AD/A-006 641

A FEASIBILITY STUDY FOR MONITORING SYSTEMS OF FATIGUE DAMAGE TO HELICOPTER COMPONENTS

R. B. Johnson, et al

Technology, Incorporated

Prepared for:

Army Air Mobility Research and Development Laboratory

January 1975

EUSTIS DIRECTORATE POSITION STATEMENT

This report is considered to provide a reasonable assessment of the monitoring concepts evaluated, and establishes the feasibility of a flight condition monitoring system.

Mr. James P. Waller of the Structures Area, Technology Applications Division served as Project Engineer for this effort.

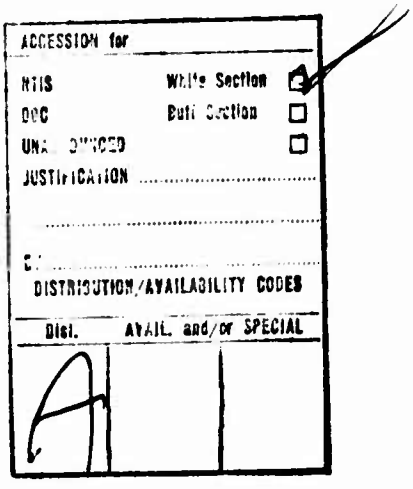

DISCLAIMERS

The findings in this report are not to be construed as an official Department of the Army position unless so designated by other authorized documents.

When Government drawings, specifications, or other data are used for any purpose other than in connection with a definitely related Government procurement operation, the United States Government thereby incurs no responsibility nor any obligation whatsoever; and the fact that the Government may have formulated, furnished, or in any way supplied the said drawings, specifications, or other data is not to be regarded by implication or otherwise as in any manner licensing the holder or any other person or corporation, or conveying any rights or permission, to manufacture, use, or sell any patented invention that may in any way be related thereto.

Trade names cited in this report do not constitute an official endorsement or approval of the use of such commercial hardware or software.

DISPOSITION INSTRUCTIONS

Destroy this report when no longer needed. Do not return it to the originator.

Unclassified

SECURITY CLASSIFICATION OF THIS PAGE (When Data Entered)

REPORT DOCUMENTATION PAGE		READ INSTRUCTIONS BEFORE COMPLETING FORM
1. REPORT NUMBER USAAMRDL-TR-74-92	2. GOVT ACCESSION NO.	3. RECIPIENT'S CATALOG NUMBER
4. TITLE (and Subtitle) A FEASIBILITY STUDY FOR MONITORING SYSTEMS OF FATIGUE DAMAGE TO HELICOPTER COMPONENTS		5. TYPE OF REPORT & PERIOD COVERED Final Report: March 1973 to August 1974 6. PERFORMING ORG. REPORT NUMBER
7. AUTHOR(s) R.B. Johnson G.L. Martin M.S. Moran		8. CONTRACT OR GRANT NUMBER(s) DAAJ02 /3-C-0053
9. PERFORMING ORGANIZATION NAME AND ADDRESS Technology Incorporated Dayton, Ohio 45431		10. PROGRAM ELEMENT, PROJECT, TASK AREA & WORK UNIT NUMBERS Task 1F162204A17002
11. CONTROLLING OFFICE NAME AND ADDRESS Eustis Directorate, U.S. Army Air Mobility Research & Development Lab, Fort Eustis, Virginia 23604		12. REPORT DATE January 1975 13. NUMBER OF PAGES 194
14. MONITORING AGENCY NAME & ADDRESS (if different from Controlling Office)		15. SECURITY CLASS. (of this report) Unclassified 15a. DECLASSIFICATION/DOWNGRADING SCHEDULE

16. DISTRIBUTION STATEMENT (of this Report)

Approved for public release; distribution unlimited.

17. DISTRIBUTION STATEMENT (of the abstract entered in Block 20, if different from Report)

18. SUPPLEMENTARY NOTES

19. KEY WORDS (Continue on reverse side if necessary and identify by block number)

helicopters
Structural Integrity Program
fatigue-critical components
fatigue damage monitoring
recording systems
flight condition monitoring
life-cycle costs

20. ABSTRACT (Continue on reverse side if necessary and identify by block number)

To monitor and record the in-flight operations of UH-1H and CH-47C helicopters for the subsequent assessment of the fatigue damage to their structures, four types of monitoring were investigated: (1) flight condition monitoring, (2) component-load monitoring, (3) mission-type monitoring, and (4) direct monitoring. After the recording systems and corresponding data processing systems were identified for each monitoring type, each type

DD FORM 1 JAN 73 1473 EDITION OF 1 NOV 65 IS OBSOLETE

Unclassified

SECURITY CLASSIFICATION OF THIS PAGE (When Data Entered)

20. was tested for its technical acceptability and cost-effectiveness. Study results indicated that the flight condition monitoring is best for the UH-1H and also for the CH-47C provided that the monitoring of gross weight for the latter model becomes technically acceptable.

PREFACE

Technology Incorporated, Dayton, Ohio, prepared this report to document its efforts on a program to investigate and determine the best type of UH-1H and CH-47C helicopter monitoring for the subsequent assessment of the structural fatigue damage to these helicopter models. This program was sponsored by the Eustis Directorate, U. S. Army Air Mobility Research and Development Laboratory, Fort Eustis, Virginia, under Contract DAAJ02-73-C-0053, DA Task 1F162204A17002, entitled "Structural Integrity Program." The project monitor for the Army was Mr. J. P. Waller.

The principal Technology Incorporated personnel on this program were R. B. Johnson, G. L. Martin, M. C. Tyler, L. E. Clay, R. I. Rockafellow, M. J. Ernst, and M. S. Moran.

Acknowledgement is given to Mr. J. P. Waller (USAAMRDL) whose assistance in obtaining data was invaluable, Mr. R. Redman (AVSCOM) for assistance in obtaining reports on the UH-1H, Mr. J. Perniciaro (AVSCOM) for assistance in the investigation of the RAMMIT system, Mr. H. H. Steinmann (Boeing-Vertol) for assistance on the analysis of the CH-47C, and Mr. R. E. Johnson for his role in the definition and direction of this effort.

TABLE OF CONTENTS

TABLE OF CONTENTS - Concluded

LIST OF ILLUSTRATIONS

LIST OF TABLES

INTRODUCTION

U. S. Army Contract DAAJ02-73-C-0053, entitled "Structural Integrity Program," was performed to investigate the feasibility of monitoring helicopter usage data for the assessment of fatigue damage to individual helicopter components. The study included the investigation of various methods of recording in-flight data, various methods of assessing fatigue damage, the evaluation of both recording and assessment methods, the selection of candidate monitoring systems, the detailed development of the selected systems, a life-cycle cost analysis of the selected systems, and the recommendation of a single monitoring system for a pilot-test program.

The investigation of recording methods was conducted to identify off-the-shelf hardware that could be used to monitor helicopter data. The investigation included a survey of available analog and digital magnetic tape-recording devices. A target cost of $2000, the ability to operate reliably in the helicopter environment, and a computer-compatible output were established as the selection criteria for the recording device. None of the off-the-shelf tape recorders surveyed could meet the cost and performance criteria, so an alternative recording method was identified.

The investigation of methods for assessing fatigue damage considered four concepts: flight condition monitoring (FCM), component load monitoring (CLM), direct monitoring (DM), and mission-type monitoring (MTM). FCM involves recording flight parameters to identify flight conditions, such as hover, forward level flight, and maneuvers. CLM involves recording component loads either directly or indirectly. DM of phenomena related to fatigue involves tracking particular phenomena (such as acoustic emission, annealed foil resistance, and material inductance levels). MTM involves tracking the mission assignments of the individual aircraft. Since each concept requires monitoring different information, the assessment of fatigue damage varies with the concept. Monitoring systems, including the parameters to be monitored, were identified for each concept and were evaluated for technical acceptability and cost-effectiveness.

The evaluation of both recording and assessment methods for technical acceptability and cost-effectiveness was based on the concept that fatigue-critical components could be retired according to the observed usage, if the usage were monitored. Technical acceptability tested the ability of the monitoring system to extend component retirement lives, and the cost-effectiveness tested the economic advantage of doing so. For technical acceptability, the retirement life of each component was established by conventional fatigue analysis for the three test spectra (mild, normal, and severe) identified in this

study. These retirement lives represented upper bounds on the retirement of the components. The manufacturer's recommended retirement life[1],[2] was used as a lower bound. A monitoring system was then considered technically acceptable if it projected retirement lives between the upper and lower bounds for each test usage. The cost-effectiveness compared the savings generated by extending component retirements and the costs associated with developing, implementing, and operating the monitoring system. When savings exceeded cost, the monitoring system was considered cost-effective.

The monitoring systems that were technically acceptable and cost-effective were then selected as candidate monitoring systems. For the UH-1H, the system was identified as 2CA; for the CH-47C, as VII. The selected systems were then identified in greater detail for the life-cycle cost analysis. The final configuration and operation of the recorder and retrieval units were identified and the steps for data processing were outlined. Costs were then estimated to develop, implement, and operate the detailed monitoring systems.

The life-cycle cost analysis compared the detail costs and savings, again, generated by extending component retirements. If savings exceeded cost, then the monitoring system was considered feasible. The effect on the life-cycle cost of two factors, fleet size and usage severity, was considered. Based on the results of the life-cycle cost analysis, the candidate monitoring systems were then ranked and the monitoring system to be developed in a pilot-test program was recommended.

---

[1] Orr, P., McLeod, G., and Goddell, J., FATIGUE LIFE SUBSTANTIATION OF DYNAMIC COMPONENTS FOR THE UH-1D HELICOPTER EQUIPPED WITH THE 48-FOOT DIAMETER ROTOR, Bell Helicopter; Report No. 205-099-135, May 1964.

[2] Thakkar, H., and MacDonald, P., CH-47C DYNAMIC SYSTEM FATIGUE ANALYSIS--FINAL REPORT, Boeing Vertol Division; Report No. 114-SS-723, March 1970.

RECORDING SYSTEM SURVEY CRITERIA

A target cost was established to provide a guide in the selection of the recording device. The target cost was defined as the difference between preliminary estimates of the component savings and the expected system cost except for the recording device itself. Included in this determination was an estimate of a desired return on the initial investment. The savings were estimated on the saved replacements of fatigue critical components. By recording the usage of the helicopter, fatigue damage may be assessed accordingly and the fatigue life may be extended relative to the design life. As a measure of the extension of the service usage, the upper bounds on the fatigue life of the critical components (see Evaluation Criteria) for the three test spectra were used. Assuming that the recorder would be in operation for 10 years, the service life of the components would be 6600 hours at a rate of 55 hours per month. By comparing the upper bounds with the 6600 hours, the number of replacements was determined for each of the test spectra (Table 1). Similarly, by comparing the recommended replacement life of the components with the 6600 hours, the number of replacements for the current practice was determined. The difference between the replacements for the upper bounds and for the current practice was the number of saved replacements (Table 2). Considering the number of saved replacements, the spectrum weighting factors (see Evaluation Criteria) and the estimated component acquisition costs, the total component savings was computed at $12,500 per unit. Assuming a fleet of 2000 aircraft, the gross savings amounts to $25 million. The target cost was defined as the difference between preliminary estimates of the component savings and the expected system cost except for the recording device itself. Included in this determination was an estimate of a desired return on the initial investment.

The costs associated with implementing a recording program on a fleet of 2000 units for a 10-year period were also estimated. Costs included start-up costs (exclusive of recorder hardware costs) and support costs. On the basis of company experience on related programs, the start-up costs were estimated at $3 million and the support costs at $8 million for the 10-year period. In addition, a return to the Army of $10 million on the initial investment was considered reasonable for a 10-year program. Subtracting these costs and the return from the gross savings yields a net value of $4 million as the target cost for the recorder hardware. For a fleet of 2000 aircraft, this amounts to $2000 per unit.

In addition to the target cost, the survey criteria included two technical requirements: that the recorder (1) be capable

of withstanding the helicopter loadings, particularly shock and vibration, and (2) that the recorder have a computer-compatible output.

TABLE 1. COMPONENT REPLACEMENTS FOR A 6600-HOUR LIFETIME FOR THE UH-1H BASED ON DESIGN AND TEST SPECTRA

Component	Replacements			
	Design	Mild	Normal	Severe
Main Rotor				
Blade	2	0	1	2
Drag Brace	1	0	0	0
Yoke	1	0	0	0
Pitch Horn	1	0	0	0
Scissors	1	0	0	1
Stabilizer Bar	1	0	0	0
Retention Strap	2	0	0	1
Swashplate Support	1	0	0	0
Collective Lever	1	0	0	0

TABLE 2. SAVED COMPONENT REPLACEMENTS FOR A 6600-HOUR LIFETIME FOR THE UH-1H BASED ON THE TEST SPECTRA

Component	Saved Replacements		
	Mild	Normal	Severe
Main Rotor			
Blade	2	1	0
Drag Brace	1	1	1
Yoke	1	1	1
Pitch Horn	1	1	1
Scissors	1	1	0
Stabilizer Bar	1	1	1
Retention Strap	2	2	1
Swashplate Support	1	1	1
Collective Lever	1	1	1

RECORDING SYSTEM SURVEY

An industry survey for information on off-the-shelf products that could be used for a helicopter recording system was initiated in May 1973. Manufacturers were obtained from selected categories in the Thomas Register and the Instruments and Control System's Buyers Guide as listed below:

Source	Category	No. of Manufacturers
Thomas Register	Recorders, Magnetic Tape	58
Thomas Register	Recorders, Speed	18
Thomas Register	Recorders, Stress and Strain	8
Thomas Register	Recorders, Tape	43
Thomas Register	Recorders, Vibration	5
Thomas Register	Instruments, Aeronautical	78
Thomas Register	Instrument Work-Experimental	87
Thomas Register	Recorders, Electronic	41
I&CS Buyer's Guide	Recorders, Analog Tape, Cassette, and Digital Tape	90
I&CS Buyer's Guide	Transducers, Pressure	103
	Acceleration	48
	Gyroscopes	19
	TOTAL	598

Over 500 survey letters were mailed (some manufacturers were listed under more than one category), but the response was poor with over 50 percent not responsive. Most of the responding manufacturers did not comply with the request for pricing information. Data concerning environmental capability and reliability was similarly absent. Followup inquiries were made of several manufacturers in specific areas of interest. Because of this lack of data, products of similar capabilities could not be adequately compared.

SURVEY RESULTS

The available recorders were surveyed to find off-the-shelf hardware that could be used to monitor helicopter usage. Responses to the questionnaire were evaluated relative to the criteria defined for the recorder. To facilitate the evaluation, the responses were grouped by recorder type, computer compatibility, and environmental capability, as shown in Table

3. It became apparent early in the study that analog tape recorders would not meet the survey criteria primarily because of cost. Consequently, digital recorders, capable of discrete operations, became the focal point of the survey.

TABLE 3. SURVEY RESULTS ON MAGNETIC TAPE RECORDERS

Class*	Respondents
AC1	Astro Science Borg Warner Genisco Pemtek Precision Instruments
AC2	Bell and Howell Lockheed Electronics Sagamo Teledyne Geotech Video Research
AC3	Dallas Instruments Teac
DC1	Ampex Astro Science Precision Instruments
DC2	Cipher Daconics Digi-Data Iotape Kennedy Precision Instruments
DC3	Brush Chalco Cipher Datel Datum Hecon Interdyne Iotape Kennedy Memodyne Metrodata MFE Redaction Ross Controls Sykes
DN1	Echo Science Lockheed Electronics

* Class Three Letter Codes:

A - Analog C - Format Computer Compatible
D - Digital N - Format NOT Computer Compatible

1 - Specification Environment Capability
2 - Limited Environment Capability
3 - Little Environment Capability

Class DC1 recorders were ideal from a technical standpoint but were unacceptable in price. The recorders in this group, which would include the Air Force ASIP recorder, range in

price from $20,000 to $30,000, which is well beyond the target cost of $2000. Class DC2 recorders were the second types considered, but the price range here is $4000 to $5000, making these recorders unacceptable on cost also. By decreasing the financial return to the Army, a recorder cost of $5000 could be met, but the decreased return coupled with the limited operational capability made the Class DC2 recorders undesirable. Classes DC3 and DN1 were not seriously considered because of their technical shortcomings. Class DC3 lack environmental capability, and Class DN1 are not computer-compatible. Typical environmental limits are 0-50°C and 90 percent humidity with no condensation. Consequently, the survey of available recorders revealed that no off-the-shelf tape system could be used to record the usage data. As a result, an alternative means of monitoring usage data was investigated according to the monitoring concepts presented in this report. The survey indicated that numerous manufacturers produce transducers which would be satisfactory for the recording system.

ALTERNATE RECORDING METHOD

The alternate method of recording in-flight data replaces the magnetic tape recorder with an electronic memory device. A complementary metal-oxide silicon (CMOS) random access memory (RAM) would accumulate the in-flight data in the form of counts rather than in the real-time, sequential format of the magnetic tape. The alternative method has three basic advantages over the magnetic tape recorder: cost, data compression, and a reduction of the data processing task. Overall system cost is reduced since each aircraft need not have a magnetic tape drive system on board. Data compression is significant since data is accumulated in several categories, regardless of the length of operation. Consequently, the number of tape cassettes and the required handling are greatly reduced. This reduction consequently reduces the amount of data processing, further lowering system operating cost.

Since the memory does not produce output, such as magnetic tape, a retrieval unit would be required to extract the accumulated data from the memory. The retrieval unit would contain the magnetic tape recorder which would write the accumulated data on magnetic tape for transfer to the data processing center.

The on-board recorder, shown schematically in Figure 1, contains the following basic elements: parameter transducers, parameter comparators, a logic network, storage registers (within the RAM), and a count generator (clock for elapsed-time counters). Although not shown, a battery is also a necessary component, since power must always be applied to the RAM to retain the accumulated counts. Since the power requirements are minimal (about 5 microwatts), the battery size and life would not present a problem.

The retrieval unit, shown schematically in Figure 2, is portable and contains the magnetic tape drive and cassette, diagnostic equipment, and a rechargeable battery. Getting the in-flight data on magnetic tape in this manner eliminates the need for a large number of tape drives qualified for the helicopter environment. A single retrieval unit can service a large number of aircraft, say, at each base of operation. Since the tape drives need not be qualified for the severe environment, the unit costs will be lower, further reducing the cost of getting the in-flight data on magnetic tape (for data processing). The diagnostic equipment would include circuitry for a series of tests for the accumulated data (the tests would be performed automatically and the test results would be written on the magnetic tape), and a voltmeter for manual tests of comparator thresholds, transducer outputs, battery condition (both on-board and retrieval units), and power supply voltages. The entire unit would be packaged in a rugged transit case, complete with hinged cover and handle, and would weigh less than 25 pounds so as not to be cumbersome. The accumulated data would be read on a standard cassette in a format compatible with a computer terminal, allowing direct access for the data processing tasks.

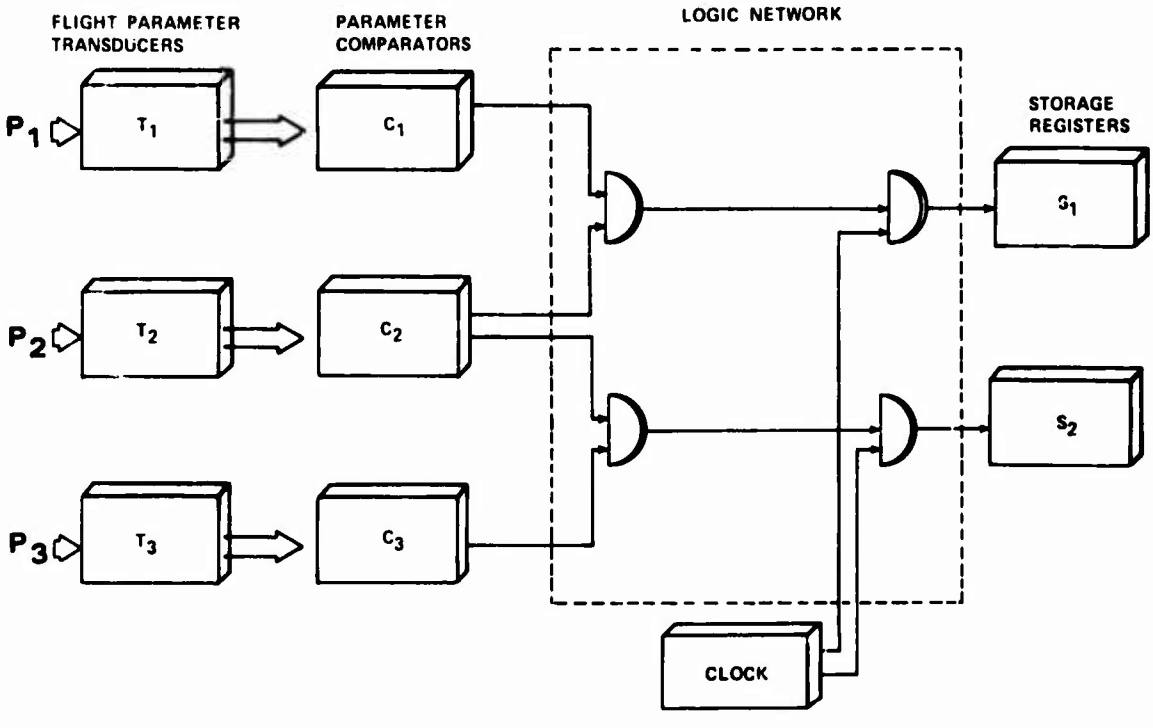

Figure 1. Schematic of FCM Recorder.

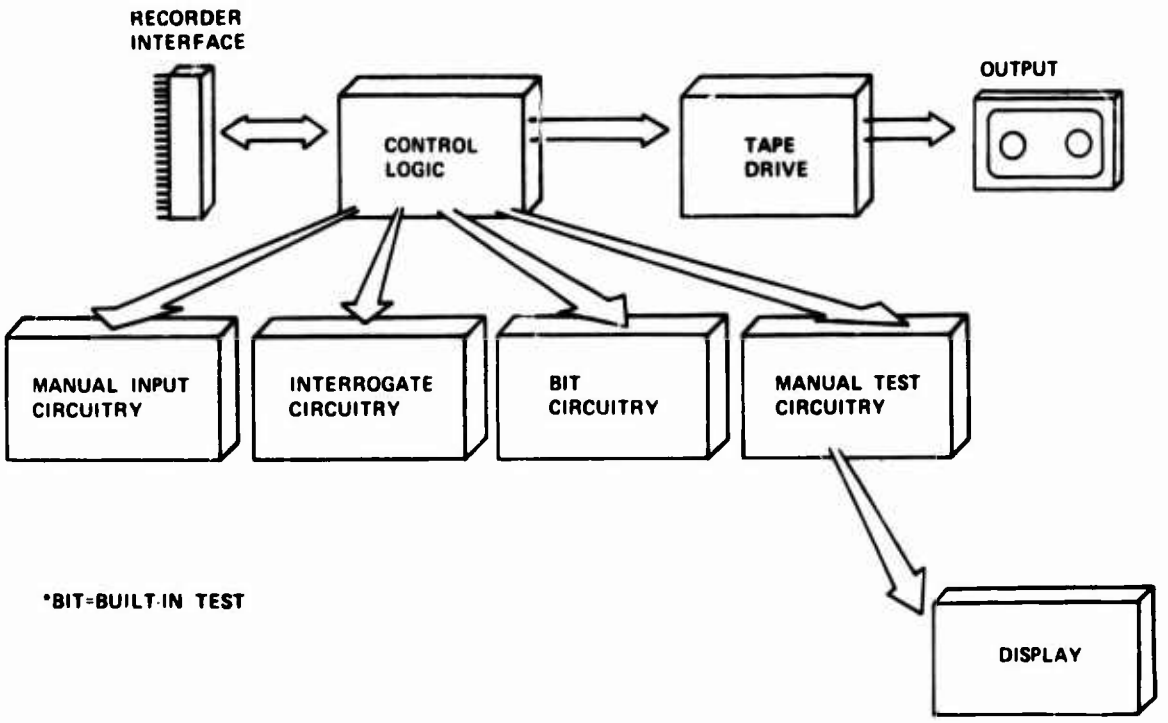

Figure 2. Schematic of Retrieval Unit.

MONITORING METHODS

INTRODUCTION

Four types of in-flight aircraft monitoring--FCM, CLM, DM, and MTM--were identified, investigated, and evaluated individually and relatively to define potential means for monitoring the operational usage of the UH-1H and CH-47C helicopters. The following section discusses the concepts and associated assumptions of each of the four monitoring types.

FLIGHT CONDITION MONITORING

The FCM collects flight condition data for fatigue damage assessment. Similar to the manufacturer's fatigue analysis, where damage is assigned to various flight conditions of a design spectrum, the fatigue analysis with FCM data is based on the actual flight time spent in various flight conditions.

The fatigue damage assessment is based on a damage rate per unit of time for each selected flight condition and the total time spent in the given flight condition; that is,

$$D(I) = C(I) \cdot T(I) \qquad (1)$$

where D = damage for a given flight condition
C = damage rate for a given flight condition
T = total time spent in the given flight condition

Therefore, in comparison to the classical method of computing fatigue damage where applied cycles (n) of specific load levels are compared with the corresponding number of cycles to failure (N), the FCM concept is based on the assumption that the actual time spent in a flight condition can be used to identify the applied cycles (n) and that the number of cycles to failure (N) can be assumed for the flight condition. For the number of cycles to failure, the manufacturer's top-of-scatter load or stress level is assumed for the flight condition. Since the number of applied cycles of the load level is also assumed, the damage fraction for the flight condition is another assumption. The damage fraction is then divided by the duration of the flight condition to produce a conservative damage rate. Since the load level is the top-of-scatter load for the flight condition, the damage fraction and the resulting damage rate are both conservative. Finally, to complete the fatigue damage assessment, the flight conditions and the means of monitoring them must be identified.

The flight conditions considered damaging to the UH-1H and CH-47C are listed in Tables 4 and 5, respectively. These tables are based on the 100 flight hours specified in the design spectrum.

TABLE 4. FLIGHT CONDITIONS FOR THE UH-1H

	Flight Condition		Percent of Flight Time
I.	Ground Conditions		1.000
II.	Power-On Flight		
	A	Vertical Takeoff	0.400
	B	Hover	3.520
	C	Norm Acceleration	1.000
	D	Norm Deceleration	1.000
	E	Max Acceleration	0.250
	F	Max Deceleration	0.250
	G	Sideward Flt	0.500
	H	Rearward Flt	0.250
	I	Full Pwr Climb	4.000
	J	Fwd Level Flt	77.000
	K	Part Power Descent	1.000
	L,M	Turns	4.000
	N,O	Pull-Ups	0.500
	P	Control Reversals	1.000
	Q	Norm Landing	1.000
III.	Transition		
	A	Power to Auto	0.350
	B	Auto to Power	0.350
IV.	Autorotation		
	A	Steady Forward Flight	2.000
	B	60-Kn Control Reversal	0.030
	C,D	Turns	1.000
	E	Autorotation Landing/ Power Recovery	0.200
	F	Full Auto Landing	0.250

TABLE 5. FLIGHT CONDITIONS FOR THE CH-47C

Flight Conditions	Duration
Level Flight,	
Hover	10 Percent
Transition (Hover to Forward Flight)	15 Percent
60 percent V_{NE}*	25 Percent
90 percent V_{NE}	20 Percent
100 percent V_{NE}	20 Percent
110 percent V_{NE}	10 Percent
Maneuvers,	
Flare, Landing	4/hr
Turn,	
Right	5/hr
Left	5/hr
Pull-Up,	
Collective	3/hr
Longitudinal	1/hr
Control Reversals,	
Longitudinal	4/hr
Lateral	4/hr
Directional	4/hr
Other Conditions	
Gross Weight,	
27000 lb	50 Percent
33000 lb	25 Percent
46000 lb	25 Percent
Center of Gravity,	
Forward	50 Percent
Aft	50 Percent
Altitude,	
0 to 6000 ft	50 Percent
6000 to 10000 ft	40 Percent
10000 ft and above	10 Percent

*V_{NE} = velocity never exceeded

In the CH-47C spectrum, the total time is divided among the level flight conditions and maneuvers which are considered as discrete events of no duration; in the UH-1H spectrum, the duration of all maneuvers was considered. Consequently, the duration of maneuvers[3] was used (see Table 6) and the flight condition spectrum was so adjusted.

[3] Herskovitz, A., and Steinmann, H., CH-47A DESIGN AND OPERATIONAL FLIGHT LOADS STUDY, Boeing, Philadelphia, Pennsylvania; USAAMRDL Technical Report 73-40, U.S. Army Air Mobility Research and Development Laboratory, Fort Eustis, Virginia, November 1973, AD772949.

TABLE 6. DURATION OF MANEUVERS FOR THE CH-47C

Maneuver	Duration (seconds)
Flare, Landing	30.0
Turn	58.5
Pull-Up	7.1
Control Reversal,	
Longitudinal	7.5
Lateral	8.0
Directional	6.4

With this information and the damage accrued by each fatigue-critical component, the flight conditions were ranked according to their severity in producing damage to the helicopter as a whole. The results of the ranking procedure are listed in Tables 7 and 8 for the UH-1H and CH-47C, respectively. For both helicopter models, the flight conditions producing the most damage are pull-ups, control reversals, and landings; some turns and level flight conditions also contribute damage. Consequently, the definition of the recording systems concentrated on the higher-ranked flight conditions.

The flight conditions are identified by monitoring those parameters that reflect specific helicopter conditions. Table 9 lists the parameters for the UH-1H. As noted, a collective pull-up at 90 percent V_H (limit forward airspeed) is the most damaging flight condition. To individually identify the collective pull-ups, the recorder must monitor the indicated airspeed, the collective stick position, the pitch rate, and the vertical acceleration. The stick position is monitored to identify the control input, that is, to differentiate the collective pull-up from other conditions causing similar helicopter responses, such as longitudinal pull-ups and reversals. The airspeed is monitored to determine whether the maneuver is performed at 90 percent V_H; pitch rate and vertical acceleration are monitored to identify the helicopter response. Similarly, the other parameters listed in Table 9 were identified by the damaging flight conditions listed in Table 10. This latter table presents the 23 flight conditions producing the most fatigue damage, the parameters required to monitor each flight condition individually, and the type of monitoring required.

TABLE 7. RANKING OF FLIGHT CONDITIONS FOR THE UH-1H

Rank	Flight Condition	Rank Value
1	Pull-Up at 90 Percent V_H, Collective	80.740
2	Hovering, in Ground Effect, Control Reversal, Longitudinal	17.000
3	Pull-Up at 90 Percent V_H, Cyclic	10.440
4	Control Reversal at 90 Percent V_H, Lateral	7.740
5	Power Off Landing, with No Power Recovery	5.6240
6	Control Reversal at 90 Percent V_H, Longitudinal	4.680
7	Landing, Normal at 9500 Lb Gross Weight	4.650
8	Transition, Power Off to Power On at 80 Percent V_H	4.6
9	Main Rotor Start/Stop Cycles	3.924
10	Power Off, Landing Approach with Power Recovery in Ground Effect at 40 Percent V_H	3.450
11	Deceleration, Maximum Rate	2.536
12	Transition, Power Off to Power On at 60 Percent V_H	2.160
13	Landing, Normal at 8500 Lb Gross Weight	2.075
14	Pull-Up at 60 Percent V_H, Collective	1.645
15	Turn, Right at 90 Percent V_H	1.600
16	Turn, Left at 90 Percent V_H	1.482
17	Sideward Flight, Right	.852
18	Turn, Left at 60 Percent V_H	.415
19	Landing, Normal at 7500 Lb Gross Weight	.383
20	Forward Flight, at 20 Percent V_{NE}	.271
21	Forward Flight, at 30 Percent V_{NE}	.230
22	Turns, Right at 60 Percent V_H	.130
23	Deceleration, Normal	.127

TABLE 8. RANKING OF FLIGHT CONDITIONS FOR THE CH-47C

Rank	Flight Condition	Alt/Gross Wt	Percent of Flight Time
1	Cyclic Pull-Up	0-6000 ft/33000 lb	.020
2	Longitudinal Reversal	10000 ft-above/27000 lb	.030
3	Cyclic Pull-Up	6000-10000 ft/33000 lb	.020
4	Longitudinal Reversal	0-6000 ft/27000 lb	.170
5	Longitudinal Reversal	6000-10000 ft/27000 lb	.140
6	Exceed V_{ne}	10000 ft-above/33000 lb	.210
7	Landing Flare	0-6000 ft/46000 lb	.390
8	Longitudinal Reversal	0-6000 ft/33000 lb	.080
9	Collective Pull-Up	0-6000 ft/33000 lb	.060
10	Longitudinal Reversal	6000-10000 ft/33000 lb	.070
11	Collective Pull-Up	6000-10000 ft/33000 lb	.050
12	Cyclic Pull-Up	10000 ft-above/27000 lb	.010
13	Collective Pull-Up	6000 ft-above/46000 lb	.060
14	Longitudinal Reversal	10000 ft-above/33000 lb	.020
15	Lateral Reversal	6000 ft-above/46000 lb	.090
16	Lateral Reversal	0-6000 ft/46000 lb	.090
17	Lateral Reversal	6000-10000 ft/27000 lb	.150
18	Lateral Reversal	0-6000 ft/27000 lb	.180
19	Transition	0-6000 ft/46000 lb	1.520
20	Lateral Reversal	10000 ft-above/27000 lb	.040
21	Lateral Reversal	0-6000 ft/33000 lb	.090
22	Cyclic Pull-Up	6000 ft-above/46000 lb	.020
23	Lateral Reversal	6000-10000 ft/33000 lb	.070
24	Left Turn	6000 ft-above/46000 lb	.850
25	Left Turn	10000 ft-above/33000 lb	.170
26	Longitudinal Reversal	0-6000 ft/46000 lb	.080
27	Longitudinal Reversal	6000 ft-above/46000 lb	.090
28	Exceed V_{ne}	0-6000 ft/46000 lb	1.010
29	Right Turn	0-6000 ft/46000 lb	.820
30	Directional Reversal	0-6000 ft/33000 lb	.070
31	Directional Reversal	6000-10000 ft/33000 lb	.060
32	70% V_{ne}	6000 ft-above/46000 lb	2.620
33	Directional Reversal	0-6000 ft/27000 lb	.140
34	70% V_{ne}	0-6000 ft/46000 lb	2.530
35	Directional Reversal	6000-10000 ft/27000 lb	.120
36	Exceed V_{ne}	6000-10000 ft/33000 lb	.840
37	Right Turn	6000 ft-above/46000 lb	.850
38	Exceed V_{ne}	0-6000 ft/33000 lb	.990
39	Right Turn	0-6000 ft/33000 lb	.810
40	Left Turn	0-6000 ft/33000 lb	.810
41	Right Turn	10000 ft-above/27000 lb	.340
42	Right Turn	10000 ft-above/33000 lb	.170
43	Left Turn	10000 ft-above/27000 lb	.340
44	Rotor Start/Stop	--	.250
45	Left Turn	0-6000 ft/46000 lb	.820
46	Right Turn	6000-10000 ft/33000 lb	.680
47	Right Turn	0-6000 ft/27000 lb	1.610
48	Left Turn	6000-10000 ft/33000 lb	.680
49	Right Turn	6000-10000 ft/27000 lb	1.360

TABLE 9. MONITORING PARAMETERS FOR THE UH-1H

Indicated Airspeed
Main Rotor RPM
Longitudinal Stick Position
Lateral Stick Position
Collective Stick Position
Pitch Rate
Roll Rate
Yaw Rate
Vertical Acceleration
Longitudinal Acceleration
Lateral Acceleration
Landing Gear Touchdowns
Engine Torque
Gross Weight

The type of monitoring specifies that the flight condition be monitored on an occurrence or time basis. For example, rotor start/stops (#2) are monitored as occurrences where an excursion of rotor rpm from below 25 percent of normal to above 85 percent of normal and to below 25 percent of normal is considered as a single occurrence of a rotor start/stop cycle. An example of a flight condition monitored on a time basis is forward flight at 20 percent V_H (#15) where the flight time would be accrued when the indicated airspeed was approximately 20 percent V_H and the vertical acceleration was in a level flight range (typically, 0.8g to 1.2g). The code numbers in Table 10 define the type of monitoring by specifying how the parameter is to be monitored. Where more than one code is shown, the manner of monitoring is optional, depending on the desired complexity of the recording system.

Monitoring all the parameters listed in Table 9, however, proved to be too costly. Consequently, the parameters monitoring the control stick inputs were eliminated and only those monitoring the helicopter response were retained.

TABLE 10. MONITORING PARAMETERS VERSUS DAMAGING FLIGHT CONDITIONS FOR THE UH-1H

FLIGHT CONDITION	Indicated Airspeed	Main Rotor RPM	Altitude	Longitudinal Stick Position	Lateral Stick Position	Collective Stick Position	Pitch Gyro (Rate)	Roll Gyro (Rate)	Yaw Gyro (Rate)	Vertical Acceleration	Longitudinal Acceleration	Lateral Acceleration	Landing Gear Touchdown	Engine Torque	Gross Weight (Gear Pressure)	Type of Monitoring
1. Collective Pull-up .9V_H	13,14					13	13,14			13,14						0
2. Rotor Stop/Start		11														0
3. Full Auto Landing		14,31				13				13			11	13	14	0
4. Right Turn .9V_H	23,24				31			31	31			31				T
5. Left Turn .9V_H	23,24				31			31	31			31				T
6. Normal Landing (9500 lb)										13			11		14	0
7. Max.Rate Deceleration	31			31			31				13,14					0
8. Cyclic Pull-up .9V_H	13,14			13			13,14			13,14						0
9. Auto to Power .6V_H	14	14,31				13								11,31		0
10. Left Turn .6V_H	23,24				31			31	31			31				T
11. Normal Landing (8500 lb)										13			11		14	0
12. Lateral Control Reversal .9V_H	13,14				14,31			14,31				13				0
13. Collective Pull-up.6V_H	13,14					13	13,14			13,14						0
14. Auto Ldg.Approach/Pwr Rec IGE .4V_H		14,31				31				31			11	31	14	0
15. Forward Flight .2V_{ne}	23,24									12,13						T
16. Long.Control Reversal	13,14			14,31			14,31			13						0
17. Forward Flight .3V_{ne}	23,24									12,13						T
18. Auto to Power .8V_H	13,14	14,31				31								11,31		0
19. Sideward Flight-Right					24,31			24,31				31				T
20. Long. Control Reversal-Hover IGE	12			14,31			14,31			13						0
21. Right Turn .6V_H	23,24							31	31			31				T
22. Normal Deceleration	31			31			31				13,14					0
23. Normal Landing (7500 lb)										13			11		14	0

CODE:

11 - Occurrence of event
12 - Occurrences in range
13 - Occurrence above threshold
14 - Occurrence in ranges above threshold
22 - Time in ranges
23 - Time above threshold
24 - Time in ranges above threshold
31 - Time history above threshold
0 - Occurrence
T - Time

As a result, such flight conditions as collective and longitudinal pull-ups could not be differentiated, since the helicopter response is similar for both flight conditions. These flight conditions could, however, still be monitored as elements of a flight condition category where flight conditions causing similar helicopter responses could be included in the same recorded data. Thus, instead of recording collective and longitudinal pull-ups as separate flight conditions, both would be recorded in a category where the vertical acceleration and pitch rate exceed specified thresholds. As presented in Appendix A, the various recording systems for the UH-1H were based on the reduced set of parameters. As an example, Table 11 lists the parameters considered for the candidate monitoring system on the UH-1H, System 2CA, and Table 12 indicates how these parameters are combined to form categories of damaging flight conditions. Table 12 also lists by number the design spectrum flight conditions that should be recorded in each of the categories; the flight condition numbers correlate with those presented in Table A-1, and the asterisks denote damaging conditions. Note that the recorded time in categories will include time from damaging as well as nondamaging flight conditions. The damage rate, however, is based on the total time in the flight condition category for the design spectrum. This, again, is a conservative assumption. Table 13 lists the resultant damage rates for each of the flight condition categories for system 2CA, and Appendix A presents the same information for the other recording systems considered for the UH-1H helicopter.

TABLE 11. MONITORING PARAMETERS FOR RECORDING SYSTEM 2CA FOR THE UH-1H

Indicated Airspeed
Main Rotor RPM
Pitch Rate
Roll Rate
Vertical Acceleration
Landing Gear Touchdown
Engine Torque

A similar development was undertaken for the FCM method of recording data for the CH-47C helicopter. The flight conditions shown in Table 5 were selected on the basis of producing 1 percent or more of the total damage to any of the fatigue-critical components. Table 8 lists the flight conditions ranked according to the severity of damage produced on the helicopter as a whole. As for the UH-1H, the parameters reflecting CH-47C conditions were identified to record primarily those flight conditions most damaging to fatigue-critical components.

TABLE 12. SYSTEM 2CA

Flight Condition Category	Parameters	Thresholds (& Tolerance)	Flight Conditions Included
0	Clock time	--	2, 3, 4, 5, 6*, 7, 8, 11, 12*, 13*, 14 15, 16, 17*, 18*, 19, 20, 26, 27, 30, 44, 47, 50, 53, 54, 55, 56, 59, 62*, 63, 64, 45, 46
1	Landing gear touchdown	--	40, 41*, 42*, 43*,
2	Power buss & landing gear	--	65*
3	Rotor rpm	100 rpm ±10 rpm	1*
4	A/S above threshold Vertical accel above threshold Pitch rate below threshold	80 kt ±3 kt 1.2 g ±.0375 g 10°/sec ±.5°/sec	34*, 36*, 37*
5	A/S above threshold Vertical accel above threshold Pitch rate above threshold	80 kt ±3 kt 1.2 g ±.0375 g 10°/sec ±.5°/sec	29*, 32*
6	A/S between threshold Vertical accel above threshold Pitch rate below threshold	55-80 kt 1.2 g ±.0375 g 10°/sec ±.5°/sec	33, 35*
7	A/S between threshold Vertical accel above threshold Pitch rate above threshold	55-80 kt 1.2 g ±.0375 g 10°/sec ±.5°/sec	28, 31* 48*, 49*
8	A/S above threshold Vertical accel betw. "g" threshold	80 kt ±3 kt .8g < Nz < 1.2g	24, 25, 38*, 39
9	A/S between threshold Vertical accel betw. "g" threshold	55-80 kt .8g < Nz < 1.2g	9, 10*, 21, 22, 23 51, 52, 57, 58, 60, 61

* Damaging flight conditions; flight condition numbers correlate with those presented in Table A-1.

TABLE 13. DAMAGE RATES, C_{ij}, FOR UH-1H FCM SYSTEM 2CA

*FLIGHT CONDITION CATEGORY	COMPONENT(i)									
	1	2	3	4	5	6	7	8	9	10
	MAIN ROTOR RETENTION STRAP	MAIN ROTOR YOKE	STABILIZER BAR	MAIN ROTOR DRAG BRACE	SWASHPLATE SUPPORT	COLLECTIVE LEVER	MAIN ROTOR PITCH HORN	MAIN ROTOR SCISSORS	MAIN ROTOR GRIP	MAIN ROTOR BLADE
0	0.	0.	0.	.5[illegible]E-04	0.	0.	.[illegible]E-05	.[illegible]E-05	.[illegible]E-0[illegible]	.[illegible]E-03
1	0.	0.	0.	0.	0.	0.	0.	0.	.[illegible]E-02	.[illegible]E-02
2	0.	0.	.[illegible]E+00	0.	.[illegible]E-01	.[illegible]E-01	0.	.1[illegible]E-02	0.	.[illegible]E-02
3	.[illegible]E-01	0.	0.	0.	0.	0.	0.	0.	0.	0.
4	0.	.[illegible]E-01	0.	.17[illegible]E+00	.[illegible]E-01	.[illegible]E-01	.[illegible]E-01	.[illegible]E-01	.13[illegible]E-01	.[illegible]E-01
5	0.	0.	0.	0.	.[illegible]E-02	.[illegible]E-02	.1[illegible]E-01	.[illegible]E-01	0.	.[illegible]E-02
6	0.	0.	0.	0.	.[illegible]E-02	.[illegible]E-02	.[illegible]E-02	.[illegible]E-02	.1[illegible]E-02	.[illegible]E-02
7	0.	0.	0.	0.	.[illegible]E-03	.[illegible]E-03	.[illegible]E-04	.[illegible]E-04	0.	.[illegible]E-02
8	0.	0.	0.	.1[illegible]E-03	.[illegible]E-05	.[illegible]E-05	.[illegible]E-05	.[illegible]E-05	.[illegible]E-05	.[illegible]E-04
9	0.	0.	0.	0.	0.	0.	0.	.[illegible]E-05	0.	.[illegible]E-04

*FLIGHT CONDITION CATEGORY

0 TOTAL FLIGHT TIME NOT RECORDED IN CATEGORIES 4-9

1 NUMBER OF LANDING GEAR TOUCHDOWNS

2 NUMBER OF FULL AUTOROTATIVE LANDINGS

3 NUMBER OF ROTOR SHUTDOWNS

4 TIME AT V<80 KT, n_z<1.2 g, P<PT

5 TIME AT V>80 KT, n_z<1.2 g, P<PT

6 TIME AT 55 KT<V<80 KT, n_z<1.2 g, P<PT

7 TIME AT 55 KT<V<80 KT, n_z<1.2 g, P<PT

8 TIME AT V<80 KT, .8 g<n_z<1.2 g

9 TIME AT 55 KT<V<80 KT, .8 g<n_z<1.2 g

Based on the UH-1H FCM development, the parameters to be monitored were restricted to helicopter response and related conditions exclusive of control inputs. Table 14 lists the selected parameters, and Table 15 presents the monitoring required for each. Among the parameters to be monitored is the helicopter gross weight. This information has been considered essential for fatigue damage assessment since the CH-47C has a flight envelope that is very sensitive to gross weight, as typified by a reduction in V_{NE} (velocity never exceeded) with increasing altitude and gross weight.

TABLE 14. MONITORING PARAMETERS FOR THE CH-47C

Indicated Airspeed
Rotor RPM
Pitch Rate
Roll Rate
Yaw Rate
Vertical Acceleration
Landing Gear Touchdowns
Gross Weight
Altitude
Longitudinal Cyclic Speed Trim (LCST) Position

TABLE 15. MONITORING PARAMETERS VERSUS DAMAGING FLIGHT CONDITIONS FOR THE CH-47C

Flight Condition	Gross Weight	Altitude	Indicated Airspeed	Pitch Rate	Roll Rate	Yaw Rate	Vertical Accel	Landing Gear Touchdown	LCST Position	Rotor RPM
1. Cyclic Pull-Up	12	22	23,24	23,24			23,24			
2. Long. Control Rev.	12	22	24,31	24,31			24,31			
3. Landing Flare	12	22					13	11		
4. Collective Pull-Up	12	22	23,24	23,24			23,24			
5. Lateral Control Rev.	12	22	24,31		24,31		24,31			
6. Transition (Hover to Fwd Flight)	12	22	23,24							
7. Exceed Vne	12	22	23,24						11	
8. Left Turn	12	22	23,24		31					
9. Directional Control Rev.	12	22	23,24			24,31				
10. Level Flight (70 Percent Vne)	12	22	23,24							
11. Right Turn	12	22	23,24		31					
12. Rotor Start/Stop										11

CODE:

11 - Occurrence of event

12 - Occurrence in range

13 - Occurrence above threshold

14 - Occurrence in ranges above threshold

22 - Time in ranges

24 - Time in ranges above threshold

31 - Time history above threshold

Of the FCM recording systems considered for the CH-47C, System VII is presented as an example. Table 16 lists the selected parameters for System VII, and Table 17 indicates how the parameters are combined to form categories of damaging flight conditions. Table 17 also lists by number the flight conditions recorded in the flight condition categories; the flight condition numbers correlate with those presented in Table A-2, and the asterisks denote damaging conditions. The resulting damage rates for System VII are reported in Table 18. The remaining FCM recording systems for the CH-47C are presented in Appendix A.

TABLE 16. MONITORING PARAMETERS FOR RECORDING SYSTEM VII FOR THE CH-47C

Indicated Airspeed
Rotor RPM
Pitch Rate
Vertical Acceleration
Landing Gear Touchdown
Gross Weight
Altitude
Longitudinal Cyclic Speed Trim (LCST) Position

TABLE 17. SYSTEM VII

Flight Condition Category	Parameters	Thresholds (& Tolerance)	Flight Conditions Included
0	Clock time	--	1,2,7,14*,15,16,21,28*,29, 30,35,42,43,44,49,56*,57, 58,63,70*,71,72,77,84,85, 86*,98,99,100,112
1	Airspeed LCST Position	V < 60 kt Extended	--
2	Airspeed Gross Weight Altitude	60 kt < V < .9 Vne GW < 33000 ALT < 5000	3
3	Airspeed Gross Weight Altitude	60 kt < V < .9 Vne 33000 < GW < 40000 ALT < 5000	45
4	Airspeed Gross Weight Altitude	60 kt < V < .9 Vne 40000 < GW < 46000 ALT < 5000	--
5	Airspeed Gross Weight Altitude	60 kt < V < .9 Vne GW > 46000 ALT < 50000	87*
6	Airspeed Gross Weight Altitude	60 kt < V < .9 Vne GW < 33000 5000 < ALT < 9000	17
7	Airspeed Gross Weight Altitude	60 kt < V < .9 Vne 33000 < GW < 40000 5000 < ALT < 9000	59
8	Airspeed Gross Weight Altitude	60 kt < V < .9 Vne 40000 < GW < 46000 5000 < ALT < 9000	--
9	Airspeed Gross Weight Altitude	60 kt < V < .9 Vne GW > 46000 5000 < ALT < 9000	101*

* Damaging flight conditions; flight condition numbers correlate with those presented in Table A-2.

TABLE 17 - Continued

Flight Condition Category	Parameters	Thresholds (& Tolerance)	Flight Conditions Included
10	Airspeed Gross Weight Altitude	60 kt < V < .9 Vne GW < 33000 ALT > 9000	31
11	Airspeed Gross Weight Altitude	60 kt < V < .9 Vne 33000 < GW < 40000 ALT > 9000	73
12	Airspeed Gross Weight Altitude	60 kt < V < .9 Vne 40000 < GW < 46000 ALT > 9000	--
13	Airspeed Gross Weight Altitude	60 kt < V < .9 Vne GW > 46000 ALT > 9000	--
14	Airspeed Gross Weight	V > Vne GW < 33000	6,20,34
15	Airspeed Gross Weight	V > Vne 33000 < GW < 40000	48*,62*,76*
16	Airspeed Gross Weight	V > Vne 40000 < GW < 46000	--
17	Airspeed Gross Weight	V > Vne GW > 46000	90*,104
18	Airspeed LCST Position	V > Vne Retracted	--
19	Vertical Accel above Threshold Pitch Rate above Threshold Gross Weight	1.2 g ±.0375 g 10°/sec ±.5°/sec GW < 33000	11,12*,25,26*,39*,40*
20	Vertical Accel above Threshold Pitch Rate below Threshold Gross Weight	1.2 g ±.0375 g 10°/sec ±.5°/sec 33000 < GW < 40000	53*,54*,67*,68*,81,82*
21	Vertical Accel above Threshold Pitch Rate below Threshold Gross Weight	1.2 g ±.0375 g 10°/sec ±.5°/sec 40000 < GW < 460(	--

* Damaging flight conditions; flight condition numbers correlate with those presented in Table A-2.

TABLE 17 - Continued

Flight Condition Category	Parameters	Thresholds (& Tolerance)	Flight Conditions Included
22	Vertical Accel above Threshold Pitch Rate above Threshold Gross Weight	1.2 g ±.0375 g 10°/sec ±.5°/sec GW > 46000	95,96*,109*,110*
23	Vertical Accel above Threshold Pitch Rate above Threshold Gross Weight	1.2 g ±.0375 g 10°/sec ±.5°/sec GW < 33000	10,24,38
24	Vertical Accel above Threshold Pitch Rate below Threshold Gross Weight	1.2 g ±.0375 g 10°/sec ±.5°/sec 33000 < GW < 40000	52*,66*,80
25	Vertical Accel above Threshold Pitch Rate above Threshold Gross Weight	1.2 g ±.0375 g 10°/sec ±.5°/sec 40000 < GW < 46000	--
26	Vertical Accel above Threshold Pitch Rate below Threshold Gross Weight	1.2 g ±.0375 g 10°/sec ±.5°/sec GW > 46000	94,108*
27	Roll Rate above Threshold Gross Weight	5°/sec ±.1°/sec GW < 33000	8,9*,13*,22,23*,27*,36*,37* 41*
28	Roll Rate above Threshold Gross Weight	5°/sec ±.1°/sec 33000 < GW < 40000	50*,51*,55*,64*,65*,69*,78*, 79*,83
29	Roll Rate above Threshold Gross Weight	5°/sec ±.1°/sec 40000 < GW < 46000	--
30	Roll Rate above Threshold Gross Weight	5°/sec ±.1°/sec GW > 46000	92*,93*,97*,106*,107*,111*
31	Landing Gear Touchdown Gross Weight	GW > 46000	91*,105
32	Rotor rpm	100 rpm ±10 rpm	113*
33	Airspeed Gross Weight Altitude	.9 Vne < V < Vne GW < 33000 0 < ALT < 5000	4,5

* Damaging flight conditions; flight condition numbers correlate with those presented in Table A-2.

TABLE 17 - Concluded

Flight Condition Category	Parameters	Thresholds (& Tolerance)	Flight Conditions Included
34	Airspeed Gross Weight Altitude	.9 Vne < V < Vne 33000 < GW < 40000 0 < ALT < 5000	46,47
35	Airspeed Gross Weight Altitude	.9 Vne < V < Vne 40000 < GW < 46000 0 < ALT < 5000	--
36	Airspeed Gross Weight Altitude	.9 Vne < V < Vne GW > 46000 0 < ALT < 5000	88,89
37	Airspeed Gross Weight Altitude	.9 Vne < V < Vne GW < 33000 5000 < ALT < 9000	18,19
38	Airspeed Gross Weight Altitude	.9 Vne < V < Vne 33000 < GW < 40000 5000 < ALT < 9000	60,61
39	Airspeed Gross Weight Atltitude	.9 Vne < V < Vne 40000 < GW < 46000 5000 < ALT < 9000	--
40	Airspeed Gross Weight Altitude	.9 Vne < V < Vne GW > 46000 5000 < ALT < 9000	102,103
41	Airspeed Gross Weight Altitude	.9 Vne < V < Vne GW < 33000 ALT > 9000	32,33
42	Airspeed Gross Weight Altitude	.9 Vne < V < Vne 333000 < GW < 40000 ALT > 9000	74,75
43	Airspeed Gross Weight Altitude	.9 Vne < V < Vne 40000 < GW < 46000 ALT > 9000	--
44	Airspeed Gross Weight Altitude	.9 Vne < V < Vne GW > 46000 ALT > 9000	--

* Damaging flight conditions; flight condition numbers correlate with those presented in Table A-2.

TABLE 18. DAMAGE RATES, C_{ij}, FOR CH-47C FCM SYSTEM VII

*FLIGHT CONDITION CATEGORY	COMPONENT(i)									
	1	2	3	4	5	6	7	8	9	10
	AFT ROTOR SHAFT P/N	AFT ROTOR PITCH SHAFT	FWD ROTOR PITCH SHAFT	AFT HUB	AFT HORIZ HINGE PIN	AFT ROTOR BLADE	AFT ROTOR BLADE SOCKET	FWD ROTOR BLADE SOCKET	AFT TIE BAR	FWD TIE BAR
0	0.	0.	.3970E-05	0.	0.	.3050E-03	.4370E-04	.4480E-04	0.	0.
1	0.	0.	0.	0.	0.	0.	0.	0.	0.	0.
2	0.	0.	0.	0.	0.	0.	0.	0.	0.	0.
3	0.	0.	0.	0.	0.	0.	0.	0.	0.	0.
4	0.	0.	0.	0.	0.	0.	0.	0.	0.	0.
5	0.	0.	0.	0.	0.	.3110E-03	0.	0.	0.	0.
6	0.	0.	0.	0.	0.	0.	0.	0.	0.	0.
7	0.	0.	0.	0.	0.	0.	0.	0.	0.	0.
8	0.	0.	0.	0.	0.	0.	0.	0.	0.	0.
9	0.	0.	0.	0.	0.	.3660E-03	0.	0.	0.	0.
10	0.	0.	0.	0.	0.	0.	0.	0.	0.	0.
11	0.	0.	0.	0.	0.	0.	0.	0.	0.	0.
12	0.	0.	0.	0.	0.	0.	0.	0.	0.	0.
13	0.	0.	0.	0.	0.	0.	0.	0.	0.	0.
14	0.	0.	0.	0.	0.	0.	0.	0.	0.	0.
15	.5810E-02	.1620E-02	0.	.2720E-03	.2720E-03	.1570E-02	.1530E-03	0.	0.	0.
16	0.	0.	0.	0.	0.	0.	0.	0.	0.	0.
17	.1560E-02	.1200E-02	0.	0.	0.	.1060E-03	.2230E-04	0.	0.	0.
18	0.	0.	0.	0.	0.	0.	0.	0.	0.	0.
19	.1510E-01	.1750E-01	.2420E-01	.8780E-02	.8780E-02	.1000E-01	.1340E-01	.1530E-01	0.	0.
20	.1060E-01	.1370E-01	.1380E-01	.1130E-01	.1130E-01	.5690E-02	.3570E-02	.1320E-01	0.	0.
21	0.	0.	0.	0.	0.	0.	0.	0.	0.	0.
22	0.	.4890E-02	0.	.4760E-04	.4760E-04	.9100E-03	.7760E-02	.1900E-03	0.	0.

*FLIGHT CONDITION CATEGORY

0 FLIGHT TIME NOT RECORDED IN CLASSES 2-45
1 TIME AT A/S < 60 KT AND LCST EXTENDED
2 TIME AT 60 KT < A/S < .9 VNE, GW < 33000, AND ALT < 5K
3 TIME AT 60 KT < A/S < .9 VNE, 33000 < GW < 40000, AND ALT < 5K
4 TIME AT 60 KT < A/S < .9 VNE, 40000 < GW < 46000, AND ALT < 5K
5 TIME AT 60 KT < A/S < .9 VNE, GW > 46000, AND ALT < 5K
6 TIME AT 60 KT < A/S < .9 VNE, GW < 33000, AND 5K < ALT < 9K
7 TIME AT 60 KT < A/S < .9 VNE, 33000 < GW < 40000, AND 5K < ALT < 9K
8 TIME AT 60 KT < A/S < .9 VNE, 40000 < GW < 46000, AND 5K < ALT < 9K
9 TIME AT 60 KT < A/S < .9 VNE, GW > 46000, AND 5K < ALT < 9K
10 TIME AT 60 KT < A/S < .9 VNE, GW < 33000, AND ALT < 9K
11 TIME AT 60 KT < A/S < .9 VNE, 33000 < GW < 40000, AND ALT > 9K
12 TIME AT 60 KT < A/S < .9 VNE, 40000 < GW < 46000, AND ALT > 9K
13 TIME AT 60 KT < A/S < .9 VNE, GW > 46000, AND ALT > 9K
14 TIME AT A/S > VNE AND GW < 33000
15 TIME AT A/S > VNE AND 33000 < GW < 40000
16 TIME AT A/S > VNE AND 40000 < GW < 46000
17 TIME AT A/S > VNE AND GW > 46000
18 TIME AT A/S > VNE AND LCST RETRACTED
19 NZ > 1.2, P > PT, AND GW < 33000
20 NZ > 1.2, P > PT, AND 33000 < GW < 40000
21 NZ > 1.2, P > PT, AND 40000 < GW < 46000
22 NZ > 1.2, P > PT, AND GW > 46000

TABLE 18 - Concluded

*FLIGHT CONDITION CATEGORY	COMPONENT(i)									
	1	2	3	4	5	6	7	8	9	10
	AFT ROTOR SHAFT P/N	AFT ROTOR PITCH SHAFT	FWD ROTOR PITCH SHAFT	AFT HUB	AFT HORIZ HINGE PIN	AFT ROTOR BLADE	AFT ROTOR BLADE SOCKET	FWD ROTOR BLADE SOCKET	AFT TIE BAR	FWD TIE BAR
23	.7750E-03	.1130E-03	0.	.2250E-03	.2250E-03	0.	.1400E-02	0.	0.	0.
24	.8090E-02	.1340E-01	.7250E-03	.1090E-01	.1090E-01	.3630E-02	.7450E-02	.3160E-02	0.	0.
25	0.	0.	0.	0.	0.	0.	0.	0.	0.	0.
26	.7170E-03	.6350E-02	.1610E-02	.5170E-03	.5170E-02	.4260E-02	.4940E-02	.1170E-02	0.	0.
27	.6050E-03	.3160E-03	0.	0.	0.	0.	.6330E-03	.4490E-03	0.	0.
28	.6080E-03	.2180E-03	0	.5260E-04	.5260E-04	.7000E-04	.5500E-03	.4910E-03	0.	0.
29	0.	0.	0.	0.	0.	0.	0.	0.	0.	0.
30	.2380E-03	.2040E-02	.2900E-04	.1080E-02	.1080E-02	.9860E-04	.1400E-02	.1790E-03	0.	0.
31	0.	0.	.2730E-02	0.	0.	.1960E-01	.3080E-04	.3300E-02	0.	0.
32	0.	0.	0.	0.	0.	0.	0.	0.	.2130E-02	.2130E-02
33	0.	0.	0.	0.	0.	0.	0.	0.	0.	0.
34	0.	0.	0.	0.	0.	0.	0.	0.	0.	0.
35	0.	0.	0.	0.	0.	0.	0.	0.	0.	0.
36	0.	0.	0.	0.	0.	0.	0.	0.	0.	0.
37	0.	0.	0.	0.	0.	0.	0.	0.	0.	0.
38	0.	.3890E-05	0.	0.	0.	0.	.7190E-05	0.	0.	0.
39	0.	0.	0.	0.	0.	0.	0.	0.	0.	0.
40	0.	0.	0.	0.	0.	0.	0.	0.	0.	0.
41	0.	0.	0.	0.	0.	0.	0.	0.	0.	0.
42	0.	0.	0.	0.	0.	0.	0.	0.	0.	0.
43	0.	0.	0.	0.	0.	0.	0.	0.	0.	0.
44	0.	0.	0.	0.	0.	0.	0.	0.	0.	0.

*FLIGHT CONDITION CATEGORY

23 NZ > 1.2, P > PT, AND GW < 33000
24 NZ > 1.2, P > PT, AND 33000 < GW < 40000
25 NZ > 1.2, P > PT, AND 40000 < GW < 46000
26 NZ > 1.2, P > PT, AND GW > 46000
27 R > RT AND GW < 33000
28 R > RT AND 33000 < GW < 40000
29 R > RT AND 40000 < GW < 46000
30 R > RT AND GW > 46000
31 LANDING GEAR TOUCHDOWN AND GW > 46000
32 ROTOR START/STOP CYCLES
33 TIME AT .9 VNE < A/S < VNE, GW < 33000 AND 0 < ALT < 5K
34 TIME AT .9 VNE < A/S < VNE, 33000 < GW < 40000, AND 0 < ALT < 5K
35 TIME AT .9 VNE < A/S < VNE, 40000 < GW < 46000, AND 0 < ALT < 5K
36 TIME AT .9 VNE < A/S < VNE, GW > 46000, AND 0 < ALT < 5K
37 TIME AT .9 VNE < A/S < VNE, GW < 33000, AND 5K < ALT < 9K
38 TIME AT .9 VNE < A/S < VNE, 33000 < GW < 40000, AND 5K < ALT < 9K
39 TIME AT .9 VNE < A/S < VNE, 40000 < GW < 46000, AND 5K < ALT < 9K
40 TIME AT .9 VNE < A/S < VNE, GW > 46000, AND 5K < ALT < 9K
41 TIME AT .9 VNE < A/S < VNE, GW < 33000, AND ALT > 9K
42 TIME AT .9 VNE < A/S < VNE, 33000 < GW < 40000, AND ALT > 9K
43 TIME AT .9 VNE < A/S < VNE, 40000 < GW < 46000, AND ALT > 9K
44 TIME AT .9 VNE < A/S < VNE, GW > 46000, AND ALT > 9K

COMPONENT LOAD MONITORING

With the CLM, flight-measured component loads are used to assess fatigue damage. This method of assessing fatigue damage is comparable to the manufacturer's analysis where component loads are related to various flight conditions. In the CLM concept, however, the recorded loads need not be associated with flight conditions since the loads are recorded on a real-time basis. Like the FCM, the CLM records elapsed time within a specified range of the component load. Consequently, the fatigue damage is again assessed on a rate basis:

$$D(I) = C(I) \cdot T(I) \qquad (1)$$

where D = damage for a given load range,
C = damage rate for the given load range, and
T = elapsed time spent in the load range.

This damage assessment is similar to the classical method of computing fatigue damage: The applied cycles (n) of the loads in the range are derived from T(I), and the damage rate (1/N) is conservatively based on the maximum load in the load range. In the ideal recorder, the monitored loads would be the critical loads of the fatigue-critical components. This, however, would require instrumentation beyond the scope of a cost-effective system. Slip rings, multiplexing equipment, and circuitry to calculate loads from recorded strains would make the recorder costs prohibitive. Since the ideal component loads recorder is not practicable, a compromise was made on the loads to be monitored to simplify the recorder and to make it feasible.

The compromise consisted of expressing the loads on the dynamic components of the helicopter rotor system as a linear function of the loads in the stationary control system. This compromise was based on the fact that the Boeing cruise guide indicator (CGI) monitors the loads on two components (fixed link and pivoting actuator) in the aft rotor fixed control system. The higher of the two loads is displayed on a cockpit indicator.[4] The dial face of the indicator is divided into three segments representing endurance limits of 0 to 100 percent, 100 to 150 percent, and 150 to 200 percent, respectively. The theory of this monitoring is that the two components sense the most critical fatigue loads in the helicopter, and therefore these loads define the allowable structural

---

[4] Brown, W.P., and Stienmann, H.H., THE CH-47C CRUISE GUIDE INDICATOR, Boeing-Vertol Division, Proceedings of the Annual National Forum of the American Helicopter Society, Preprint No. 453, presented at the 26th Annual National Forum of the American Helicopter Society, June 1970.

flight envelopes. The figures in Reference 4 exhibit a linear relationship between the percentage of endurance limit displayed on the cockpit indicator and that experienced by several of the dynamic components.

The CLM refines the CGI data. By recording the magnitude and occurrence of selected stationary control loads, the magnitude and occurrence of the loads on the fatigue-critical dynamic components can be determined. From this, the accrued fatigue damage to each dynamic component can be calculated. Assuming the linear relation of component loads, transfer functions were developed in this study by a computer program which utilized dynamic and stationary loads from the flight load surveys on the test-bed aircraft.[5],[6] A function of the following form was sought:

$$\hat{L}_R = \alpha_o + \alpha_1 L_{F1} + \ldots + \alpha_n L_{Fn} \qquad (2)$$

where $\hat{L}_R$ = approximation to the rotating component load

L_{Fn} = actual fixed component loads

α_n = coefficients which define the transfer function

The approximated loads were then used by the program to calculate component fatigue lives which were maximized with the provision that the approximation to the rotating component load be greater than or equal to the actual rotating component load; i.e.,

$$\hat{L}_R \geq L_R \qquad (3)$$

The computer program entitled CLMMOD whose technique and procedure are discussed in Appendix B was used to determine the transfer functions. The transfer functions for the UH-1H components were based on 170 flight conditions reported in Reference 5. The 170 flight conditions were selected because they produced fatigue damage on at least one of the components. Similarly, the transfer functions for the CH-47C components were based on 217 flight conditions reported in Reference 6. Since only the

---

[5] Garrison, J., LOAD LEVEL TEST OF UH-1D HELICOPTER IN 48-FOOT DIAMETER MAIN ROTOR CONFIGURATION, VOLS III AND IV, Bell Helicopter; Report No. 205-099-049, April 1964.

[6] Hartman, L.J., CH-47C STRESS AND MOTION SURVEY, Boeing-Vertol Division; Report No. 114 FT-708, April 1969.

maximum load for each component was reported, it was assumed that the reported loads occurred simultaneously during the flight condition.

After the transfer functions were established, the rotating component loads were approximated for the respective loads, and retirement lives were computed from the approximated loads. The resulting retirement lives, however, were not acceptable for most of the components analyzed. The acceptability of the computed retirement lives was determined by the function error (E) computed as follows:

$$E = 1 - \frac{\text{approximate retirement life}}{\text{actual retirement life}} . \qquad (4)$$

The function error for the unacceptable retirement lives was close to unity, indicating a large error in the computation. A function error of zero indicated very small errors in the computation.

The results of the CLMMOD analysis for the UH-1H helicopter are presented in Table 19. The components considered were the main rotor blade, main rotor grip, main rotor drag brace, main rotor yoke, main rotor stabilizer bar, main rotor pitch horn, swashplate support, and collective lever. The constants, α_n, are shown in the table along with the value of the function error. Only the swashplate support and collective lever show function errors of zero, indicating acceptable fatigue lives. Since the actual retirement life of each component was based on the collective lever loads, the transfer function was unity. Therefore, the approximate and actual loads and retirement lives were the same.

The results of the CLMMOD analysis for the CH-47C are shown in Table 20. Only the aft rotor pitch link was selected for analysis because this component was expected to yield the best results. Good results were also expected because of the Reference 4 correlation of pitch link loads and several stationary component loads. In addition, the reported linear relationship agrees with the previously stated assumption. Six tests of pitch link load versus stationary component loads were run, including the combination of the component loads cited in Reference 4. In all tests, the function error was nonzero, indicating that the approximate retirement lives are unacceptable.

Accordingly, since it was concluded that the CLM technique would not produce acceptable retirement lives for any of the UH-1H or CH-47C components, the technique was judged technically unfeasible and its further study was curtailed.

TABLE 19. RESULTS OF COMPONENT LOADS MONITORING MODEL (CLMMOD) FOR THE UH-1H

	Monitored Loads	DYNAMIC COMPONENT LOADS								
		MR Blade	MR Grip	Drag Brace	MR Yoke	S/P Support	Coll. Lever	Stab. Bar	Pitch Horn	Scissors
α_0		.468E+04	.863E+03	.348E+04	.988E+04	.000E-00	.000E-00	.229E+01	-.186E+03	.118E+03
α_1	R. Cyc. Cont Tube (Mean)	.181E+01	.691E-01	-.158E-00	-.163E+01	.000E-00	.000E-00	-.116E-00	.162E-00	.185E-00
α_2	R. Cyc. Cont. Tube (Osc.)	.436E-01	.104E+01	.299E+01	.650E+01	.000E-00	.000E-00	-.109E-00	-.649E-00	-.136E-00
α_3	L. Cycl. Cont. Tube (Mean)	-.106E+01	-.640E-00	-.202E+01	-.204E+01	.000E-00	.000E-00	-.257E-00	-.105E-01	-.445E-01
α_4	L. Cyc. Cont. Tube (Osc.)	.315E+01	.792E-00	.196E+01	.143E+01	.000E-00	.000E-00	.147E+01	-.200E-00	.243E-00
α_5	Coll. Cont. Tube (Mean)	-.653E+01	-.192E+01	-.514E+01	-.669E+01	.000E-00	.000E-00	-.153E+01	.858E-00	.261E-00
α_6	Coll. Cont. Tube (Osc.)	.323E-00	.697E-01	.102E+01	.282E+02	.100E+01	.100E+01	.312E-00	.166E+01	.519E-00
α_7	C.G. Vert. Accel. (G)	.285E+04	.729E+03	.263E+04	.775E+04	.000E-00	.000E-00	.826E+03	.835E+03	.140E+03
	Function Error	.995E-00	.971E-00	.996E-00	.994E-00	.000E-00	.000E-00	.949E-00	.838E-00	.594E-00

The Load approximation for each dynamic component load has the form:

Dynamic Component Load = α_0 + α_1 *(R.CYC.CONT.TUBE LOAD-MEAN) + α_2 *(R.CYC.CONT.TUBE LOAD-OSC.)
+ α_3 *(L.CYC.CONT.TUBE LOAD-MEAN) + α_4 *(L.CYC.CONT.TUBE LOAD-OSC.)
+ α_5 *(COLL.CONT.TUBE LOAD-MEAN) + α_6 *(COLL.CONT.TUBE-OSC.)
+ α_7 *(CG VERT.ACCEL-G)

TABLE 20. RESULTS OF COMPONENT LOADS MONITORING MODEL (CLMMOD) FOR THE CH-47C AFT PITCH LINK

Test Case	α_0	α_1	α_2	α_3	Error Function
1	.296E+04	.238E-00	.000E-00	.000E-00	.929E-00
2	.301E+04	.000E-00	.542E-00	.000E-00	.949E-00
3	.489E+04	.000E-00	.000E-00	-.154E-00	.983E-00
4	.250E+04	.219E+02	.160E-00	.000E-00	.894E-00
5	.123E+04	.812E+02	.000E-00	-.296E-00	.944E-00
6	.348E+04	.000E-00	.343E-00	.102E-00	.955E-00

The load approximation for each test case has the form:

Pitch Link Load = α_0 + α_1 (Swiv Act Load)
+α_2 (Fixed Link Load) + α_3 (Pivot Act Load)

DIRECT MONITORING

The DM method uses data gathered on various fatigue-related phenomena to assess fatigue damage. The phenomena include the change in metal conductivity due to cold-working, the acoustic emission of metals under stress, and the change in magnetic field strength as a result of fatigue loads. Unlike the FCM and CLM methods, the DM method empirically associates the monitored data with the accrued fatigue damage. This association would therefore be determined through tests of full-scale components measuring both the monitored data and the accrued component fatigue damage. From these tests, the criteria for retirement life projection and component removal would be established in terms of the monitored data.

Since the DM methods require empirical definition, they cannot be evaluated in terms of extended retirement lives for the components of the test-bed aircraft. However, the applicability of the DM methods for assessing component fatigue damage is discussed in Appendix A for all the DM methods - resistance change (as typified by the annealed foil fatigue gage), acoustic emission, and inductance testing - and is summarized in the following paragraphs.

The annealed foil fatigue gage has shown promise as a passive fatigue damage indicator. However, since currently available gages lack consistency in their responses, a given percentage of resistance change cannot be correlated with the actual fraction of the fatigue life expended for a component outside the controlled laboratory environment.

The monitoring of acoustic emission during periodic proof stressing provides a means of detecting the presence and growth of fatigue cracks. Good results have been obtained in controlled situations where the damaging loads and the proof loads are applied similarly. However, to proof-load components of a helicopter rotor system equivalent to the complex loads experienced during flight could require new hardware or disassembly of the system. Additionally, impending fatigue failure has been successfully detected only for materials exposed to low-cycle fatigue and not for high-cycle fatigue typically encountered in helicopter components.

Inductive sensing was shown to be capable of detecting microcracks in metals. Wherever cracks propagated normal to the surface of beam specimens were detected early, cracks propagated parallel to the surface of roll specimens were detected much later. Although the tests have indicated that an inductive sensing system is of some value in detecting metal fatigue during vibratory beam tests, a model has not been developed to analytically predict signal amplitudes as a function of either the number of fatigue cycles or the crack propagation rate. Additionally, the degree of uncertainty is high whenever the first signal encountered is of high amplitude. It is therefore difficult to predict the remaining fatigue life by comparing such laboratory data with that taken by relatively continuous monitoring. Therefore, inductive sensing cannot be considered a satisfactory means of monitoring the fatigue life of helicopter components.

MISSION TYPE MONITORING

With the MTM concept, the functional assignment of each helicopter is used to assess the fatigue damage to the fatigue-critical components. Table 21 lists the functional assignments for Army helicopters in the alphabetical order of their three-letter codes. The functional assignment of each aircraft is monitored in the Reliability and Maintainability Management Improvement Techniques (RAMMIT) Reporting System by aircraft serial number. The assignments are reported monthly in the Chronological, Historical Aircraft Ownership Summary (CHAOS) report. The fatigue damage to the fatigue-critical components is assessed according to the flight time spent by the aircraft in each functional assignment (FA). This time is also reported in the CHAOS report. The damage would be assessed similarly as in the FCM method; that is, damage is computed as the product of flight time and a theoretical damage rate for the functional assignment under consideration:

$$D = T_N \cdot C_N \qquad (5)$$

where D = damage to the component under consideration

T_N = time spent in the functional assignment N

C_N = theoretical damage rate for the functional assignment N

TABLE 21. LISTING OF FUNCTIONAL ASSIGNMENT OF HELICOPTERS

Code	Functional Assignment	Typical Distribution % of Fleet UH-1H	CH-47C
AGA	Combat Mission - Active Army	47.1	44.5
AGB	Direct Combat Training - Active Army	1.0	1.1
AGE	Combat Mission - Reserve Forces	3.1	-
AGF	Direct Combat Training - Reserve Forces	-	-
BGC	Direct Combat Support - Active Army	15.8	29.5
BGG	Direct Combat Support - Reserve Forces	1.4	-
BGI	Direct Combat Training - ARADCOM	-	-
BGJ	Direct Combat Support - ARADCOM	0.6	-
CFB	Indirect Logistical Support	-	-
CIC	Executive Transport	2.5	-
CID	Proficiency Flight Time	.4	-
CIF	Weather Service	-	-
CIG	Photographic and Survey	.1	-
CIH	Aeromedical	.5	-
CIJ	Intelligence and Classified Projects	-	-
CIK	Attaches, Missions and MAGG	.1	-
CIL	Special Missions	1.9	-
D1IA	Flight Training	7.6	1.1
D2IA	Technical Operations and Maintenance Training	.4	1.6
D3IA	Training Support	.9	-
LIL	Test and Evaluation	.6	2.7
GIL	Test Support	1.4	-

This damage assessment requires that a theoretical damage rate be determined for each of the functional assignments identified in Table 21. To determine the theoretical damage rates requires such information as the definition of typical mission profiles for each functional assignment, the frequency of occurrence of flight conditions for the mission profiles, and the corresponding component loads. Since information on mission profiles and flight condition frequencies for each functional assignment was not available, the theoretical damage rates for the functional assignments were not calculated. Rather, an alternative means of gathering mission-type information was considered where theoretical damage rates could be determined.

The alternative MTM method was based on the mission segment (MS) concept which assumes that the mission profile can be subdivided into several segments, for example, ascent, steady state, maneuver, and descent. Fatigue damage to the components, therefore, can be assessed for the flight time spent in the various mission segments:

$$D = C_A \cdot T_A + C_S \cdot T_S + C_M \cdot T_M + C_D \cdot T_D \qquad (6)$$

where D = fatigue damage to the component under consideration

C_i = theoretical damage rate for the ith mission segment

T_i = flight time in the ith mission segment

A,S,M,D = mission segment ascent, steady state, maneuvers, descent

As in the FCM method, the theoretical damage rates can be determined by considering the flight conditions that the mission segments would include. A single test case was developed by using the manufacturer's design data (Reference 1). The flight conditions were assigned to the mission segments as shown in Table 22. The resulting theoretical damage rates are presented in Table 23.

TABLE 22. ASSIGNMENT OF FLIGHT CONDITIONS TO MISSION SEGMENTS

Flight Condition		Mission Segment
I	Ground Conditions	Ground
II	Power-On Flight	
A	Vertical T/O	Ascent
B	Hover	Hover
C	Norm Accel	Ascent
D	Norm Decel	Descent
E	Max Accel	Ascent
F	Max Decel	Descent
G	Sideward Flt	Steady
H	Rearward Flt	Steady
I	Full Pwr Climb	Ascent
J	Fwd Level Flt	Steady
K	Part Pwr Des	Descent
L,M	Turns	Maneuver
N,O	Pull-ups	Maneuver
P	Control Rev	Maneuver
Q	Norm Land	Descent
III	Transition	
A	Power to Auto	Descent
B	Auto to Power	Ascent
IV	Autorotation	
A	Steady Forward Flight	Steady
B	60 Kn Control Reversal	Maneuver
C,D	Turns	Maneuver
E	Autorotation Landing/Pwr Rec	Descent
F	Full Auto Landing	Descent

TABLE 23. DAMAGE RATES, C_{ij}, FOR UH-1H MTM SYSTEM MS

MISSION SEGMENT CATEGORIES	COMPONENT(i)									
	1	2	3	4	5	6	7	8	9	10
	MAIN ROTOR RETENTION STRAP	MAIN ROTOR YOKE	STABILIZER BAR	MAIN ROTOR DRAG BRACE	SWASHPLATE SUPPORT	COLLECTIVE LEVER	MAIN ROTOR PITCH HORN	MAIN ROTOR SCISSORS	MAIN ROTOR GRIP	MAIN ROTOR BLADE
0	.3200E-01	0.	0.	0.	0.	0.	0.	0.	0.	0.
1	0.	0.	0.	0.	.1178E-03	.1164E-03	.2222E-04	.4171E-04	0.	.8750E-03
2	0.	0.	0.	0.	0.	0.	0.	0.	0.	.4836E-04
3	0.	.2687E-02	0.	.8906E-02	.4508E-02	.3892E-02	.4109E-02	.6610E-02	.7337E-03	.2066E-02
4	0.	0.	.1086E-01	0.	.3244E-02	.2749E-02	0.	.1379E-03	.1881E-03	.4163E-02
5	0.	0.	0.	.3060E-03	0.	0.	0.	0.	.4261E-05	.2628E-03

Each of the MTM methods presented here has its advantages and disadvantages. The functional assignment technique is an extremely simple monitoring method. Since the CHAOS report of the RAMMIT system already monitors the functional assignment and flight time of each aircraft, the functional assignment method requires no on-board recording. Rather, a system which interfaces with the RAMMIT system is all that is necessary to monitor the fatigue damage. The interfacing system would call out the appropriate information (functional assignment code and flight time), apply the theoretical damage rates (once determined) to the flight time, and report the assessed fatigue damage to the appropriate serialized components. The flight time for the aircraft and the fatigue damage to the serialized components would be correlated in a component status file. This file would be maintained by the composite 2410/2407 file of the RAMMIT system, which monitors component change information. The entire system, therefore, could be developed by interfacing a new file with the current RAMMIT system. The disadvantage of the functional assignment method is the identification of theoretical damage rates for the functional assignments. A detailed recording program on sample aircraft would be required to identify the mission profile of each functional assignment. The theoretical damage rate would then be calculated according to the sample data, and then applied to all the aircraft in the particular functional assignment. Consequently, the theoretical damage rate will be a function of the missions flown by the sample aircraft and will only be as representative of the functional assignment as these missions allow.

The mission segment method requires an on-board recorder to identify the flight time accrued in each of the mission segments. Although the resultant monitoring will be more complex than that in the functional assignment method, the recording will provide better information for fatigue damage assessment. In addition, theoretical damage rates can be identified for the mission segment method, as previously discussed. The definition of theoretical damage rates permits evaluating this method for technical acceptability; this evaluation capability gives the mission segment method an advantage over the functional assignment method. The disadvantage of the mission segment method is its increased complexity and, therefore, its increased cost.

EVALUATION OF METHODS

EVALUATION CRITERIA

To test the technical acceptability of the various monitoring systems, a usage spectrum which represented the composite fleet operation was derived. Because of the difficulty in formulating a single composite spectrum representative of the entire fleet operation, and because of the difficulties of trying to vary fleet operations to determine the monitoring system sensitivity to spectrum variations, three representative spectra were defined. These spectra portrayed a mild, normal, and severe utilization of the two helicopter models; for both models, these spectra were defined not as the worst-case usage, but rather as representative of a severe or mild utilization which might be expected to occur with some regularity. Weighting factors, which approximate the distribution of the usage spectra among the fleet, were also defined. Consequently, each spectrum and its weighting factor form an approximation of the utilization of each fleet of helicopters.

This approach (using three usage spectra of varying degrees of severity and associated weighting factors to approximate average fleet usage) allowed for an estimate of the sensitivity of each candidate monitoring system to usage spectrum variations. Therefore, a candidate monitoring system which is technically acceptable for the average fleet usage could also be tested for the severe usage without forming a separate spectrum by simply varying the weighting factors. In this manner, the monitoring system could be evaluated for the entire range of usage.

The three spectra for each helicopter class were generated similarly by using data obtained from various operational surveys[7,8,9]. Since both the UH-1H and CH-47C helicopters are used in the direct combat support function for a large percentage of their operational life, the data from these references provide a representative base from which to derive the required test usage spectra. The test usage spectra were developed by distributing the flight time from the operational surveys in various flight conditions.

---

[7] Johnson, Raymond B., Clay, Larry E., and Meyers, Ruth E., OPERATIONAL USE OF UH-1H HELICOPTERS IN SOUTHEAST ASIA, Technology Incorporated, Dayton, Ohio; USAAMRDL Technical Report 73-15, U.S. Army Air Mobility Research and Development Laboratory, Fort Eustis, Virginia, May 1973, AD764260.

The distribution of the flight time was based on the assumption that each flight condition can be described as having a particular combination of flight-measured parameters such as airspeed, altitude, rate of climb, torque, and normal acceleration. Since References 7 through 9 present tables of time in concurrent ranges of measured parameters, the tables could be divided so that time in each block was related to a flight condition.

As an example, the tables of rate of climb versus torque permitted determining the time in steady level flight, accelerated flight, full-power climb, partial power descent, and decelerating flight. By cross-referencing with tables of airspeed versus torque, a further division can be made into hover and forward flight. By working such a division among the times in each flight parameter table and performing all multiple correlations as necessary to obtain fine divisions, a flight spectrum was derived. This spectrum was defined as the severe spectrum. The normal and mild spectra were derived by modifying the severe spectrum so that those conditions which would contribute significant fatigue damage were reduced in occurrence. In general, the normal and mild spectra reflected larger cruise times and less maneuvers. It should again be noted that the terms "severe spectrum" and "mild spectrum" are not intended to convey the impression of the worst or best usage to which the particular fleet might be exposed. Rather, these terms are used in this study to describe the two extremes to which a reasonable percentage of the fleet might be exposed.

Tables 24 and 25 present the three test spectra and the design spectrum for the UH-1H and CH-47C helicopters, respectively. The three representative spectra will be used to establish upper bounds on component life for various selected critical components.

---

[8] Giessler, F. Joseph, and Braun, Joseph F., FLIGHT LOADS INVESTIGATION OF COMBAT ARMED AND ARMORED CH-47A HELICOPTERS OPERATING IN SOUTHEAST ASIA, Technology Incorporated, Dayton, Ohio; USAAVLABS Technical Report 68-1, U. S. Army Aviation Materiel Laboratories, Fort Eustis, Virginia, March 1968, AD671672.

[9] Giessler, F. Joseph, and Braun, Joseph F., FLIGHT LOADS INVESTIGATION OF CARGO AND TRANSPORT CH-47A HELICOPTERS OPERATING IN SOUTHEAST ASIA, Technology Incorporated, Dayton, Ohio; USAAVLABS Technical Report 68-2, U.S. Army Aviation Materiel Laboratories, Fort Eustis, Virginia, April 1968, AD672842.

TABLE 24. UH-1H USAGE SPECTRA

	Design	Mild	Normal	Severe
I. Ground				
A. Normal Start	.500	.250	.500	.75
B. Normal Shutdown	.500	.250	.500	.75
II. Power-On Flight				
A. Vertical Takeoff	.400	1.000	1.500	1.000
B. Hover I.G.E.				
1. Steady	3.290	2.000	2.500	1.000
2. Right Turn	.100	.080	.230	.500
3. Left Turn	.100	.080	.240	.500
4. Control Reversal				
a. Longitudinal	.010	.005	.010	.020
b. Lateral	.010	.005	.010	.020
c. Rudder	.010	.005	.010	.010
C. Normal Acceleration	1.000	.500	1.000	1.500
D. Normal Deceleration	1.000	.500	1.000	1.500
E. Max. Rate Acceleration	.250	.150	.200	.500
F. Max. Rate Deceleration	.250	.150	.200	.500
G. Sideward				
1. Right	.250	.100	.200	.250
2. Left	.250	.100	.200	.250
H. Rearward	.250	.050	.250	.300
I. Full Power Climb	4.000	4.000	5.000	5.000
J. Fwd Level Flight				
1. 0.2 V_{ne}	1.000	.300	.500	.500
2. 0.3	1.000	.500	.800	.500
3. 0.4	2.000	1.200	1.200	1.000
4. 0.5	3.000	4.600	3.800	4.000
5. 0.6	7.000	19.500	13.500	6.000
6. 0.7	8.000	32.500	26.300	13.3
7. 0.8	15.000	20.500	21.000	22.800
8. 0.9	25.000	4.460	9.100	16.200
9. V_{ne}	15.000	.400	1.200	10.000
K. Partial Power Descent	1.000	3.000	3.000	3.000
L. Right Turn				
1. 0.3 V_H	.500	.200	.200	.200
2. 0.6 V_H	1.000	.500	.800	.900
3. 0.9 V_H	.500	.200	.350	.400
M. Left Turn				
1. 0.3 V_H	.500	.200	.200	.200
2. 0.6 V_H	1.000	.500	.800	.900
3. 0.9 V_H	.500	.200	.350	.400
N. Cyclic Pull-Up				
1. 0.6 V_H	.200	.030	.070	.150
2. 0.9 V_H	.050	.010	.015	.030
O. Collective Pull-Up				
1. 0.6 V_H	.200	.030	.070	.150
2. 0.9 V_H	.050	.010	.015	.030
P. 0.9 V_H Cont. Reversal				
1. Longitudinal	.050	.005	.010	.015
2. Lateral	.050	.005	.010	.015
3. Rudder	.050	.005	.010	.020
Q. Normal Landing				
1. 6500 lb	.100	.200	.300	.200
2. 7500 lb	.300	.250	.300	.350
3. 8500 lb	.450	.300	.350	.550
4. 9500 lb	.150	0	.050	.100
III. Transitions				
A. Power to Auto				
1. 0.3 V_H	.100	.015	.050	.070
2. 0.6 V_H	.200	.030	.100	.140
3. 0.9 V_H	.050	.015	.050	.070

TABLE 24 - Concluded

	Design	Mild	Normal	Severe
B. Auto to Power				
1. 0.4 V_H	.100	.015	.050	.070
2. 0.6 V_H	.200	.030	.100	.140
3. 0.8 V_H	.050	.015	.050	.070
IV. Autorotation				
A. Steady				
1. 0.4 V_H	.800	.100	.250	.500
2. 0.6 V_H	1.000	.300	.500	1.000
3. 0.8 V_H	.200	.100	.250	.500
B. 60 Kt. Control Rev.				
1. Longitudinal	.010	.005	.008	.010
2. Lateral	.010	.005	.008	.010
3. Rudder	.010	.005	.008	.010
C. Right Turn				
1. 0.4 V_H	.200	.030	.090	.150
2. 0.6 V_H	.250	.090	.150	.250
3. 0.8 V_H	.050	.020	.040	.050
D. Left Turn				
1. 0.4 V_H	.200	.030	.090	.150
2. 0.6 V_H	.250	.090	.150	.250
3. 0.8 V_H	.050	.020	.040	.050
E. Auto Landing Appr. with Pwr Recovery				
1. 0.4 V_H	.080	.005	.026	.050
2. 0.6 V_H	.100	.020	.050	.080
3. 0.8 V_H	.020	.010	.015	.020
F. Full Autorotation Ldg.	.250	.050	.075	.100

TABLE 25. CH-47C USAGE SPECTRA

GW: 27,000 lb Alt: 0-6,000 ft

Flight Condition	Percent Flight Time			
	Design	Mild	Normal	Severe
Hover	1.980	.920	1.310	1.410
Transition	2.970	2.310	2.630	2.640
70% V_{ne}	4.950	14.770	10.950	9.140
90% V_{ne}	3.960	3.230	3.720	3.510
100% V_{ne}	3.960	1.150	2.190	2.990
Exceed V_{ne}	1.980	.690	1.100	1.410
Landing Flare	1.320	.290	.370	.510
Left Turn	1.610	1.350	1.420	1.430
Right Turn	1.610	.750	1.391	1.430
Collective Pull-Up	.120	.045	.043	.043
Longitudinal Pull-Up	.040	.042	.043	.043
Longitudinal Reversal	.170	.030	.070	.090
Lateral Reversal	.180	.020	.050	.065
Directional Reversal	.140	.020	.020	.035

TABLE 25 - Continued

GW: 27,000 lb — Alt: 6,000 ft-10,000 ft

Flight Condition	Design	Percent Flight Time Mild	Normal	Severe
Hover	1.670	.740	1.050	1.120
Transition	2.510	1.850	2.100	2.110
70% V_{ne}	4.180	11.820	8.760	7.310
90% V_{ne}	3.350	2.580	2.980	2.810
100% V_{ne}	3.350	.920	1.750	2.390
Exceed V_{ne}	1.670	.550	.880	1.120
Landing Flare	.000	.230	.290	.410
Left Turn	1.360	.600	1.140	1.140
Right Turn	1.360	.600	1.105	1.140
Collective Pull-Up	.100	.036	.035	.036
Longitudinal Pull-Up	.030	.035	.035	.036
Longitudinal Reversal	.140	.020	.050	.060
Lateral Reversal	.150	.020	.040	.048
Directional Reversal	.120	.010	.090	.100

GW: 27,000 lb — Alt: 10,000 ft +

Flight Condition	Design	Percent Flight Time Mild	Normal	Severe
Hover	.420	.180	.260	.280
Transition	.630	.460	.530	.530
70% V_{ne}	1.050	2.950	2.190	1.830
90% V_{ne}	.840	.650	.740	.700
100% V_{ne}	.840	.230	.440	.600
Exceed V_{ne}	.420	.140	.220	.280
Landing Flare	.000	.060	.070	.100
Left Turn	.340	.150	.280	.290
Right Turn	.340	.180	.157	.218
Collective Pull-Up	.020	.009	.009	.012
Longitudinal Pull-Up	.010	.005	.009	.012
Longitudinal Reversal	.030	.010	.010	.030
Lateral Reversal	.040	.004	.010	.030
Directional Reversal	.030	.003	.010	.020

TABLE 25 - Continued

GW: 33,000 lb Alt: 0-6,000 ft

Flight Condition	Design	Percent Flight Time		
		Mild	Normal	Severe
Hover	.990	.460	.660	.700
Transition	1.490	1.150	1.310	1.320
70% V_{ne}	2.480	7.380	5.480	4.570
90% V_{ne}	1.980	1.620	1.860	1.760
100% V_{ne}	1.980	.580	1.100	1.490
Exceed V_{ne}	.990	.532	.880	.895
Landing Flare	.660	.140	.180	.260
Left Turn	.810	.380	1.313	.710
Right Turn	.810	.380	.715	.710
Collective Pull-Up	.060	.023	.022	.030
Longitudinal Pull-Up	.020	.011	.022	.036
Longitudinal Reversal	.080	.010	.030	.035
Lateral Reversal	.090	.010	.020	.080
Directional Reversal	.070	.010	.020	.030

GW: 33,000 lb Alt: 6,000 ft - 10,000 ft

Flight Condition	Design	Percent Flight Time		
		Mild	Normal	Severe
Hover	.840	.370	.530	.560
Transition	1.260	.920	1.050	1.050
70% V_{ne}	2.090	5.910	4.380	3.650
90% V_{ne}	1.670	1.290	1.490	1.410
100% V_{ne}	1.670	.460	.880	1.190
Exceed V_{ne}	.840	.280	.440	.560
Landing Flare	.000	.120	.150	.210
Left Turn	.680	.300	.570	.570
Right Turn	.680	.300	.559	.570
Collective Pull-Up	.050	.018	.017	.041
Longitudinal Pull-Up	.020	.009	.017	.039
Longitudinal Reversal	.070	.010	.030	.060
Lateral Reversal	.070	.010	.020	.060
Directional Reversal	.060	.010	.040	.044

TABLE 25 - Continued

GW: 33,000 lb Alt: 10,000 ft +

Flight Condition	Design	Percent Flight Time		
		Mild	Normal	Severe
Hover	.210	.090	.130	.140
Transition	.310	.230	.260	.260
70% V_{ne}	.520	1.480	1.100	.910
90% V_{ne}	.420	.320	.370	.350
100% V_{ne}	.420	.120	.220	.300
Exceed V_{ne}	.210	.070	.122	.217
Landing Flare	.000	.030	.040	.050
Left Turn	.170	.080	.140	.140
Right Turn	.170	.080	.110	.140
Collective Pull-Up	.010	.005	.004	.006
Longitudinal Pull-Up	.004	.002	.004	.006
Longitudinal Reversal	.020	.002	.010	.010
Lateral Reversal	.020	.002	.005	.020
Directional Reversal	.010	.001	.002	.010

GW: 46,000 lb Alt: 0-6,000 ft

Flight Condition	Design	Percent Flight Time		
		Mild	Normal	Severe
Hover	1.010	.810	1.150	1.233
Transition	1.520	1.497	1.858	2.050
70% V_{ne}	2.530	10.926	6.227	8.000
90% V_{ne}	2.030	2.830	3.260	3.080
100% V_{ne}	2.030	1.010	1.920	2.610
Exceed V_{ne}	1.010	.610	.624	1.230
Landing Flare	.390	.250	.320	.360
Left Turn	.820	.660	1.240	1.250
Right Turn	.820	.660	.930	1.250
Collective Pull-Up	.060	.040	.038	.053
Longitudinal Pull-Up	.020	.020	.031	.047
Longitudinal Reversal	.080	.030	.078	.078
Lateral Reversal	.090	.020	.040	.140
Directional Reversal	.070	.010	.090	.110

TABLE 25 - Concluded

GW: 46,000 lb Alt: 6,000 ft - 10,000 ft

Flight Condition	Design	Percent Flight Time		
		Mild	Normal	Severe
Hover	1.050	.120	.160	.180
Transition	1.570	.290	.330	.330
70% V_{ne}	2.620	1.840	1.192	2.052
90% V_{ne}	2.090	.400	.460	.440
100% V_{ne}	2.090	.140	.270	.370
Exceed V_{ne}	1.050	.090	.140	.180
Landing Flare	.000	.040	.050	.060
Left Turn	.850	.090	.180	.360
Right Turn	.850	.090	.130	.135
Collective Pull-Up	.060	.006	.005	.008
Longitudinal Pull-Up	.020	.003	.005	.008
Longitudinal Reversal	.090	.003	.010	.020
Lateral Reversal	.090	.002	.010	.020
Directional Reversal	.070	.002	.005	.020

Having developed test spectra for each helicopter, weighting factors were derived to account for the variability of usage within the fleet. These weighting factors approximate the fraction of the fleet which experiences any one of the three spectra. In developing these factors, two considerations were included: first, the knowledge of helicopter assignment among the various usage categories, and second, a knowledge of the distribution of usage severity within each category. From these two considerations, a weighting factor for each usage category may be derived according to the following equation:

$$F_i = \sum_j A_{ij} B_j \qquad (7)$$

where F_i = weighting factor for the ith spectrum

A_{ij} = proportion of time in the ith spectrum for helicopters in the jth mission

B_j = proportion of helicopters in the jth mission

Values of the A_{ij} factor were obtained from a survey of the usage of helicopters in each mission category. The values were estimated from a review of operational data presented in various documents, including References 7 through 9. The A_{ij} for each spectrum for the general mission category of combat assault, direct combat support, training and testing, and miscellaneous are presented in Table 26 for the UH-1H and CH-47C helicopters. For any given mission category, the sum of the values equals one.

TABLE 26. A_{ij} FOR THE UH-1H AND CH-47C

		Mission			
Helicopter	Usage Severity	Combat Assault	Direct Combat Support	Training and Testing	Misc.
UH-1H	Mild	0.20	0.30	0.20	0.70
	Normal	0.50	0.60	0.60	0.20
	Severe	0.30	0.10	0.20	0.10
CH-47C	Mild	0.16	0.31	0.08	0.20
	Normal	0.45	0.56	0.67	0.60
	Severe	0.39	0.13	0.25	0.20

The B_j factor was obtained from fleet assignment information[10,11]. The distribution of fleet assignment for the last 6 years was plotted and then projected into the future to determine approximate values for B_j. The frequency distribution for the B_j's by year and the future projection are presented in Figures 3 and 4 for the UH-1H and CH-47C helicopters, respectively. The projected values of B_j for each helicopter are presented in Table 27.

The weighting factor, F_i, was calculated from the A_{ij} and B_j factors for each of the test spectra by using Equation 7. The resulting weighting factors for each helicopter are presented in Table 28.

---

[10] AIRCRAFT OPERATIONAL UTILIZATION - UH-1H FLEET, Directorate for Product Assurance, U.S. Army Aviation Systems Command, St. Louis, Missouri.

[11] AIRCRAFT OPERATIONAL UTILIZATION - CH-47B,C FLEET, Directorate for Product Assurance, U.S. Army Aviation Systems Command, St. Louis, Missouri.

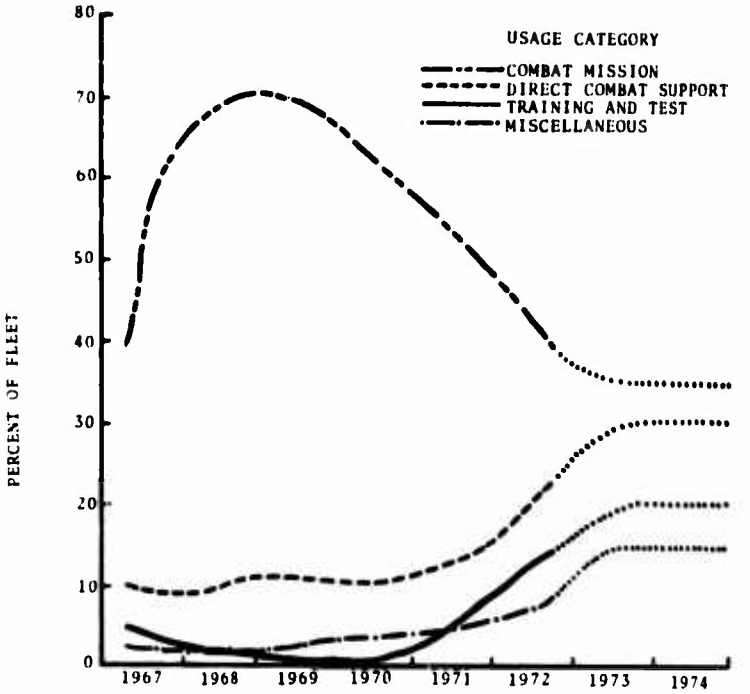

Figure 3. UH-1H Mission Frequency Distribution.

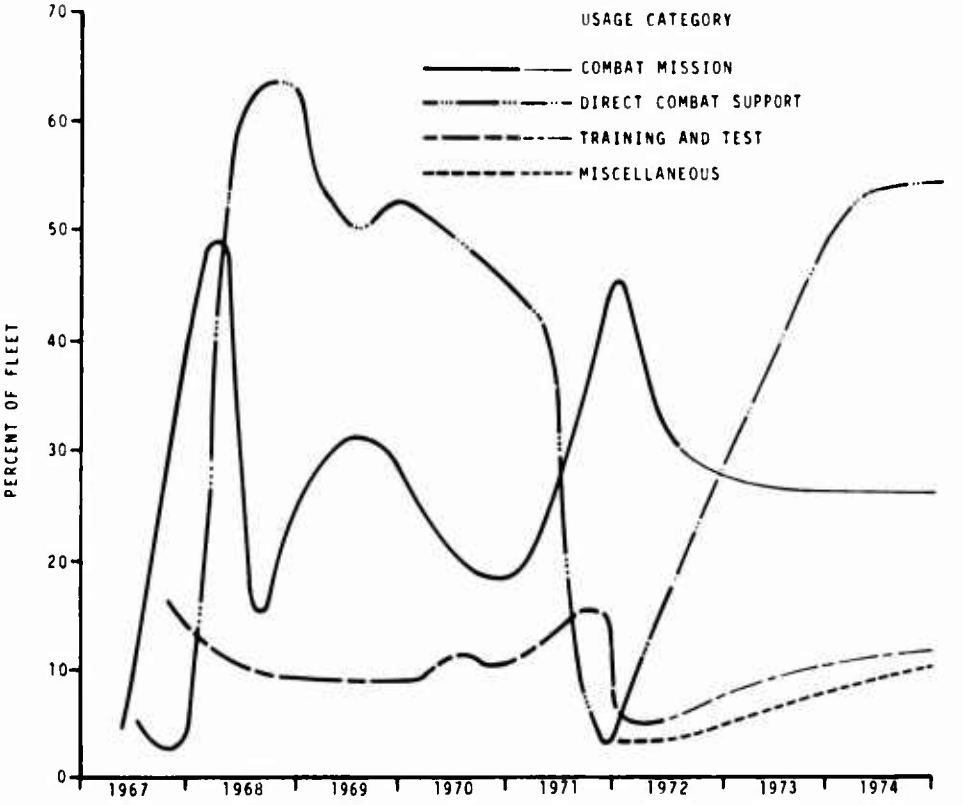

Figure 4. CH-47C Mission Frequency Distribution.

TABLE 27. PROJECTED B_j FOR THE UH-1H AND CH-47C

Helicopter	Mission Assignment	Projected B_j
UH-1H	Combat Assault	0.35
	Direct Combat Support	0.30
	Training and Testing	0.20
	Miscellaneous	0.15
CH-47C	Combat Assault	0.31
	Direct Combat Support	0.52
	Training and Testing	0.12
	Miscellaneous	0.05

TABLE 28. WEIGHTING FACTORS FOR THE UH-1H AND CH-47C

Helicopter	Usage Spectrum	Weighting Factor
UH-1H	Mild	0.31
	Normal	0.50
	Severe	0.19
CH-47C	Mild	0.23
	Normal	0.54
	Severe	0.23

Critical high cost dynamic components of the UH-1H and CH-47C helicopters were reviewed and selected on the basis of their impact on the life-cycle cost of each helicopter. The selection of components was based on the cost per helicopter for component acquisition, spares acquisition, spares inventory, and component removal and replacement. The selected components for each helicopter, together with quantity per helicopter, calculated replacement time, and recommended replacement time, are presented in Tables 29 and 30. The calculated replacement time is the number of hours computed in the manufacturer's substantiation analysis. The recommended replacement time is the number of hours that the manufacturer recommends for the actual replacement of components. Only nine components were identified on the UH-1H helicopter, because the components in the tail rotor system could not be considered in this study. These components were eliminated because of the large variation between the calculated and recommended replacement times.

TABLE 29. SELECTED FATIGUE-CRITICAL COMPONENTS FOR THE UH-1H

Component	Quantity	Replacement Lives	
		Manufacturer Calculated	U.S. Army Recommended
Main Rotor			
Blade	2	2958	2500
Drag Brace	2	3716	3300
Yoke	1	14628	5000
Pitch Horn	2	7080	3300
Scissors	2	4247	3300
Stabilizer Bar	1	6795	3300
Retention Strap	2	3099	2200
Swashplate Support	1	5173	3300
Collective Lever	1	5966	3300

TABLE 30. SELECTED FATIGUE-CRITICAL COMPONENTS FOR THE CH-47C

Component	Quantity	Replacement Lives	
		Manufacturer Calculated	U.S. Army Recommended
Aft Rotor			
Shaft	1	3680	3600
Hub	1	9790	UL*
Horizontal Pin	3	9790	2280
Blade Socket	3	4490	4000
Tie Bar	3	2400	2400
Blade	6	4400	4000
Pitch Shaft	3	3820	3800
Forward Rotor			
Blade Socket	3	6600	6000
Tie Bar	3	2400	2400
Pitch Shaft	3	8340	3800

* UL - Unlimited Life

Limits (bounds) were then established for the usage of the components. The recommended retirement life, the most severe usage expected, was considered the lower limit. Then the three test spectra were used in a substantiation analysis to establish the upper limits for mild, normal, and severe

usage. Then these bounds served as the criteria for evaluating the recording systems. Essentially, the fatigue assessment model for each recording system must predict the component fatigue lives between the upper and lower limits for each of the three test spectra. Tables 31 and 32 present the upper and lower bounds for the UH-1H and CH-47C helicopter components, respectively.

TABLE 31. UPPER AND LOWER BOUNDS FOR UH-1H COMPONENTS

Component	Lower Bounds	Upper Bounds: Mild Spectrum	Upper Bounds: Normal Spectrum	Upper Bounds: Severe Spectrum
Blade	2500	9096.	5025.	3116.
Grip	Unlimited (38,956)	244835.	129150.	64938.
Drag Brace	3300	19967.	12279.	6425.
Yoke	5000	72625.	48417.	24208.
Pitch Horn	3300	21418.	12326.	9339.
Scissors	3300	13394.	7849.	5821.
Drive Link	Unlimited (33,133)	104538.	61219.	44744.
Swpl. Support	3300	22131.	13388.	8395.
Collective Lev.	3300	25545.	15379.	9622.
Stab Bar.	3300	33719.	22479.	16860.
Retention Strap	2200	6197.	3099.	2066.

TABLE 32. UPPER AND LOWER BOUNDS FOR CH-47C COMPONENTS

Component	Lower Bounds	Upper Bounds: Mild Spectrum	Upper Bounds: Normal Spectrum	Upper Bounds: Severe Spectrum
Aft Rotor				
Shaft	3600.	12,303.	7,203.	4,372.
Hub	9790.	38,113.	21,064.	12,194.
Horizontal Pin	2280.	38,113.	21,064.	12,194.
Blade Socket	4000.	16,412.	8,783.	6,083.
Tie Bar	2400.	7,209.	3,378.	2,501.
Blade	4000.	7,249.	5,384.	4,613.
Pitch Shaft	3800.	14,435.	8,575.	5,017.
Forward Rotor				
Blade Socket	6000.	27,395.	13,546.	10,039.
Tie Bar	2400.	7,209.	3,378.	2,501.
Pitch Shaft	3800.	37,824.	19,872.	13,194.

TECHNICAL ACCEPTABILITY

The technical acceptability of the monitoring systems was based on the ability to predict the fatigue lives for all components between the upper and lower bounds for all the test spectra. To simulate the prediction of component fatigue lives (the task of the data processing in the monitoring system), a computer program, SIMULE, was formulated. To predict fatigue lives, the SIMULE program must identify the output of the on-board recorder, assess fatigue damage to the components according to the recorder output, and compute the fatigue life of the components on the basis of the fatigue damage assessments and the accumulated flight time. The SIMULE program was run for a 100-hour sample of each of the test spectra from which the recorder output was simulated. The output of the recorder was simulated by assigning the flight conditions of the test spectra to the flight condition categories according to the anticipated vehicle response. The time and counts of the flight conditions in the 100-hour sample were then accumulated in the flight condition categories of the monitoring system. As in a standard fatigue analysis, the fatigue computation in the SIMULE program was based on Miner's Rule of Cumulative Fatigue Damage. Damage fractions were computed from the recorded output and theoretical damage rates (Equation 1) and then summed to determine the damage accumulated by the components in the 100-hour sample. Assuming the 100-hour sample was an average, the component fatigue life was computed. Thus, the SIMULE program computed the fatigue lives anticipated for the usage identified by the test spectra. These fatigue lives were then compared with the upper and lower bounds in the test for technical acceptability.

Of the ten monitoring systems for the UH-1H, six were tested for technical acceptability: the four FCM methods, 1B, 2C, 2CA, and 3A; and the other two MTM methods, functional assignment (FA) and mission segment (MS). The CLM method was not evaluated because the transfer functions that determine fatigue-critical component loads from stationary component loads were not identified. The DM methods were not evaluated because the assessment of fatigue damage must be derived empirically for each application.

The results of the technical acceptability test for the four FCM methods are shown graphically in Table 33, which illustrates the relationships of the SIMULE-computed fatigue life of the components to the upper and lower bounds for each test spectrum. When the computed fatigue lives were between the upper and lower bounds, indicating technical acceptability, the corresponding space in the figure was left blank. When the computed fatigue life exceeded the upper bound, indicating technical unacceptability, the corresponding space was filled with an X. When the computed fatigue life was less than the lower bound, also indicating technical unacceptability, the corresponding space was filled with a dot (•).

Thus, when a monitoring system is technically acceptable, all the spaces corresponding to the components and all three test spectra are blank.

The results of the technical acceptability tests were as follows: FCM method 1B was not technically acceptable because the computed fatigue life of the main rotor stabilizer bar was outside the bounds established for technical acceptability. Adjustments were made to the model to improve the assessment of fatigue damage with no improvement in the assessment of damage to the stabilizer bar. FCM method 2C was not technically acceptable for the same reason as stated for FCM method 1B. Adjustments made to this method did not improve the assessment of fatigue damage to the stabilizer bar. The difficulty in assessing fatigue damage for the stabilizer bar was traced to the assessment of damage for landings. Of all landings, only full autorotative landings are damaging to the stabilizer bar. In methods 1B and 2C, the autorotative and power-on landings are combined in the same flight condition category. Thus damage would be assessed for all landings and not just for autorotative landings; consequently, the assessment of damage for the stabilizer bar would be overly conservative.

FCM method 2CA was technically acceptable, since SIMULE computed fatigue lives for all the components between the upper and lower bounds for all of the test spectra. FCM method 3A was technically unacceptable because the computed fatigue life for the main rotor drag brace was above the upper bound for the severe spectrum. The unconservative assessment of fatigue damage was attributed to the flight condition category containing the flight condition of lateral control reversals while hovering with a ground effect. Since this category contained less total time, it produced the unconservative (lower) assessment of fatigue damage. Consequently, of the four FCM methods, only 2CA was technically acceptable.

The two MTM methods, MS and FA, were also evaluated for technical acceptability. Since the MS method also computed damage according to recorded elapsed time and theoretical damage rates, it could be evaluated by the SIMULE program. As previously discussed, a test case for the MS method was generated from the design spectrum. With the test case data as input into SIMULE, the component fatigue lives were computed. Table 33 compares the computations with the upper and lower bounds. The MS method was too conservative in the assessment of fatigue damage to the stabilizer bar, main rotor drag brace, swashplate support, collective lever, and main rotor blade; therefore, it was technically unacceptable. Since no damage rates were identified for the FA method, this method could not be evaluated directly. Instead, its technical acceptability was based on the acceptability of the MS method. Since the MS method monitors in-flight data, whereas the FA

method does not, it was assumed that the MS approach would yield better predictions of the component fatigue lives. Moreover, the FA method applies a single damage rate to the entire fleet and differentiates damage only by flight time. Since the MS method was technically unacceptable, it was assumed that the FA method was also technically unacceptable. As a result, the MTM system was judged technically unacceptable for both helicopter models.

TABLE 33. TECHNICAL ACCEPTABILITY RESULTS FOR THE UH-1H

COMPONENT	SYSTEM	1B	2C	2CA	3A	MS
	SPECTRUM	M N S	M N S	M N S	M N S	M N S
Retention Strap						
Yoke						
Stabilizer Bar		●	●			● ● ●
Drag Brace					X	● ●
Swashplate Support						● ●
Collective Lever						●
Pitch Horn						
Scissors						
Blade						● ●

blank - fatigue life between upper and lower bounds

● - fatigue life below lower bound

X - fatigue life above upper bound

Of the ten monitoring systems for the CH-47C, the six FCM methods were evaluated. The CLM method was not evaluated because transfer functions that determine fatigue-critical component loads from stationary component loads were not identified. The DM methods were not evaluated because the assessment of fatigue damage must be empirically defined for the particular application. The MTM methods were not evaluated because of the results for the UH-1H helicopter.

The results of the evaluation of the FCM methods for the CH-47C are shown graphically in Table 34. Again, the spaces are blank for technically acceptable results, filled with an X where the computed fatigue life exceeds the upper bound, and filled with a dot (•) where the computed fatigue life is less than the lower bound. All the FCM methods

were technically unacceptable, primarily because of overly conservative assessments of fatigue damage to most of the components. The conservatism in the fatigue damage assessments was a result of condensing the extensive information of the fatigue substantiation by recording only one of the four parameters considered. The fatigue substantiation of the CH-47C accounted for gross weight, altitude, center of gravity (CG) position, and cargo configuration. In the methods I through VA, either gross weight or altitude was monitored since these appeared to be the important fatigue-damage parameters. Assumed as unimportant parameters, CG position and cargo configuration were not included in the consideration of the CH-47C flight conditions. Since methods I, II, IIA, and IIIA monitored only gross weight, the time in each flight condition was combined for various gross weights, CG positions, and cargo configurations. In all the methods, the combination of flight conditions resulted in spreading the assessment of fatigue damage over a greater proportion of the flight time, which produced the overly conservative assessments.

TABLE 34. TECHNICAL ACCEPTABILITY RESULTS FOR THE CH-47C

COMPONENT	SYSTEM	I	II	IIA	IIIA	IVA	VA
	SPECTRUM	M N S	M N S	M N S	M N S	M N S	M N S
AFT ROTOR							
Shaft		●		●●●		X X X	X X
Hub and Horizontal Pin		●●●	X X		●●	X	X
Blade Socket		●●●	●	●●	●●	X	X
Tie Bar							
Blade		●	X X X	●●●	●●●	X X X	X X X
Pitch Shaft		●●	X	●●		X	X
FORWARD ROTOR							
Blade Socket		●●●	●●●	●●	●●	X	X
Tie Bar							
Pitch Shaft		●●●			●●	X	X

blank - fatigue life between upper and lower bounds

● - fatigue life below lower bound

X - fatigue life above upper bound

Two basically new methods, VI and VII, were considered in order to find a technically acceptable monitoring system for the CH-47C. Method VI monitored altitude variations like IVA but with fewer categories. In addition, n_z peaks were counted rather than timed for each altitude range. Method VII monitored both gross weight and altitude as the basis of most of the flight condition categories. The results of the technical acceptability test for these methods are shown graphically in Table 35. Although method VI improved the assessment of fatigue damage to the components, the improvement was not sufficient to pass the test. Fatigue damage to the aft rotor shaft, the aft rotor blade, and the aft rotor pitch shaft was still assessed too conservatively. Method VII was technically acceptable since the computed fatigue lives for all the components were within bounds for all the test spectra. Consequently, it was concluded that gross weight and altitude must both be monitored for reasonable assessments of fatigue damage.

TABLE 35. TECHNICAL ACCEPTABILITY RESULTS FOR REVISED MONITORING SYSTEMS FOR THE CH-47C

COMPONENT	SYSTEM	VI	VII				
	SPECTRUM	M N S	M N S	M N S	M N S	M N S	M N S
AFT ROTOR							
Shaft		● ● ●					
Hub and Horizontal Pin							
Blade Socket							
Tie Bar							
Blade		● ● ●					
Pitch Shaft		● ● ●					
FORWARD ROTOR							
Blade Socket							
Tie Bar							
Pitch Shaft							

blank - fatigue life between upper and lower bounds

● - fatigue life below lower bound

X - fatigue life above upper bound

The monitoring of gross weight poses a technical problem since accurate measurements of helicopter gross weight are difficult in an operational environment[12]. Gross weight measurements were accurate only for a level-ground rotors-static condition. Therefore, because of the limited accuracy of the gross weight measurements, Method VII was judged technically acceptable with reservation.

SUMMARY

Of the six candidate monitoring systems for the UH-1H and eight for the CH-47C, only one system for each helicopter was technically acceptable: system 2CA for the UH-1H and system VII for the CH-47C. System VII was technically acceptable based on the assumption that gross weight could be monitored accurately and reliably. Since Reference 12 indicated that existing state-of-the-art systems could not accurately monitor gross weight, the detailed definition of the candidate monitoring system, as presented in the next section, was limited to system 2CA for the UH-1H helicopter. However, the basic recording system and data processing/component tracking system would be identical for either system.

---

[12] Dybvad, Richard L., HELICOPTER GROSS WEIGHT AND CENTER OF GRAVITY MEASUREMENT SYSTEM, Electro Development Corporation, USAAMRDL Technical Report 73-66, U.S. Army Air Mobility Research and Development Laboratory, Fort Eustis, Virginia, August 1973, AD771955.

ON-BOARD RECORDER

The on-board recorder is basically a data storage unit with transducers to sense flight parameters, comparator circuits to detect threshold crossings, and circuitry to accumulate counts in the storage device. The unit also includes a battery which applies continuous power to the storage device. The following describes the recorder components and their operation.

The transducers sense airspeed, vertical acceleration, pitch rate, engine torque, main rotor rpm, and landing gear touchdown. Specific transducers were not identified, since several of each type are available. The final selection of transducers would depend on acquiring more detailed information on the power requirements and the reliability of the transducers.

The electrical output of each transducer is conditioned by a low-pass filter and then fed into a comparator circuit as shown in the schematic of Figure 5. The low-pass filter eliminates noise from the transducer output. The breakpoint is set by using a resistor (R) and capacitor (C) such that 1/RC equals the maximum frequency desired. In this application, the comparator circuit identifies the airspeed threshold crossings. The threshold values for the 2CA recorder are tentatively set at 55 and 80 knots. These thresholds, and the other parameter thresholds, are tentative in that the final threshold levels should be determined by a flight test program. Altering the threshold level does not present a problem because the threshold can be reset by setting the resistances R_2 and R_3 of Figure 5 to values defined by the relationship

$$V_T = 15\, R_2/R_3 \tag{8}$$

where V_T = voltage output of transducer at threshold level
R_2 and R_3 = circuit resistances

Thus, if the airspeed transducer output is 0.6 volt, the 55-knot threshold, then an R_2 of 40 ohms and an R_3 of 1000 ohms would produce the desired result. The output of the comparator, therefore, will be high when the transducer output exceeds 0.6 volt, indicating that 55 knots has been exceeded. The 80-knot comparator would be set up similarly. Representing the output of each comparator as V_{55} and V_{80}, respectively, the comparator outputs for the airspeed ranges are as follows: $\overline{V_{55}}$* for airspeeds less than 55 knots, $V_{55} \cdot \overline{V_{88}}$ for airspeeds between 55

* $\overline{V_{55}}$ denotes a false logic output of the comparator circuit, indicating that the airspeed has not reached 55 knots.

and 80 knots, and V_{80} for airspeeds above 80 knots. These thresholds can be maintained within ±0.5 knot with relatively inexpensive operational amplifiers. To avoid the "ping-pong" effect, which occurs when the transducer output oscillates about the threshold level, a secondary threshold would be built into the recorder. This secondary threshold will allow a counter to continue to accumulate data until a threshold lower than the identified threshold is crossed. After the lower threshold is crossed, the data would then be accumulated in another counter. The secondary threshold is illustrated in Figure 6 for the situation where the "ping-pong" effect would occur.

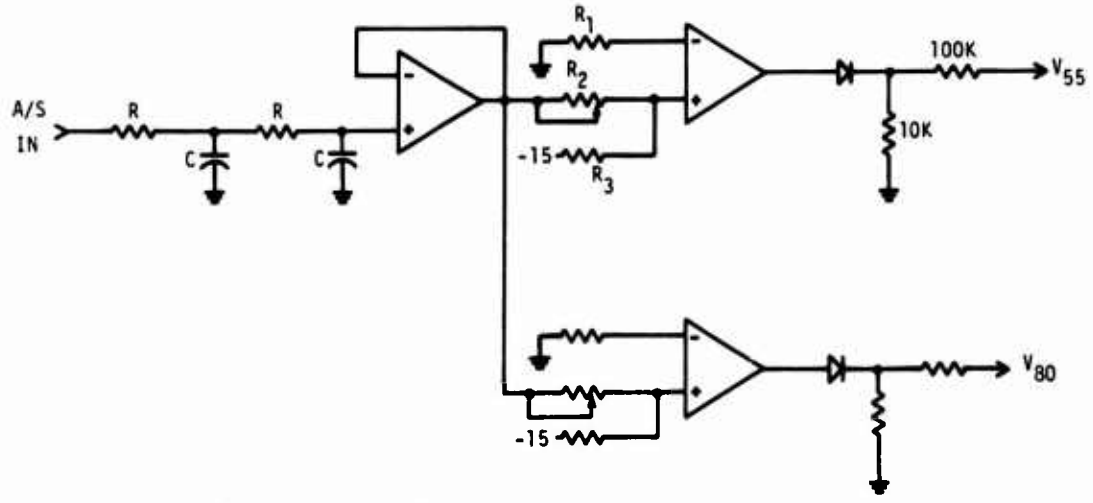

Figure 5. Schematic of Filter Comparator Circuit for Airspeed.

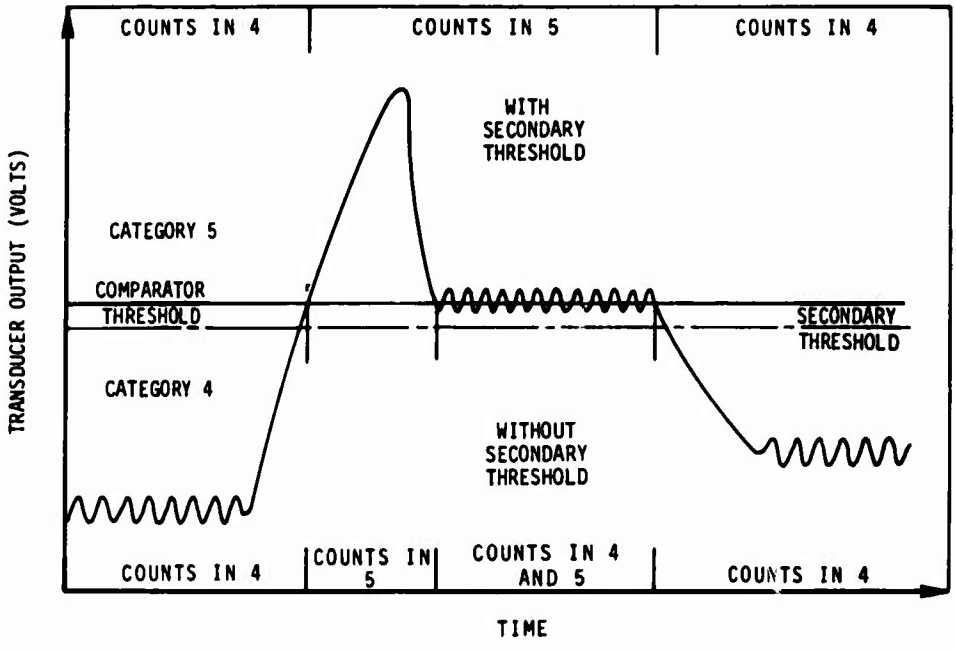

Figure 6. Effect of Secondary Threshold on Recorder Operation.

The output of the other transducers will be fed through similar filter-comparator circuits which would produce outputs similar to those identified for the airspeed transducer. The various comparator outputs will then be combined by a logic network that will associate the parameters and their thresholds to identify the flight condition categories of system 2CA. The representation of the parameters and their thresholds for the flight condition categories is presented in Table 36. Built-in electronic logic (CMOS) would then use the comparator output to direct the accumulation of counts in the storage unit.

TABLE 36. DESCRIPTION OF FLIGHT CONDITION CATEGORIES AS COMPARATOR OUTPUTS

Flight Condition Category	Comparator Output*	Flight Condition Category	Comparator Output*
0	$\overline{V_{55}}$	5	$V_{80} \cdot G_{1.2} \cdot \overline{P_{10}}$
1	$T_L \cdot \overline{Q_E}$	6	$V_{55} \cdot \overline{V_{80}} \cdot G_{1.2} \cdot P_{10}$
2	$T_L \cdot Q_E$	7	$V_{55} \cdot \overline{V_{80}} \cdot G_{1.2} \cdot \overline{P_{10}}$
3	N_{25}, N_{85}, N_{25}	8	$V_{80} \cdot \overline{G_{1.2}}$
4	$V_{80} \cdot G_{1.2} \cdot P_{10}$	9	$V_{55} \cdot \overline{V_{80}} \cdot \overline{G_{1.2}}$

* The outputs of the parameter transducers are:

V_{55}	indicated airspeed above 55 KT
V_{80}	indicated airspeed above 80 KT
N_{25}	main rotor RPM above 25%
N_{85}	main rotor RPM above 85%
P_{10}	pitch rate above 10°/sec
R_{10}	roll rate above 10°/sec
$G_{1.2}$	vertical acceleration above 1.2 g
T_L	occurrence of a landing gear touchdown
Q_E	occurrence of autorotation identified by engine power buss.

The storage unit consists of two CMOS RAM chips. Each chip contains 256 x 1 bits and is divided into eight 32-bit groups. Thus, counter 1 occupies bits 1 to 32 of the first chip, counter 2 occupies bits 33 through 64, etc. Each group is a counter with a capacity of 2^{31} bits of data. (At a rate of one count every 0.1 second, it would take 6.8 years of continuous recording to fill each counter.) Since the system 2CA only requires 11 counters (the 11th to track total flight time for data processing), counters 12 through 16 are spares but could easily be utilized by identifying the appropriate CMOS logic. Each counter will consume about 5 microwatts of power in the standby mode, amounting to 80 microwatts for both RAM chips. Two lithium primary batteries, 0.64 inch in diameter by 1.2 inch in length, are adequate to power the memory in the standby mode for 10 years.

The counters are accessed sequentially by a binary counter as shown in Figure 7. The binary counters address each of the 512 bits of the two RAM chips in sequence as follows: the divide-by-32 binary counter addresses each of the 32 bits (starting with the least significant bit (LSB)) in each counter; the divide-by-8 binary counter addresses each of the counters on a RAM chip; and the divide-by-2 binary counter addresses each of the RAM chips. Thus the status of the divide-by-8 and divide-by-2 binary counters identifies which of the 16 counters is being accessed.

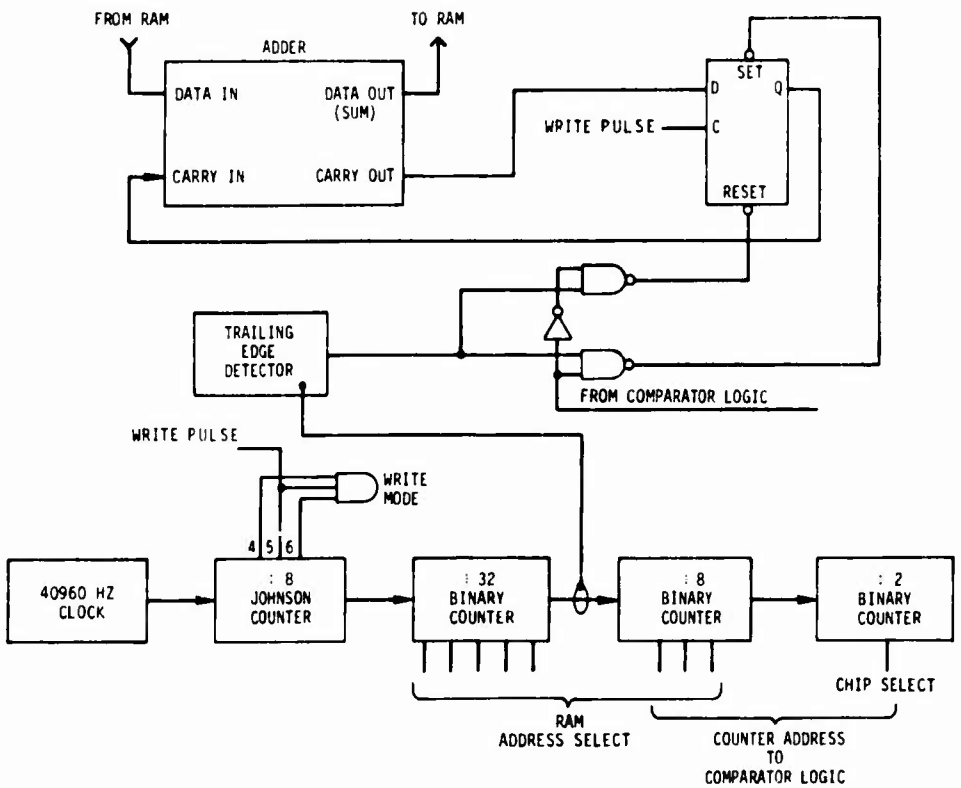

Figure 7. Schematic of Counter Access and Operation.

The status of these binary counters is therefore fed to the comparator CMOS logic to enable the appropriate counter. The three binary counters are run by a 40960-Hz clock so that all 16 counters can be addressed and incremented, as necessary, in a 0.1-second interval. To permit the incrementing of counter values, a divide-by-8 counter is inserted between the clock and binary counters. This counter separates the time spent in each bit into read and write modes, where the write mode is identified as states 4, 5, and 6 of the counter. During the read mode, the value of the bit is placed on the "data-in" line of the adder circuit. (The bit is specified by the status of the three binary counters.) The bit value is then incremented by the "carry-in" value of the adder circuit at state 4 of the counter, and the updated value is written on the bit from the "data-out" line at state 5 of the counter. Simultaneously, the "carry-out" value of the adder circuit is specified. The "carry-in" value of the adder circuit is set equal to 1 if the bit being considered is the LSB of the counter to be incremented (identified by the comparator CMOS logic); for the LSB of all other counters the "carry-in" value would be zero. When the LSB has been incremented by 1, the value of the "carry-out" line will depend on the previous "data-in" value. For example, if the previous "data-in" value was 0, the "data-out" value would be 1 and the "carry-out" value would be zero. If the previous "data-in" value was 1, the "data-out" value would be 0 and the "carry-out" value would be 1 As each of the remaining 31 bits of the counter are read, they are updated by the carry flip-flop until the trailing edge detector identifies the end of the counter (change in the divide-by-32 counter from state 31 to state 0). At this point, the flip-flop is set or reset depending on the output of the comparator logic. If the next counter is to be incremented, then the flip-flop is set; otherwise, the flip-flop is reset. In this fashion, the flight time is divided among the various elapsed-time categories. A separate circuit would be used for each of the event counters, such as the rotor start/stop counter.

The data is extracted from the RAM chips by simply applying the 512 sequential addresses to the RAM circuits and writing the contents on the playback cassette of the retrieval unit.

RETRIEVAL UNIT

The retrieval unit is a portable device whose primary function is to extract stored data from the recorder while it is installed on the aircraft. Secondary functions include an automatic test of the recorder logic, calibration of the recorder comparators, and ground test of the various transducers.

The retrieval unit will be designed to simplify the operator's

task and yet provide him with a flexible instrument for data playback and testing. The unit will be lightweight (less than 25 lb) and shaped like a briefcase with hinged cover and handle for easy carrying. The electronics will be rigidly mounted within a rugged transit case designed to withstand flight-line use. It will contain rechargeable batteries to eliminate the need for aircraft power during data playback. A voltmeter will be included enabling flight-line calibration of comparator thresholds, static testing of transducer outputs, battery condition, and power supply voltages.

Data extracted from the recorder storage is highly condensed. A lost single bit or an undetected single bit error can drastically change the meaning of the data. Several techniques to be used to reduce the probability of an undetected error are as follows:

(1) After each reading of the recorder memory, the recorder inputs will be excited by test signals from the data retrieval unit. This test will add known values to each of the recorder storage registers. After this test, data will again be extracted from the recorder, primarily to check the recorder logic. In addition, when the difference between the two successive playbacks conforms with the known test values, the probability is very high that each playback is correct.

(2) The data from each recorder counter will be extracted and individually recorded on cassette tape. A gap on tape will separate the data in each counter. During the recording of the data in each counter, an error code will be generated and recorded. During the playback of the cassette tape, the code will permit detecting any errors whose lengths are two bits or more.

(3) The data in each counter will be extracted and recorded twice. Each recording will be separate and will contain the error code described in (2).

In the test mode, analog signals are generated and applied to the recorder comparators. If the recorder is functioning properly, a specific number of counts will be added to the contents of each counter. After the application of the test signals, the value of all counters along with the error code will be recorded twice. The data processing center will then be able to compare the before-test and after-test counter values to determine the recorder validity.

Periodically the operator will check the comparator threshold levels, the transducer static outputs, and the recorder battery voltage. The status of the comparator outputs will be indicated by lamps on the retrieval unit. The operator will

rotate a potentiometer and observe the voltage when each comparator changes state. The correct voltage readings will be shown by a card on the retrieval unit.

The operator will then connect the voltmeter to each transducer output by a thumbwheel switch and observe each output voltage. The correct readings will also be shown by a card on the retrieval unit. Another adjustment of the thumbwheel switch will connect the voltmeter to the recorder battery so that its condition may be checked.

DATA PROCESSING CENTER

At the data processing center, such as the Directorate of Product Assurance at AVSCOM, the recorded data would be converted into assessments of fatigue damage. The effort would be divided into three tasks: initial processing, fatigue damage assessment, and component tracking management. Each task was developed as a separate system, with appropriate interfaces, to form the data processing system. The function of each system is as follows:

1. The initial processing system (IPS) checks the parity and built-in-test (BIT) data to detect circuitry malfunctions and the recorded data to detect transducer malfunctions. From these checks, the recorder malfunctions would be detected and the lost and invalid data would be conservatively estimated. This system also maintains information on the status of all recorders to permit preparing reports for maintenance actions.

2. In the fatigue damage assessment system (FDAS), the fatigue damage to the individual fatigue-critical components is assessed according to the specified aircraft serial number. The damage is assessed on the basis of the accumulated counts in the flight condition categories and the conservative damage rates.

3. In the component-tracking management system (CTMS), the status of the individual fatigue-critical components is updated. The status includes the total damage accrued by the component, the rate at which damage is being accrued, and the time remaining until component removal. Files are updated after each recording for the part and are maintained until component retirement.

Reports for the fatigue-critical components are generated in the CTMS and include: an aircraft status report which details the status of all its fatigue-critical components, a logistics report that projects the demands on component spares for each base of operation, and a maintenance report which identifies the components that require retirement. The aircraft status and logistic reports are periodic, issued monthly or quarterly, and the maintenance report is a special report, issued as retirements become necessary.

The processing tasks are performed on the retrieval unit output. The general information, base of operation and date, is written on tape from circuits internal to the retrieval unit. The circuit for the base of operation is semipermanent since the thumbwheel input is covered to prevent accidental change. The circuit for the date is readily accessible, allowing the operator to input the appropriate date. The header information, recorder serial number, aircraft serial information, and aircraft log time, is written on tape from circuits internal to the on-board recorder. The recorder serial number is hard-wired into the unit; the aircraft serial number is semipermanent (the input thumbwheels are covered during installation to prevent accidental change); and the aircraft log time is manually fed in by the operator at the time of recording. The log time input can be retained as a reference value until the next recording is made. Having read the header information, the retrieval unit begins an automatic sequence whereby the recorded data is read, the built-in tests are performed, and the final counter values are written on the output tape. Each segment of the output and each counter value is separated by a gap in the tape, thus isolating each word. The output for each aircraft will be similarly separated by a larger gap. The processing operations performed on these data by the separate systems are outlined in the following.

Initial Processing System

When the cassette is received at the center, it is read into the initial processing system (IPS) where the data is checked for errors caused by recorder or retrieval unit malfunctions. The IPS basically contains, as shown schematically in Figure 8, three checks on the recorded data: the parity checks performed by the retrieval unit and IPS during the read operation, the built-in tests performed by the retrieval unit, and various checks performed on the contents of the counters. The parity checks can detect read errors down to those two bits in length, thus disclosing most of the read errors. The retrieval unit provides singly redundant output for the counters as a measure against the total loss of data when read errors do occur.

After the parity checks are completed, the BIT data are evaluated. Since the retrieval unit interrupts the transducer input

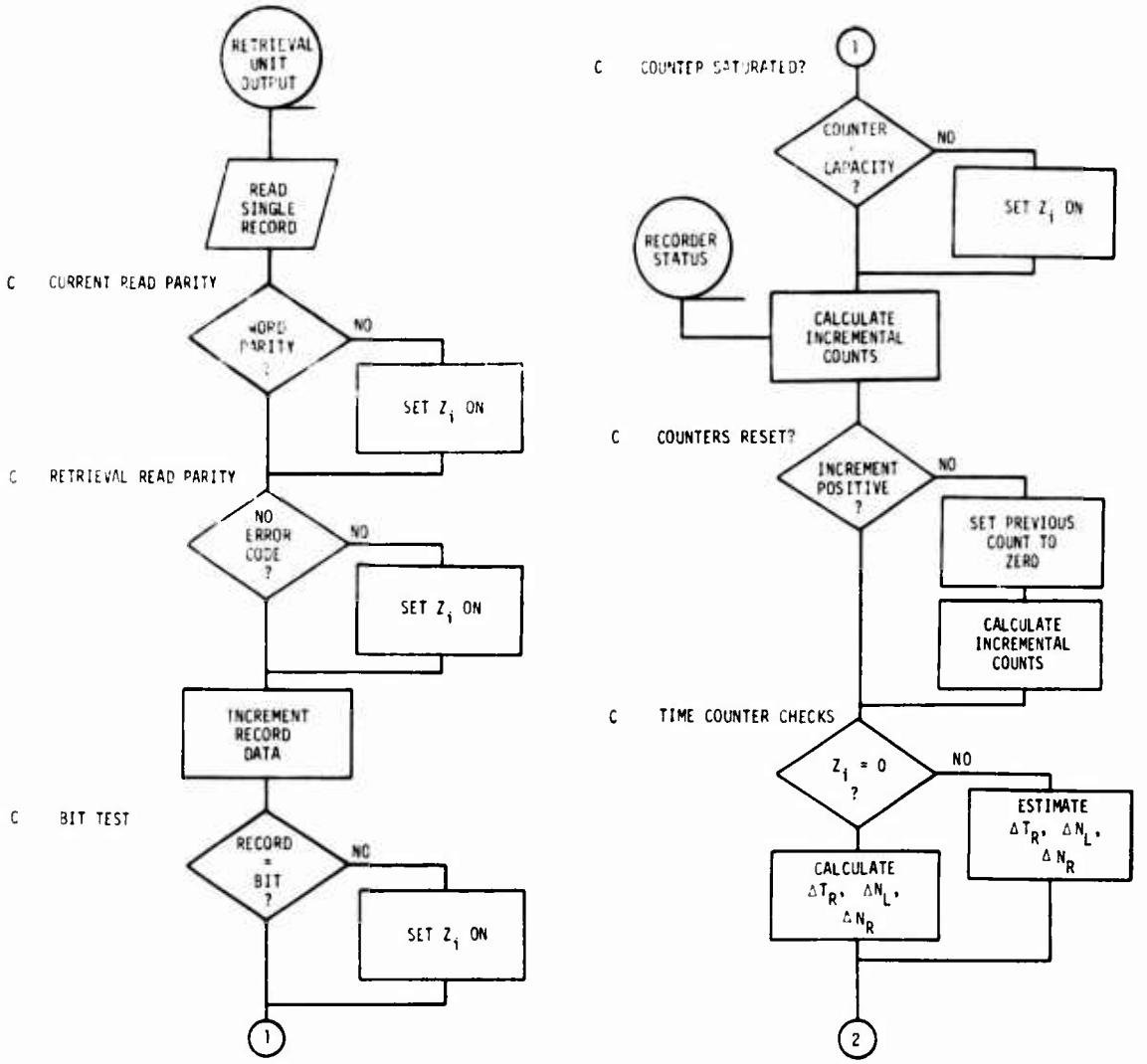

Figure 8. Flow Chart of IPS Processing.

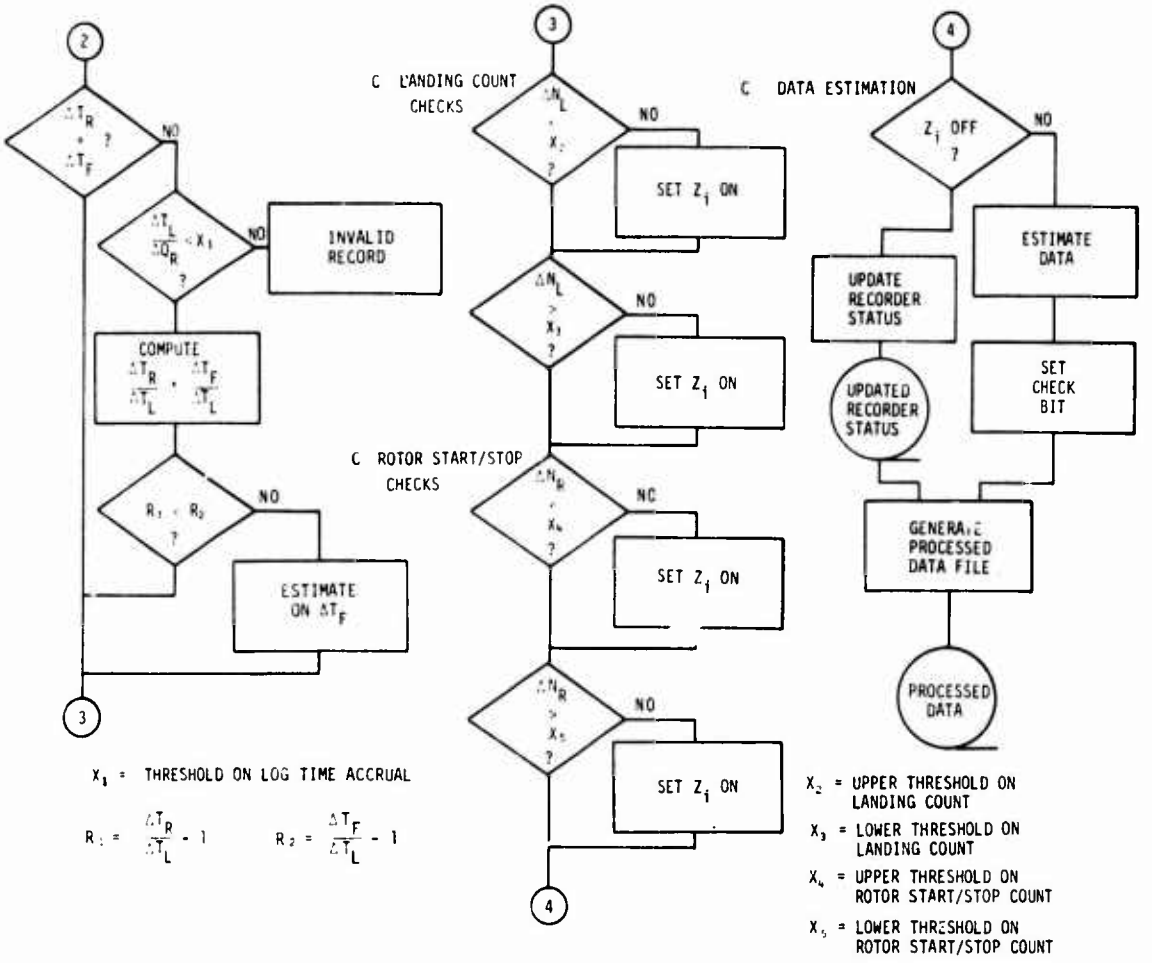

Figure 8 - Concluded

to the comparators to input a series of test inputs, the BIT data reflects a test of comparator, logic, and counter circuit operation. The test is simply a comparison of the recorded data, incremented by the predetermined number of counts in the BIT, and the final counter values. Again, a single redundancy is included to prevent loss of information by random read errors. When the BIT data and the final counter values agree, the circuitry of the recorder is presumed intact; when the values disagree, the circuit being considered is presumed to have malfunctioned. If the counter contents are presumed invalid, the error switch Z_i is set in the on position, and the data for this counter is conservatively estimated.

Since the retrieval unit does not reset the counters at the conclusion of the data extraction, the counters contain totals (inclusive of all previous data and BIT counts). Since the counter capacity is so large, 2^{31} total counts, it will not be exceeded in normal operation. However, the counter could be filled as a result of a malfunction. As a check on this mode of failure, the counter contents will be compared with its capacity. If the counter is saturated, then the data is assumed invalid, and the error switch is set in the on position. The assessment of fatigue damage is made on a record-by-record basis, and therefore the total counts accrued in the counters must be converted to incremental values. To obtain the incremental counts accrued over the last reporting period, the previous totals must be subtracted from the current readings. The previous totals are maintained by recorder serial number in a status file, along with the following information: base of operation, aircraft serial number, date of data extraction, and aircraft log time. Incremental counts are used in the assessment of fatigue damage to circumvent the problems which the use of the counter totals would produce when components or recorders would be replaced. Essentially, the problem would be that the IPS must maintain the initial event for each component in addition to the data already being maintained. This maintenance would produce a large increase in the storage requirements of the IPS and would, in a sense, duplicate the purpose of the CTMS file. By passing incremental values to the FDAS and then to the CTMS, the IPS storage for individual components can be avoided. When components are replaced, a special reading of the recorder should be made to establish the initial value from which the incremental counts for the new components can be determined. After recorder malfunctions are repaired, the counters should be reset to zero, and again a special reading should be made. In most instances, resetting the counters to zero would produce a negative increment in counts during the next processing operation. Since the IPS would be structured to prevent negative increments, the resetting of the counters could be presumed if the special reading was not conducted.

Presuming that the data have passed both parity and BIT checks and that the incremental counts have been defined, the recorded data are checked to verify the proper operation of the transducers. These checks are only general since they compare the data to reasonable limits. The checked recorded data include the record time (ΔT_R), derived as the sum of all the time counters, the number of landings (ΔN_L), and the count of rotor start/stop cycles (ΔN_R). ΔT_R is compared to the flight time (ΔT_F) which is accumulated in a separate counter by monitoring the clock. When the values of ΔT_R and ΔT_F agree, the counter contents are presumed to be valid. However, when they disagree, a malfunction is presumed to have occurred. To determine which of the two is in error, the increments in log time (ΔT_L) and calendar time (ΔQ_R) are considered. If both ΔT_R and ΔT_F are reasonable with respect to ΔT_L, then the one closest to ΔT_L with consideration of ΔQ_R will be chosen for further processing.

If ΔT_F is selected, the time counters are presumed to have malfunctioned, the error switches are set in the on position, and the data for these counters are conservatively estimated. When any of the time counters have been shown to be defective by the parity or BIT data, ΔT_R cannot be determined accurately. In this situation, the unaffected time counters will be presumed valid, and the data for the malfunctioning counters will be estimated by using ΔT_F. First, however, ΔT_F will be compared with ΔT_L to determine if it is valid.

The check on the number of landings simply compares the number of landings performed in either the record or the flight times to limits based on the maximum and minimum flight durations. For this check, the number of landings should include both the power-on and power-off landings to obtain an accurate landing rate. When the violation of either limit of landing rates is interpreted as a recorder malfunction, the error switch is set in the on position for both counters, and the data are conservatively estimated. The count of rotor start/stop cycles will be made similarly. Limits will be established for the maximum and minimum number of cycles that can be performed in either the record or the flight times. Again, the violation of the limits results in a conservative estimate of the incremental counts.

When the error switch has been placed in the on position for any counter, a conservative estimate of the recorded data will be made. The data are estimated from the maximum rate of accrual of counts for the counter considered for its base of operation and the duration of the record, ΔT_R, ΔT_F, or ΔT_L. The maximum rate of accrual for each counter for each base of operation will be maintained by the IPS in the recorder status file. The maximum rate will be continuously updated by only valid data.

After all the data checks have been completed, the recorder status file is updated with only data that have passed all the data checks. Arranged according to recorder serial number, the status file contains the following information which is updated with each valid record: base of operation, date of data extraction, index of data record, aircraft serial number, total log time (T_L), total record time (T_R), total count in each counter, total bit counts, and recorder malfunction codes (updated with each record). Other information not stored by recorder serial number but maintained by the status file includes the pre-established BIT count and the maximum count accrual rates for data estimation.

After the data has been estimated, the IPS generates an output tape which includes the processed data for each aircraft. This tape is used as input to the FDAS and includes the following information for each aircraft serial number: base of operation, date of data extraction, total log time, total record time, and check bit* and data for each flight condition category. In addition to the tape output, the IPS generates a special report on the status of the recorders. This report lists the malfunctioning recorders and their malfunction codes identifying the mode or modes of recorder failure. Each base of operation will receive a report with the records pertinent to the base. The report will list recorders by serial number and in the order of their appearance in the retrieval unit output, along with the aircraft serial number.

Fatigue Damage Assessment System

At the completion of the IPS run on the cassette from a given base of operation, an output tape containing the processed data for each aircraft serial number is generated. This information is then fed to the FDAS, where fatigue damage is assessed as shown in Figure 9. The fatigue damage to each component type is assessed according to Equation (1), expanded here for clarity:

$$\Delta D(J) = \sum_{I=1}^{N} T(I) \cdot C(I,J), \; J = 1,M \qquad (9)$$

where $\Delta D(J)$ = the incremental damage to the jth component type for the record

---

* The check bit identifies whether the data for the flight condition category is actual or estimated.

T(I) = processed counter value for the ith flight condition category (from IPS output)

C(I,J) = theoretical damage rate for the jth component type for the ith flight condition category

N = number of flight condition categories

M = number of component types

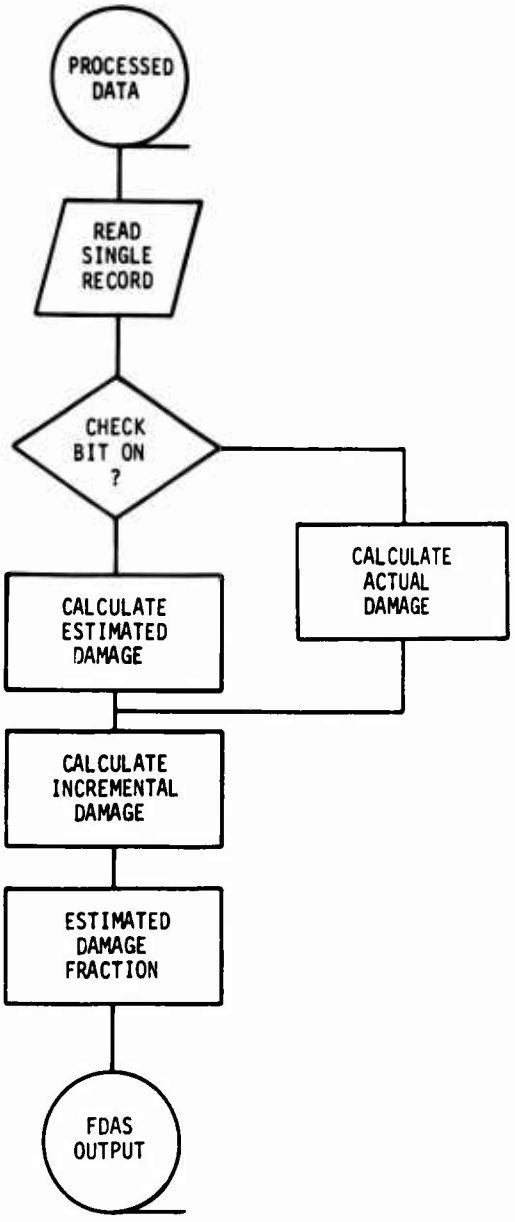

Figure 9. Flow Chart of FDAS Processing.

Since the derivation of the theoretical damage rates was discussed under the monitoring concept, it will not be repeated here. The damage rates for each component type are maintained within the FDAS file. A sample of the damage rates for the UH-1H FCM System 2CA is presented in Table 13.

Since the counter values listed on the IPS output tape may be either actual or estimated, the estimated values must be separated to compute the estimated fatigue damage. The counter values can be separated by sorting the processed data with the check bit provided for this purpose. Once the counter values are separated, the fatigue damage may be computed for both the actual and estimated data. Taking the ratio of estimated damage to the sum of actual and estimated damages yields the estimated fraction of damage for this record. The overall fraction of total damage estimated can then be determined in CTMS using this proportion and the component history.

The output of the FDAS includes the following information for each aircraft serial number: base of operation, date of data extraction, incremental damage to each component type, and fraction of the estimated incremental damage. This information is again written on tape for input to the CTMS where the incremental damage is applied to the individual components.

Component Tracking Management System

The component tracking management system (CTMS) comprises the software to accumulate and retain the fatigue damage on each of the serialized components. The function of the CTMS, therefore, is to accept the incremental damage to the component types for each aircraft serial number from the FDAS and apply it to the appropriate serialized fatigue-critical component. In addition, the CTMS generates projections on the removal of the individual components based on the fatigue damage accumulation. Finally, the CTMS produces reports on the status of the fatigue-critical components for command, logistics, and maintenance usage.

The RAMMIT system was investigated to determine whether or not the accumulation of fatigue damage to each of the serialized components could be integrated into the current reporting system. Since the RAMMIT system currently maintains information other than fatigue on some of the fatigue-critical components, the use of this system for fatigue damage information would reduce the cost and problems involved with the development of the monitoring system. Ideally, the RAMMIT system and several of its reports (namely, the TASIR, CASIR, ACTION, GLIM, and MIT) would be used for the presentation of fatigue information.

The investigation of the RAMMIT system was begun at AVSCOM with the identification of the data file structure. The composite file containing data from Forms 2410 and 2407/8 was identified as the file from which components could be tracked. This file contains information on the components by aircraft serial number. General information is included on the maintenance activity and repair codes, end item maintenance, component removal, and component installation. Modifications would be made in the component removal and installation parts of the file. Each part of the file contains similar information, as shown in Table 37. This information should be expanded to include the following: (1) total damage, (2) fraction of total damage estimated, (3) time and damage increments, (4) time to removal of component, and (5) projected date of removal.

TABLE 37. CONTENTS OF COMPONENT REMOVAL AND INSTALLATION SEGMENTS OF COMPOSITE FILE

Field	Type*
Document Number	X
Date of Component Removal (or installation)	N
Component Federal Stock Number (FSN)	X
Component Serial Number (S/N)	X
Effect Code or Man-Hours (for installation)	X,N
Time Between Overhaul (TBO)	N
Hours Since New (HSN)	N
Hours Since Last Installation (HSLI)	N
Hours Since Overhaul (HSOH)	N
Number of Overhauls	N
Filler (on installation segment only)	

*X = alphanumeric, left justified
N = numeric, right justified

To insert this information into the status file, to update the current RAMMIT system to the modified file, and to make the system compatible with the recording system requires the following modifications, which are shown schematically in Figure 10.

(1) A program will be needed to expand the existing composite file to the additional capacity. This is a simple programming effort with the input tape in the old format and the output tape in the new format. The new fields should be zero-filled on the output tape. The amount of computer time to run the job depends on the number of records and the number of tapes. This time will be significant since this file is already extremely large.

(2) The existing program which combines the 2410 file and the 2407/8 file into one will have to be modified. The actual merge on the existing sequence (A/C SN, WUC (work unit code)) can be left the same. The output tape format will have to be lengthened, and the program must be modified to zero-fill new positions.

(3) The program which merges the newly combined composite file and the existing composite file master will have format changes. Since both input tapes will now have the additional fields, the input formats specified in the program must be changed. The output format will also have to be changed.

(4) The master tape must be sorted by both component and aircraft serial number before running the program which inserts the new data. If a sort is not already available to do this, one must be set up. Most sorts used at AVSCOM are tape utility sorts. The sort fields and record length must be specified in the sort. In addition, the record length of all sorts already prepared for the composite master file will have to be changed. This change should require only repunching the RECORD card in the sort execution deck.

(5) A program to insert the new data must be written. Input to the program will be the composite file master tape sorted by component serial number and aircraft tail number and the cards with the data to be inserted. The cards are in the same sort order as the tape. If the component serial number and aircraft serial number on the input card do not match with a component serial number and an aircraft serial number on the input tape, a check message will be printed. This program will calculate the accumulation of hours and the predictions. The output tape is in the extended length format.

(6) A new report generator will be written to show the status of the component in terms of flight hours and to show the predictions calculated. This program will involve the design of the report format and the data movement to the appropriate fields. The input tape will be the master composite file tape after the insertion program has been run.

(7) All existing report generators must be changed to accept the new format of the input tape (the extended length). Any programs that use the new data file will have changes in the output header lines and the report line format; the code must be inserted to move the new fields to the report line.

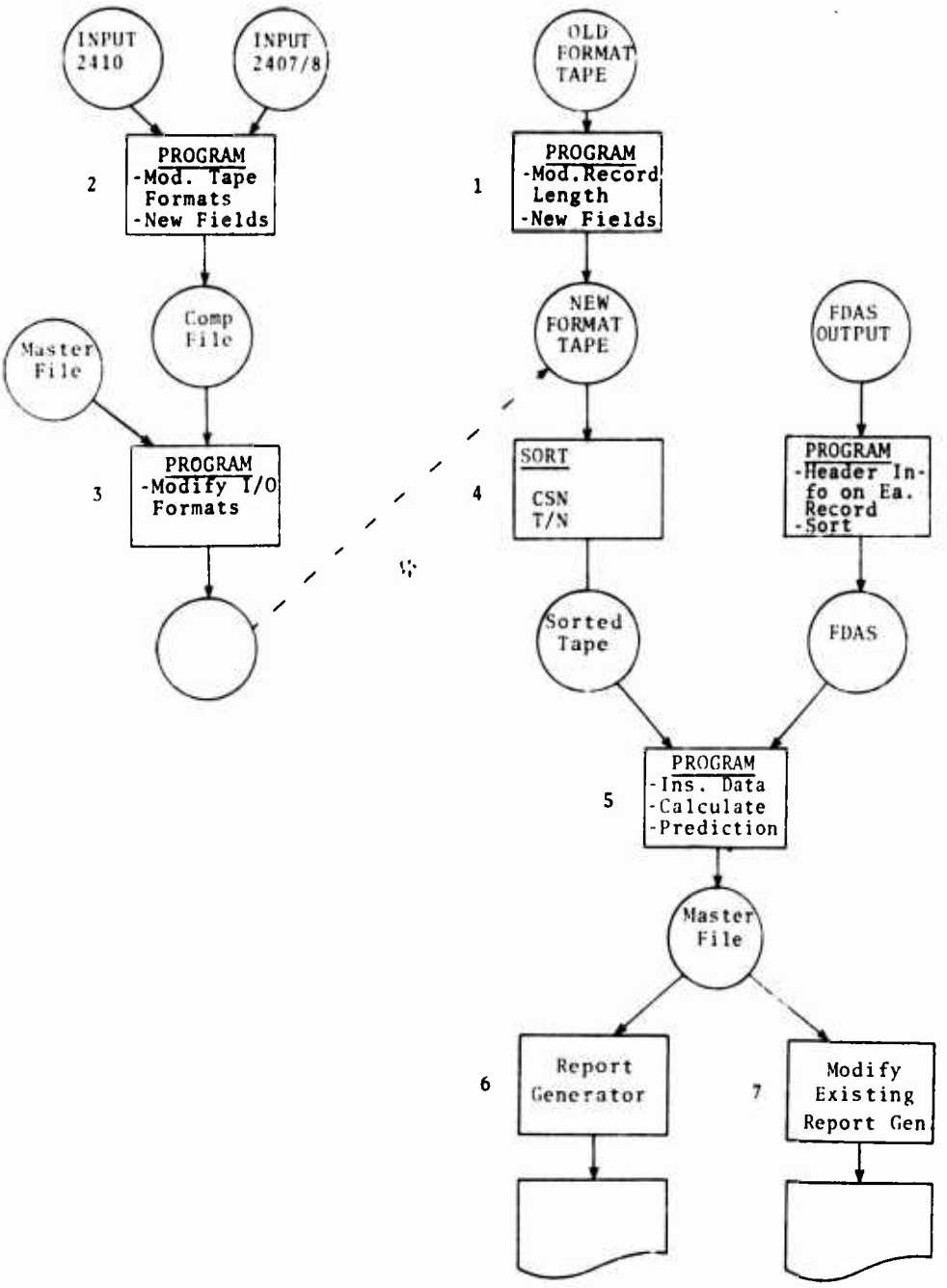

Figure 10. Modifications to the RAMMIT System.

Although these modifications to this file will permit tracking the critical components, there are three major deficiencies in the data: (1) the data entering the file has a time lag of from 9 to 12 calendar months, (2) the data in the file is incomplete, and (3) the data in the file is full of inconsistencies.

Because of these deficiencies, this file and the existing system could not yet produce useful reports. After a thorough investigation and conversations with concerned AVSCOM personnel, it was decided that new data files and report generators should be established to perform the CTMS function efficiently.

To perform the CTMS function, the separate file must contain a status file to maintain information on each serialized fatigue-critical component of each monitored aircraft. The status file must first be established for all components already in use. The information required for each component includes: an estimate of damage accrued to date, accrued flight time and damage over the previous 6 months, estimated time to removal, and date of removal. This history information may be input by card image or magnetic tape, or both. However, the program will require that the history data be sorted in the sequence of FSN part number (P/N), serial number (S/N), and aircraft serial number (T/N). Utility sorts, such as those at AVSCOM, can be used for this sequencing. To avoid duplicate inputs, the program written for the status file will flag duplicate data and check for valid inputs. The status file for the CTMS will be maintained on tape. Therefore, the output of this program and the program that updates the status file with FDAS output will be on tape. The program utilizing the FDAS output will be the working program of the CTMS, since the status of components will be updated solely by the FDAS output during the monitoring system operation.

Before the FDAS output can be accepted by the working program, it must be sorted into P/N-S/N-T/N sequence. Again, utility sorts could be used. Once accepted, the data are used to update the status file, the contents of which are shown in Table 38. The update is performed as follows:

(1) The incremental damage (ΔD) is added to the total damage.

(2) The fraction of damage estimated for the incremental data is changed to a new fraction of total damage estimated.

(3) The incremental log time (ΔT_L) is added to the time since the new (TSN).

(4) The record time (ΔT_R) is used to update the time increments $\Delta T1$ through $\Delta T6$ as follows:

$$\Delta T1 = \Delta T_R(r) \quad (10)$$

$$\Delta T2 = \Delta T_R(r) + \Delta T_1(r-1) \quad (11)$$

$$\Delta T3 = \Delta T_R(r) + \Delta T_2(r-1) \quad (12)$$

$$\Delta T4 = \Delta T_R(r) + \Delta T_3(r-1) \quad (13)$$

$$\Delta T5 = \Delta T_R(r) + \Delta T_4(r-1) \quad (14)$$

$$\Delta T6 = \Delta T_R(r) + \Delta T_5(r-1) \quad (15)$$

(5) The incremental damage is used to update the damage increments ΔD1 through ΔD6 similarly as for the time increment update.

(6) Three damage accrual rates are then computed:

$$\frac{\Delta D1}{\Delta T1}, \quad \frac{D6}{T6}, \quad \frac{D}{TSN}$$

(7) The time to removal (ΔTR) is then computed from the most severe damage accrual rate and the remaining damage fraction (0.95-D).

(8) The projected date of removal (TRCAL) is then computed according to the ΔTR, the time accrual rate, and the date of data extraction.

TABLE 38. CONTENTS OF STATUS FILE

Field	Type*
Component, Federal Stock Number, Part Number (FSN, PN)	X
Component Serial Number (S/N)	X
Aircraft Serial Number (T/N)	X
Base of Operation	X
Total Damage (D)	N
Time Since New (TSN)	N
Time Increments (ΔT1 through ΔT6)	N
Damage Increments (ΔD1 through ΔD6)	N
Time to Component Removal (ΔTR)	
Projected Date of Component Removal (TRCAL)	

*X = alphanumeric, left justified
N = numeric, right justified

Three reports are then generated from the status file, as shown in Figure 11. Each of the report generators requires a look-up table to find the proper nomenclature for each P/N-S/N combination. If not already available on a disc, this table will be stored on a disc to make the table more accessible.

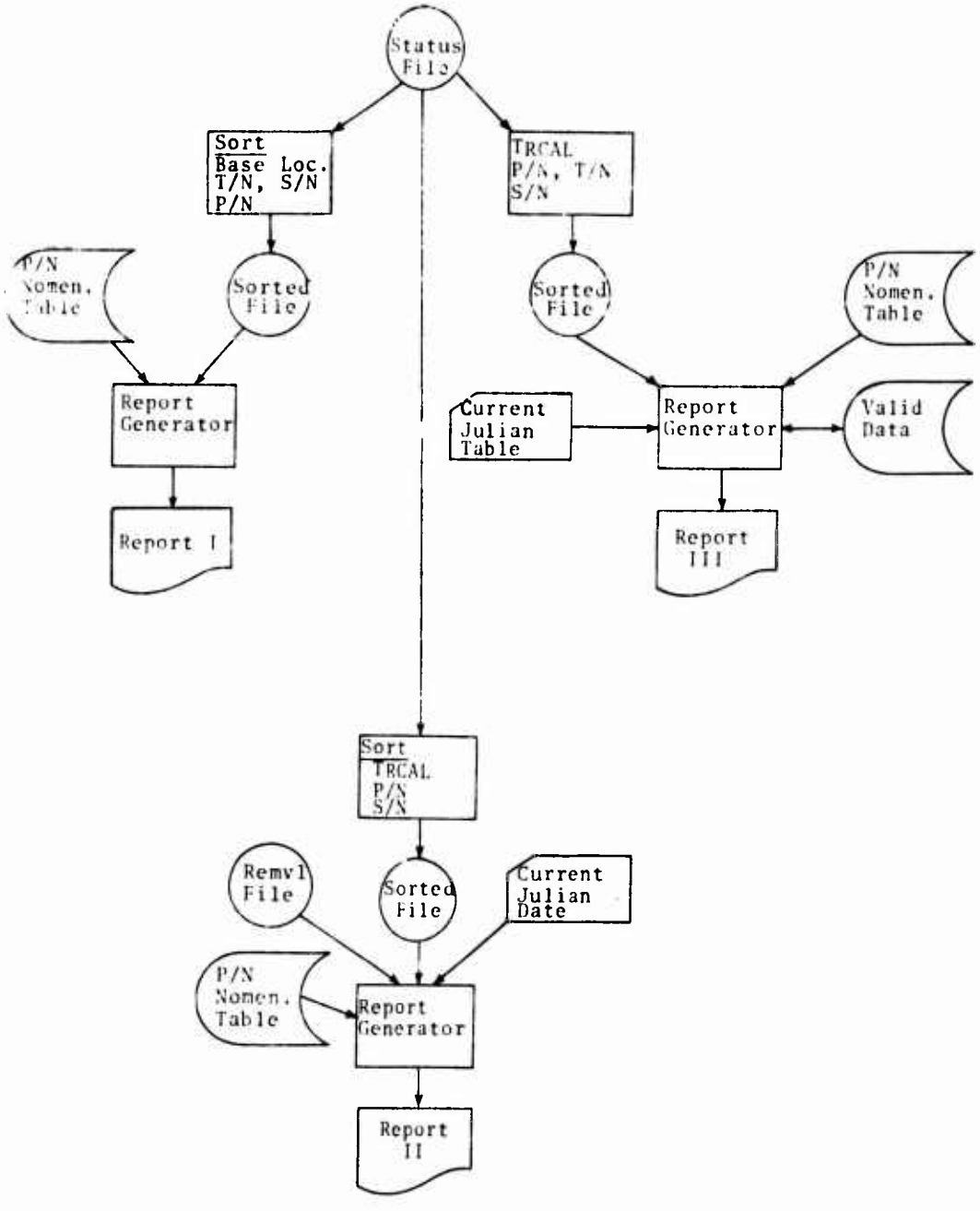

Figure 11. Report Generation Processing.

Report I is a monthly listing of the fatigue damage information (Figure 12) by T/N. The report generator requires both the status file sorted by base and in the P/N-S/N-T/N sequence and the P/N-nomenclature look-up tables as inputs. Again, the utility sort is used on the status file. Since this information is to be reported to the command, the report is generated for each base. When all the information for one base is completed, the next base is listed, etc. For each base, the information is listed by T/N. For each T/N, this table lists the component P/N, P/N nomenclature, component S/N, damage accrual rate, damage fraction, percentage of estimated damage fraction, time to removal, and projected date of removal. The component P/N, P/N nomenclature, and component S/N are self-explanatory. The damage accrual rate is the most severe damage accrual rate (in units of damage per hour of remaining life) computed in the CTMS program. The time basis of the damage accrual rate is indicated by the footnotes which specify whether the rate is based on the previous data (P), on the previous 6 months of data (S), or on the total data (T). Since the projections of replacement dates are based on the damage accrual rate, the user should know the basis for the projections. The damage fraction (relative to a scale of 1) is the amount of damage accumulated by the component at the date of the last recorded data (in this application, 1 May 1974). The percentage of the damage fraction estimated represents the damage due to recorder malfunction. The remaining life is the number of flight hours required to reach a damage fraction of 0.95 based on the reported damage accrual rate. Based on the time to removal and the flight hour accrual rate, the replacement date is the time when the remaining life will have expired. Footnotes indicate whether the replacement date is within the next 3 months or past, that is, the damage fraction of 0.95 has been exceeded. This report is generated only for those components whose damage fraction is equal to or greater than 0.7. A warning that replacement is overdue is printed on any component whose fraction is equal to or greater than 0.95.

Before the generator for Report II is run, the status file must be sorted into the TRCAL, P/N, S/N sequence (by using the utility sort). This program uses the P/N-nomenclature look-up table, the sorted status file, the sorted removal file, and an input card with the current calendar data as inputs. In Report II (Figure 13), the basic report format includes a listing of (1) the number of removals, identified by P/N and nomenclature, projected for the 0-3 month, 0-12 month, 12-15 month, and 12-24 month intervals and (2) the number of removals made in the previous 3 months. There will be two separate listings: one for the individual bases and the second for the fleet. The report is intended for inventory control since it provides advanced information on component replacements.

Report III is a quarterly maintenance report. The status file must be sorted into the TRCAL, P/N, T/N and S/N order before running the corresponding report generator. The utility sort would again be used. The required inputs are the P/N-nomenclature look-up table, the sorted status file, and an input card with the current calendar data. This program will generate listings ordered by date of replacement (TRCAL). There will be two sets of information, one for replacements due in 0-3 months and the other for overdue replacements. As shown in Figures 14 through 17, each set will be listed in two sort sequences: (1) by the TRCAL, T/N, and S/N sequence with an ordering by P/N and nomenclature, and (2) by the TRCAL, P/N, and nomenclature sequence with an ordering of T/N.

When component replacements occur, the status file must be updated. To track component removals and their replacements, a form, such as the update form shown in Figure 18 (or the input to the 2410/2407/8 file, if it were current), could be used. This information would be fed according to date to the status file to ensure that damage increments are associated with the correct serial number. Depending on the reason for component removal, the status will be updated. If the time expired or the component failed, the data in the status file would be moved to a removal file. If removed for modification, service, or as a precautionary measure, the status information will be retained in anticipation of further component usage.

TECHNOLOGY INCORPORATED HELICOPTER INTEGRITY PROGRAM

****
* *
* SELECTED COMPONENT STATUS *
* DAMAGE FRACTION GREATER THAN 0.7 *
* *
****

A/C TYPE/MODEL: CH-47C
AIRCRAFT NO: 64-13145
BASE: FT RUCKER
DATA THRU: 05/01/74
REPORT DATE: 05/15/74

COMPONENT PART NUMBER	COMPONENT NOMENCLATURE	COMPONENT SERIAL NUMBER	DAMAGE ACCRUAL RATE		DAMAGE FRACTION	PERCENTAGE OF DAMAGE FRACTION ESTIMATED	REMAINING LIFE (HRS)	REPLACEMENT DATE JULIAN DATE	
114R2196-2	PIN HORIZONTAL HINGE	PL593	.00034	P	0.971	3.2	0	74130	***
114R1543-4	BLADE SOCKET ROTOR HUB	7-5669-1	.00063	P	0.891	4.1	94	74176	*
114R2155	TIE BAR AFT ROTOR HUB	W-411-0	.00056	S	0.733	0.9	388	74330	
114R1502-33	ROTOR BLADE, AFT	5988413	.00074	T	0.784	2.7	224	74217	*
114R1543-3	BLADE SOCKET, FWD HUB	67-33921	.00042	P	0.714	1.4	557	74053	
114D3250	AFT ROTOR SHAFT	SL-4119N	.00055	T	0.711	3.2	435	74348	

*** THIS MAJOR COMPONENT HAS REACHED OR EXCEEDED 0.95 DAMAGE AND REPLACEMENT IS OVERDUE

* THIS MAJOR COMPONENT IS DUE FOR REPLACEMENT IN 0-3 MONTHS

P - DAMAGE ACCRUAL RATE BASED ON DATA FROM THE PREVIOUS MONTH

S - DAMAGE ACCRUAL RATE BASED ON DATA FROM THE PREVIOUS 6 MONTHS

T - DAMAGE ACCRUAL RATE BASED ON TOTAL PREVIOUS DATA

Figure 12. Report I, Selected Component Status.

TECHNOLOGY INCORPORATED HELICOPTER INTEGRITY PROGRAM

****
* *
* SELECTED COMPONENT *
* USEFUL LIFE PROJECTIONS *
* *
****

A/C TYPE: CH-47C
BASE: FT RUCKER
DATA PERIOD: JAN-MAR 1974
REPORT DATE: 05/15/74

COMPONENT PART NUMBER	COMPONENT NOMENCLATURE	REMOVALS LAST QUARTER	PROJECTED REMOVALS FOR 0-3 MONTHS	PROJECTED REMOVALS FOR 0-12 MONTHS	PROJECTED REMOVALS FOR 12-15 MONTHS	PROJECTED REMOVALS FOR 12-24 MONTHS
114R2050	HEAD ASSY (HUB),ROTARY	13	20	87	39	186
114R2196-2	PIN HORIZONTAL HINGE	54	63	274	110	572
114R2088	PITCH SHAFT AFT ROTOR	49	58	289	131	593
114R1543-4	BLADE SOCKET AFT ROTOR	79	50	265	99	609
114R2155	TIE BAR AFT ROTOR HUB	58	56	256	147	588
114R1502-33	AFT ROTOR BLADE	53	61	269	125	587
114D3250	AFT ROTOR SHAFT	18	22	90	41	202
114R2197	PITCH SHAFT FWD HUB	56	62	257	115	568
114R2155	TIE BAR FWD ROTOR HUB	56	53	263	122	611
114R1543-3	BLADE SOCKET FWD HUB	59	60	272	143	556

Figure 13. Report II, Selected Component Removal Projections.

TECHNOLOGY INCORPORATED HELICOPTER INTEGRITY PROGRAM

****
* *
* REPLACEMENTS DUE 0-3 MONTHS *
* *
****

A/C TYPE/MODEL: CH-47C
DATA PERIOD: MAY-JULY 1974
REPORT DATE: 05/15/74

COMPONENT PART NUMBER	COMPONENT NOMENCLATURE	COMPONENT SERIAL NUMBER	A/C NO.	BASE	REMOVAL DATE
114R2088	PITCH SHAFT AFT ROTOR	M5421	68-43110	FT RUC	05/30/74
114R2088	PITCH SHAFT AFT ROTOR	C4701	67-55462	FT RUC	06/15/74
114R1543-4	BLADE SOCKET AFT ROTOR	VY1022	67-22629	FT RUC	05/30/74
114R2196-2	PIN HORIZONTAL HINGE	A510	68-43110	FT RUC	06/03/74
114R2196-2	PIN HORIZONTAL HINGE	VY4149	67-55462	FT RUC	07/28/74
114R2155	TIE BAR AFT ROTOR HUB	PL248-14	68-43110	FT RUC	06/17/74
114R2155	TIE BAR AFT ROTOR HUB	A12-4	67-22629	FT RUC	07/09/74
114R2155	TIE BAR FWD ROTOR HUB	VF0110	67-55462	FT RUC	07/13/74
114R1502-33	AFT ROTOR BLADE	A913	67-55462	FT RUC	06/23/74
114R1502-33	AFT ROTOR BLADE	A84277	68-43110	FT RUC	07/14/74
114R2197	PITCH SHAFT FWD HUB	NL11740	67-22629	FT RUC	07/05/74
114R1543-3	BLADE SOCKET FWD HUB	VEZ0112	67-55462	FT RUC	07/15/74

Figure 14. Report III, Replacements due in 0-3 Months, by Component Number.

TECHNOLOGY INCORPORATED HELICOPTER INTEGRITY PROGRAM

****
* *
* REPLACEMENTS DUE 0-3 MONTHS *
* *
****

A/C TYPE/MODEL: CH-47C
DATA PERIOD: MAY-JULY 1974
REPORT DATE: 05/15/74

A/C NUMBER	BASE	COMPONENT PART NUMBER	COMPONENT NOMENCLATURE	COMPONENT SERIAL NUMBER	REMOVAL DATE
67-22629	FT RUC	114R1543-4	BLADE SOCKET AFT ROTOR	VY1022	05/30/74
67-22629	FT RUC	114R2197	PITCH SHAFT FWD HUB	NL11740	07/05/74
67-22629	FT RUC	114R2155	TIE BAR AFT ROTOR HUB	A1244	07/09/74
67-55462	FT RUC	114R2088	PITCH SHAFT AFT ROTOR	C4701	06/15/74
67-55462	FT RUC	114R1502-33	AFT ROTOR BLADE	A913	06/23/74
67-55462	FT RUC	114R2196-2	PIN HORIZONTAL HINGE	VY4149	07/28/74
67-55462	FT RUC	114R2155	TIE BAR FWD ROTOR HUB	VE0110	07/13/74
67-55462	FT RUC	114R1543-3	BLADE SOCKET FWD HUB	VEZ0112	07/15/74
68-43110	FT RUC	114R2088	PITCH SHAFT AFT ROTOR	M5421	05/30/74
68-43110	FT RUC	114R2196-2	PIN HORIZONTAL HINGE	A510	06/03/74
68-43110	FT RUC	114R2155	TIE BAR AFT ROTOR HUB	PL248-14	06/17/74
68-43110	FT RUC	114R1502-33	AFT ROTOR BLADE	A84277	07/14/74

Figure 15. Report III, Replacements due in 0-3 Months, by Aircraft Serial Number.

TECHNOLOGY INCORPORATED HELICOPTER INTEGRITY PROGRAM

****
* *
* OVERDUE REPLACEMENTS *
* *
****

A/C TYPE/MODEL: CH-47C
REPORT DATE: 05/15/74

COMPONENT PART NUMBER	COMPONENT NOMENCLATURE	COMPONENT SERIAL NUMBER	A/C NO.	BASE	REMOVAL DATE
114D3250	AFT ROTOR SHAFT	S5-3104	67-22629	FT RUC	01/03/74
114D3250	AFT ROTOR SHAFT	T6299	68-43110	FT RUC	04/23/74
114D3250	AFT ROTOR SHAFT	R2327	67-55462	FT RUC	05/01/74
114R2088	PITCH SHAFT AFT ROTOR	VZ10043	65-10143	FT RUC	03/03/74
114R2089	PITCH SHAFT AFT ROTOR	L439218	67-22629	FT RUC	03/28/74
114R2050	HEAD ASSY (HUB), ROTARY	EX124	66-05372	FT RUC	03/18/74
114R1502-33	AFT ROTOR BLADE	4-316-9	66-05372	FT RUC	04/10/74
114R1502-33	AFT ROTOR BLADE	4438	67-22629	FT RUC	05/01/74
114R2155	TIE BAR FWD ROTOR HUB	LB431	65-10143	FT RUC	04/11/74
114R2155	TIE BAR FWD ROTOR HUB	A6464	66-05372	FT RUC	04/30/74
114R2196-2	PIN HORIZONTAL HINGE	VA4335	65-10143	FT RUC	04/23/74
114R2197	PIN HORIZONTAL HINGE	JU52038	66-05372	FT RUC	05/02/74

Figure 16. Report III, Overdue Replacements, by Component Number.

TECHNOLOGY INCORPORATED HELICOPTER INTEGRITY PROGRAM

****
* *
* OVERDUE REPLACEMENTS *
* *
****

A/C TYPE/MODEL: CH-47C
REPORT DATE: 05/15/74

A/C NUMBER	BASE	COMPONENT PART NUMBER	COMPONENT NOMENCLATURE	COMPONENT SERIAL NUMBER	REMOVAL DATE
65-10143	FT RUC	114R2088	PITCH SHAFT AFT ROTOR	VZ10043	03/03/74
65-10143	FT RUC	114R2155	TIE BAR FWD ROTOR HUB	LB431	04/11/74
65-10143	FT RUC	114R2196-2	PIN HORIZONTAL HINGE	VA4335	04/23/74
66-05372	FT RUC	114R2050	HEAD ASSY (HUB)•ROTARY	EX124	03/18/74
66-05372	FT RUC	114R1502-33	AFT ROTOR BLADE	4-316-9	04/10/74
66-05372	FT RUC	114R2155	TIE BAR FWD ROTOR HUB	A6464	04/30/74
66-05372	FT RUC	114D3250	AFT ROTOR SHAFT	R2327	05/01/74
66-05372	FT RUC	114R2197	PIN HORIZONTAL HINGE	JU52038	05/02/74
67-22629	FT RUC	114D3250	AFT ROTOR SHAFT	S5-3104	01/03/74
67-22629	FT RUC	114R2088	PITCH SHAFT AFT ROTOR	L439218	03/28/74
67-22629	FT RUC	114R1502-33	AFT ROTOR BLADE	4338	05/01/74
68-43110	FT RUC	114D3250	AFT ROTOR SHAFT	T6299	04/23/74

Figure 17. Report III, Overdue Replacements, by Aircraft Serial Number.

TECHNOLOGY INCORPORATED HIP UPDATE FORM

BASE: A/C TAIL NO. A/C TYPE/MODEL

REPLACEMENTS ACCOMPLISHED REASON REMOVED (X)

A/C HOURS	MO/DAY/YEAR	MECHANIC	TIME EXPIRED 1	FAILED 2	PRE-CAUTION 3	MOD 4	SERVICE 5

COMPONENT REMOVALS

REMOVED PART P/N _____ S/N _____

INSTALLED PART P/N _____ S/N _____

TSN: _____ TSO: _____

REMARKS:

Figure 18. Update Form for Component Removals.

LIFE-CYCLE COST ANALYSIS

The life-cycle costs for System 2CA for the UH-1H and System VII for the CH-47C were analyzed using the Cost-Effectiveness Analysis Program (CEAP) described in Appendix B. Although System VII was not described in detail, the life-cycle costs should not differ from those of System 2CA, except for the on-board recorder and related costs.

The life-cycle costs of the candidate monitoring systems were determined for 10- and 15-year periods of operation on each fleet assuming constant 1973 dollars. Two thousand aircraft were considered for the UH-1H fleet, and 500 were considered for the CH-47C. Life-cycle costs included the development, production, implementation, and operation of the monitoring system. Development costs were further detailed for the (1) on-board recorder prototype, (2) retrieval unit prototype, (3) data processing software (IPS, FDAS, and CTMS), (4) preparation of an ECP for recording system installations, (5) recorder qualification tests, (6) recorder flight tests, and (7) technical orders and other documentation. Production costs were identified for the on-board recorder, the helicopter installation kit, and the retrieval unit. Implementation costs included (1) installing the on-board recorder, (2) compiling the data base for the computer programs, (3) outfitting the overhaul and repair stations, and (4) training Army personnel. Operational costs included maintenance man-hours for both recorder and retrieval units, spare parts, software operation and report production. Tables 39 and 40 summarize these cost factors for the UH-1H and CH-47C and present the monitoring system life-cycle costs. The non-recurring unit costs reflect the production cost of the recorder and retrieval unit. The final recorder unit cost compares very well with the target cost for the UH-1H identified in the recording system survey. The recurring unit costs represent the operational costs. For the retrieval unit, 150 units were assumed for the analysis, one for each base of operation plus spares. Spares for the recorder and retrieval units were conservatively provided for by 5% and 10% annual replacement rates for circuitry and transducers, respectively. Processing costs were based on contractor rates. Maintenance costs were based on the Army composite rate of $10.34 per hour. The life-cycle costs were computed as described in Appendix B. The life-cycle costs for the 10- and 15-year periods were $10.54 and $13.02 million for the UH-1H and $4.82 and $6.15 million for the CH-47C, respectively.

TABLE 39. MONITORING SYSTEM COSTS FOR THE UH-1H

COST FACTORS	UNIT COST (Dollars)	LIFE-CYCLE COST (Millions) 10 Yr	15 Yr
FIXED			
DEVELOPMENT	444,000	.444	.444
QUALIFICATION	29,000	.029	.029
PREPRODUCTION	10,000	.010	.010
UNIT			
NONRECURRING			
Recorder	1939	3.878	3.878
Retrieval	1419	.213	.213
Installation	500	1.000	1.000
RECURRING			
Maintenance	31.02	.620	.931
Spares,			
Recorder	148.46	2.969	4.545
Retrieval	91.35	.137	.206
Processing	62.00	1.240	1.860
		10.54	13.02

TABLE 40. MONITORING SYSTEM COSTS FOR THE CH-47C

COST FACTORS	UNIT COST (Dollars)	LIFE-CYCLE COST (Millions) 10 Yr	15 Yr
FIXED			
DEVELOPMENT	444,000	.444	.444
QUALIFICATION	29,000	.029	.029
PREPRODUCTION	10.000	.010	.010
UNIT			
NONRECURRING			
Recorder	2430	1.215	1.215
Retrieval	1419	.213	.213
Installation	500	.250	.250
RECURRING			
Maintenance	31.02	.155	.233
Spares,			
Recorder	225.28	1.126	1.690
Retrieval	91.35	.137	.206
Processing	62.00	1.240	1.860
		4.819	6.150

Savings generated by extending component retirement times were based on the component data presented in Tables 41 and 42. This data includes component cost, maintenance man-hours (MMH) required for replacement, man-hours (IMH) for the inspection of component replacements, the Army composite rate, and the representative usage for the components. The representative usage for the mild, normal, and severe spectra was determined from the analysis by the SIMULE program. Each of the three spectra were input and the program simulated the recorder output and projected retirement lives as the processing would during system operation. Savings were computed using the above information and two other assumptions. It was assumed, first, that the helicopter was flown 60 hours per month throughout the 10- and 15-year periods, and second, that the observed usage was a combination of the mild, normal, and severe spectra in the ratio of their weighting factors. As described in Appendix B, the CEA Program computed savings of $11.63 and $26.38 million for the UH-1H over the 10- and 15-year periods, and $9.35 and $34.43 million for the CH-47C over the same time periods.

TABLE 41. COMPONENT DATA FOR THE UH-1H LIFE-CYCLE COST ANALYSIS

COMPONENT	COST	MMH	IMH	RATE	USAGE			
Main Rotor					Design	Mild	Normal	Severe
Blade	3100	6.9	.17	10.34	2500	3854	2922	2602
Drag Brace	64	7.0	.17	10.34	3300	17179	10882	5862
Yoke	670	1.5	.17	10.34	5000	72472	45372	24198
Pitch Horn	33	7.0	.17	10.34	3300	15268	8770	6937
Scissors	37	7.0	.17	10.34	3300	9502	5620	4455
Stabilizer Bar	251	2.2	.17	10.34	3300	16778	11204	8403
Retention Strap	150	8.1	.17	10.34	2200	6087	3049	2032
Swashplate Support	131	3.9	.17	10.34	3300	16428	10149	6895
Collective Lever	37	2.7	.17	10.34	3300	19115	11816	8011

The benefit to the Army was computed as the difference in monitoring system life-cycle cost and the savings generated over the same time period. For the UH-1H, the benefit was $1.09 million for the 10-year period and $13.36 million for the 15-year period. For the CH-47C, the benefit was $4.53 and $28.28 million for the same time periods.

TABLE 42. COMPONENT DATA FOR THE CH-47C LIFE-CYCLE COST ANALYSIS

COMPONENT	COST	MMH	IMH	RATE	USAGE			
Aft Rotor					Design	Mild	Normal	Severe
Shaft	8472	20.0	.17	10.34	3680	7682	4765	4056
Hub	5094	10.0	.17	10.34	9790	23154	13994	10690
Horiz. Pin	604	8.7	.17	10.34	9790	23154	13994	10690
Blade Socket	1251	9.0	.17	10.34	4490	10238	6236	5420
Tie Bar	612	2.4	.17	10.34	2400	5548	2590	1968
Blade	11418	7.4	.17	10.34	4400	6756	4976	4465
Pitch Shaft	1481	1.6	.17	10.34	3820	8821	5517	4409
Forward Rotor								
Blade Socket	1280	9.0	.17	10.34	6600	13689	8410	7302
Tie Bar	612	2.4	.17	10.34	2400	5548	2590	1968
Pitch Shaft	1481	1.6	.17	10.34	8340	19272	12023	9392

Since the UH-1H System 2CA was detailed as the candidate monitoring system, the life-cycle cost analysis included the investigation of the effect of fleet size and usage severity on the benefit of the monitoring system. A range in fleet size of 1000 to 2000 aircraft was considered. The effect on the life-cycle costs is shown in Table 43 in millions of dollars for the 10- and 15-year periods. For the 10-year period, the benefit is negative for the fleet of 1000, indicating that this fleet is too small to be cost-effective. The break-even point would be approximately 1325 units for the 10-year period. For the 15-year period, the benefit is substantial for the fleet sizes considered. The break-even point is approximately 340 units.

TABLE 43. EFFECT OF FLEET SIZE ON THE LIFE-CYCLE COST ANALYSIS OF THE UH-1H FCM SYSTEM 2CA

Fleet Size	10 Year*			15 Year*		
	Savings	Cost	Benefit	Savings	Cost	Benefit
1000	5.82	6.31	-.51	13.19	7.89	5.30
1500	8.72	8.42	.30	19.78	10.46	9.32
2000	11.63	10.54	10.54	26.38	13.02	13.36

* all figures are in millions

The effect of usage severity on the UH-1H monitoring system benefit is shown in Table 44 in millions of dollars. Change in usage was expressed as changes in the weighting factors, as described in the Evaluation Criteria section. The weighting factor changes were based on the historical changes in the UH-1H usage, as depicted by Figure 3. The distribution of usage (B_j's) was identified for three different times, and weighting factors were then computed. The times were selected to represent the range of usage distribution. The resulting effect on weighting factors and the benefit are shown in the table.

TABLE 44. EFFECT OF USAGE ON THE LIFE-CYCLE COST ANALYSIS OF THE UH-1H FCM SYSTEM 2CA

Weighting Factors			10 Year*			15 Year*		
Mild	Normal	Severe	Savings	Cost	Benefit	Savings	Cost	Benefit
.31	.50	.19	11.63	10.54	1.09	26.38	13.02	13.36
.27	.52	.21	10.83	10.54	.29	25.16	13.02	12.14
.24	.50	.26	10.02	10.54	-.52	23.45	13.02	10.43

* all figures are in millions

SUMMARY AND CONCLUSIONS

In an effort to identify a means of monitoring and assessing fatigue damage to helicopter components, a feasibility study of various monitoring methods was conducted. Off-the-shelf recording systems were investigated with the result that none could capably perform the required monitoring in a cost-effective manner. Consequently, an alternative recording method, employing state-of-the-art electronics technology, was identified and found to be cost-effective.

Four methods of assessing fatigue damage were identified: FCM, CLM, DM, and MTM. Of these methods, only FCM was found technically acceptable and cost-effective as a monitoring approach and only one system was identified for each helicopter: System 2CA for the UH-1H and System VII for the CH-47C. System VII, however, required the monitoring of gross weight, which was identified as a technical problem since the accurate measurement of gross weight on helicopters has not been shown feasible in an operational environment. Although the current state-of-the-art cannot provide an accurate gross weight measurement system, should such a system become available, monitoring of the CH-47C should be considered.

Due to the nature of flight condition monitoring, conservative assumptions were used in the development of the fatigue damage assessment model. These assumptions, on threshold levels for monitored parameters and the time spent in the flight condition categories by each flight condition, should be further investigated. A flight validation program is recommended for this purpose.

Although not found technically acceptable, the CLM and DM methods would monitor fatigue damage better than the FCM or MTM methods since the data recorded by the former two methods would be more closely associated with the fatigue phenomenon. Consequently, further investigation of these methods should be considered. For the CLM, the development of transfer functions relating rotating component loads to stationary component loads should be investigated. A flight test program, where the transfer functions could be derived empirically, could be used. Of the DM methods, acoustic emission was identified as a potential means of tracking fatigue damage. The application of this method to full-scale helicopter structure should be investigated.

After the method of assessing fatigue damage was selected, the monitoring system was defined in detail. The recorder configuration and operation were detailed, and the data processing steps were identified. The processing software was designed so that it could interface with AVSCOM's RAMMIT system. Costs for the monitoring system were then identified for the life-cycle cost analysis. The life-cycle cost analysis was

conducted for both the UH-1H and CH-47C monitoring systems. Although the benefit of monitoring fatigue damage on the UH-1H is modest for the 10-year operation, the candidate does provide fleet-wide monitoring and component tracking at a low cost, and therefore would provide an excellent first-generation monitoring system. It was concluded, therefore, that the FCM System 2CA can provide an acceptable monitoring system from both technical and cost standpoints and that it should be further developed in a pilot program on the UH-1H or one of its derivatives.

RECOMMENDATIONS

It is recommended that:

1) The candidate monitoring system be further developed in a pilot program during which the assumptions or parameter thresholds and fatigue damage assessments can be validated.

2) The CLM method be further investigated to determine transfer functions for component loads. This might be accomplished by expanding the recording performed in the pilot program.

3) The use of acoustic emission be pursued as a potential fatigue damage monitor.

REFERENCES

1. Orr, P., McLeod, G., and Goddell, J., FATIGUE LIFE SUBSTANTIATION OF DYNAMIC COMPONENTS FOR THE UH-1D HELICOPTER EQUIPPED WITH THE 48-FOOT DIAMETER ROTOR, Bell Helicopter; Report No. 205-099-135, May 1964.

2. Thakkar, H., and MacDonald, P., CH-47C DYNAMIC SYSTEM FATIGUE ANALYSIS--FINAL REPORT, Boeing Vertol Division; Report No. 114-SS-723, March 1970.

3. Herskovitz, A., and Steinmann, H., CH-47A DESIGN AND OPERATIONAL FLIGHT LOADS STUDY, Boeing, Philadelphia, Pennsylvania; USAAMRDL Technical Report 73-40, U.S. Army Air Mobility Research and Development Laboratory, Fort Eustis, Virginia, November 1973, AD772949.

4. Brown, W.P., and Steinmann, H.H., THE CH-47C CRUISE GUIDE INDICATOR, Boeing Vertol Division, Proceedings of the Annual National Forum of the American Helicopter Society, Preprint No. 453, presented at the 26th Annual National Forum of the American Helicopter Society, June 1970.

5. Garrison, J., LOAD LEVEL TEST OF UH-1D HELICOPTER IN 48-FOOT DIAMETER MAIN ROTOR CONFIGURATION, VOLS III AND IV, Bell Helicopter; Report No. 205-099-049, April 1964.

6. Hartman, L.J., CH-47C STRESS AND MOTION SURVEY, Boeing-Vertol Division; Report No. 114 FT-708, April 1969.

7. Johnson, Raymond B., Clay, Larry E., and Meyers, Ruth E., OPERATIONAL USE OF UH-1H HELICOPTERS IN SOUTHEAST ASIA, Technology Incorporated, Dayton, Ohio; USAAMRDL Technical Report 73-15, U.S. Army Air Mobility Research and Development Laboratory, Fort Eustis, Virginia, May 1973, AD764260.

8. Giessler, F. Joseph, and Braun, Joseph F., FLIGHT LOADS INVESTIGATION OF COMBAT ARMED AND ARMORED CH-47A HELICOPTERS OPERATING IN SOUTHEAST ASIA, Technology Incorporated, Dayton, Ohio; USAAVLABS Technical Report 68-1, U.S. Army Aviation Materiel Laboratories, Fort Eustis, Virginia, March 1968, AD671672.

9. Giessler, F. Joseph, and Braun, Joseph F., FLIGHT LOADS INVESTIGATION OF CARGO AND TRANSPORT CH-47A HELICOPTERS OPERATING IN SOUTHEAST ASIA, Technology Incorporated, Dayton, Ohio; USAAVLABS Technical Report 68-2, U.S. Army Aviation Materiel Laboratories, Fort Eustis, Virginia, April 1968, AD 672842.

REFERENCES - Continued

10. AIRCRAFT OPERATIONAL UTILIZATION - UH-1H FLEET, Directorate for Product Assurance, U.S. Army Aviation Systems Command, St. Louis, Missouri.

11. AIRCRAFT OPERATIONAL UTILIZATION - CH-47B,C FLEET, Directorate for Product Assurance, U.S. Army Aviation Systems Command, St. Louis, Missouri.

12. Dybvad, Richard L., HELICOPTER GROSS WEIGHT AND CENTER OF GRAVITY MEASUREMENT SYSTEM, Electro Development Corporation, USAAMRDL Technical Report 73-66, U.S. Army Air Mobility Research and Development Laboratory, Fort Eustis, Virginia, August 1973, AD771955.

13. Dunegan, H.L., Harris, D.O., and Tatro, C.A., FRACTURE ANALYSIS BY USE OF ACOUSTIC EMISSION, Journal of Engineering Fracture Mechanics, Vol. 1, June 1968, p. 105-122.

14. Dunegan, H.L., and Harris, D.O., ACOUSTIC EMISSION--A NEW NON-DESTRUCTIVE TESTING TOOL, Proceedings of Third Annual Symposium on Non-destructive Testing of Welds and Materials Joining, Los Angeles, California, March 1968.

15. Gerberich, W.W., and Hartbower, C.E., MONITORING CRACK GROWTH OF HYDROGEN EMBRITTLEMENT AND STRESS CORROSION CRACKING BY ACOUSTIC EMISSION, in Proceedings of the Conference on Fundamental Aspects of Stress Corrosion Cracking (Ohio State University, Columbus, Ohio, 1967).

16. Hutton, P.H., ACOUSTIC EMISSION APPLIED TO DETERMINATION OF STRUCTURAL INTEGRITY, for presentation at the 11th Open Meeting of the Mechanical Failures Prevention Group sponsored by the Office of Naval Research at Williamsburg, Virginia, April 7 and 8, 1970.

17. Dunegan, H.L., Harris, D.O., and Tetelman, A.S., DETECTION OF FATIGUE CRACK GROWTH BY ACOUSTIC EMISSION TECHNIQUES, Materials Evaluation, Vol. 28, July-December 1970.

18. Paris, P.C., THE FRACTURE MECHANICS APPROACH TO FATIGUE, Proceedings 10th Sagamore Conference, Syracuse University Press, 1965, p. 107.

19. Dunegan, H.L., Harris, D.O., and Tetelman, A.S., PREDICTION OF FATIGUE LIFETIME BY COMBINED FRACTURE MECHANICS AND ACOUSTIC EMISSION TECHNIQUES, Proceedings of the Air Force Conference on Fatigue and Fracture of Aircraft Structures and Materials, Miami Beach, Florida, 15-18 December 1969.

20. Nakamura, T., McCauley, B.O., Gardner, A.H., Redmond, J.C., Hagemeyer, J.W., and Burton, G.M., DEVELOPMENT OF AN ACOUSTIC EMISSION MONITORING SYSTEM, General Dynamics, Ft. Worth, Texas, Report ERR-FW-901 (1969).

21. Moross, George G., INVESTIGATION TO DETERMINE THE FEASIBILITY OF DETECTING IMPENDING METAL FATIGUE FAILURE THROUGH USE OF AN INDUCTIVE SENSING DEVICE, Mechanical Technology Incorporated; USAAVLABS Technical Report 69-97, U.S. Army Aviation Materiel Laboratories, Fort Eustis, Virginia, February 1970, AD871155.

22. Harting, Dar ell R., THE -S/N-FATIGUE-LIFE GAGE: A DIRECT MEANS OF MEASURING CUMULATIVE FATIGUE DAMAGE, Experimental Mechanics, February 1966.

23. EVALUATION OF THE -S/N-FATIGUE-LIFE GAGE UNDER CONSTANT AND VARIABLE AMPLITUDE LOADING, NADC-72071-VT, Naval Air Development Center, 5 September 1972.

24. Horne, Robert S., A FEASIBILITY STUDY FOR THE DEVELOPMENT OF A FATIGUE DAMAGE INDICATOR, AFFDL-TR-66-113, Air Force Flight Dynamics Laboratory, Wright-Patterson AFB, Ohio, January 1967.

25. Horne, Robert S., and Freyre, Oscar L., ANNEALED FOIL FATIGUE SENSOR DEVELOPMENT, AFFDL-TR-71-127, Air Force Flight Dynamics Laboratory, Wright-Patterson AFB, Ohio, March 1972.

26. Maloney, Paul F., and Akeley, Carrol R., DESIGN STUDY OF REPAIRABLE MAIN ROTOR BLADES, Kaman Aerospace Corporation; USAAMRDL Technical Report 72-12, U.S. Army Air Mobility Research and Development Laboratory, Fort Eustis, Virginia, July 1972, AD749283.

27. CH-47A, B, AND C SERIES HELICOPTER ROTOR BLADE FAILURE AND SCRAP RATE DATA ANALYSIS, The Boeing Company, Vertol Division; USAAMRDL Technical Report 71-58, U.S. Army Air Mobility Research and Development Laboratory, Fort Eustis, Virginia, November 1971, AD739568.

APPENDIX A

FLIGHT CONDITION AND DIRECT MONITORING SYSTEMS

FLIGHT CONDITION MONITORING

As discussed earlier, to singularly identify each of the flight conditions of the UH-1H and CH-47C helicopters would require the monitoring of a prohibitively large number of vehicle-state parameters. Tables A-1 and A-2 list the flight conditions and percentage of flight time of each flight condition for the UH-1H and CH-47C, respectively. On the basis of a reduced set of parameters, several recording systems with varying numbers of flight condition categories were formulated for both the UH-1H and the CH-47C. The parameters selected to identify the flight condition categories for the UH-1H and CH-47C are listed in Tables 9 and 14, respectively.

Four recording systems were defined for the UH-1H. Called 1B, 2C, 2CA, and 3A, the systems have 7, 9, 10, and 15 flight condition categories, respectively. System 1B monitors landing gear touchdowns, main rotor rpm, indicated airspeed, and vertical acceleration. Table A-7 describes System 1B. Column 1 of Table A-7 labels each of the flight condition categories. Column 2 identifies the vehicle-state parameters which define each of the flight condition categories. Column 3 lists the parameter threshold value for each flight condition category, and column 4 lists the flight condition numbers grouped into each category. These numbers identify the flight conditions listed in Table A-1. The asterisks in column 4 denote damaging flight conditions. Table 7 ranks the UH-1H flight conditions from most damaging to least damaging. Flight-condition category damage rates for each component were computed by the FCMMOD program (see Appendix B); these rates are listed in Table A-17, where the column labeled "FLIGHT CONDITION CATEGORY" again identifies the flight condition categories. The next 10 columns list the flight condition category damage rates for each of the components. At the bottom of the table is a short description of each of the flight condition categories.

System 2C monitors landing gear touchdowns, main rotor rpm, indicated airspeed, vertical acceleration, and pitch rate. Table A-8 describes System 2C. Flight condition category damage rates are listed in Table A-18. System 2CA monitors landing gear touchdowns, main rotor rpm, indicated airspeed, vertical acceleration, pitch rate, roll rate, and engine torque. Table 12 describes System 2CA. Flight condition category damage rates are listed in Table 13. System 3A monitors landing gear touchdowns, main rotor rpm, indicated airspeed, vertical acceleration, pitch rate, yaw rate, roll rate, and engine torque. Table A-9 describes System 3A. Flight condition category damage rates are listed in Table A-19.

Eight recording systems were defined for the CH-47C. Called I, II, IIA, IIIA, IVA, VA, VI, and VII, the systems have 8, 20, 13, 28, 21, 15, 11, and 45 flight condition categories, respectively. Table A-2 presents the 113 CH-47C flight conditions as determined from the flight loads data. However, monitoring gross weight on the CH-47C presents certain instrumentation problems. As an alternative, two condensed flight spectra for the CH-47C were derived from Table A-2. The first, presented in Table A-3, consists of 43 flight conditions identified by gross weight. The second, presented in Table A-4, consists of 43 flight conditions identified by altitude. Recording systems I, II, IIA, and IIIA are based on the gross weight spectrum, while recording systems IVA, VA, and VI are based on the altitude spectrum. Recording system VII is based on the 113 flight condition gross weight-altitude spectrum. Rankings of the damaging flight conditions for the gross weight, altitude, and gross weight-altitude spectra are presented in Tables A-5, A-6, and 8, respectively.

System I monitors landing gear touchdowns, rotor rpm, indicated airspeed, vertical acceleration, and longitudinal cyclic speed trim position. Table A-10 describes System I. Some of the flight condition numbers in column 4 for some of the CH-47C system descriptions are followed by decimal fractions contained in parentheses. These fractions indicate that not all of the time in that flight condition occurs in a single flight condition category, but rather is distributed among two or more according to the corresponding decimal fractions. Flight condition category damage rates are listed in Table A-20.

System II monitors landing gear touchdowns, rotor rpm, indicated airspeed, vertical acceleration, LCST position, and gross weight. Table A-11 describes System II. Flight condition category damage rates are listed in Table A-21. System IIA monitors landing gear touchdowns, rotor rpm, indicated airspeed, vertical acceleration, gross weight, and LCST position. Table A-12 describes System IIA. Flight condition category damage rates are listed in Table A-22.

System IIIA monitors landing gear touchdowns, rotor rpm, indicated airspeed, vertical acceleration, pitch rate, gross weight, and LCST position. Table A-13 describes System IIIA. Flight condition category damage rates are listed in Table A-23.

System IVA monitors landing gear touchdowns, rotor rpm, indicated airspeed, vertical acceleration, pitch rate, LCST position, and altitude. Table A-14 describes System IVA. Flight condition category damage rates are listed in Table A-24.

System VA monitors landing gear touchdowns, rotor rpm, indicated airspeed, vertical acceleration, and altitude. Table A-15 describes System VA. Flight condition category damage rates are listed in Table A-25.

System VI monitors landing gear touchdowns, rotor rpm, vertical acceleration, pitch rate, roll rate, indicated airspeed, LCST position, and altitude. Table A-16 describes System VI. Flight condition category damage rates are listed in Table A-26.

System VII monitors landing gear touchdowns, rotor rpm, vertical acceleration, pitch rate, roll rate, indicated airspeed, LCST position, altitude, and gross weight. Table 17 describes System VII. Flight condition category damage rates are listed in Table 18.

TABLE A-1. FLIGHT CONDITIONS FOR UH-1H HELICOPTER

Flight Condition Number	Flight Condition	Percent of Flight Time
	Ground Conditions	
1	Normal Rotor Start/Shutdown (with Collective)	1.000
	Power-on Flight	
2	Vertical Takeoff	0.400
	Hovering I.G.E.	
3	Steady	3.290
4	Right Turn	0.100
5	Left Turn	0.100
	Control Reversal	
6	Longitudinal	0.010
7	Lateral	0.010
8	Rudder	0.010
9	Normal Acceleration	1.000
10	Normal Deceleration	1.000
11	Max Rate Acceleration	0.250
12	Max Rate Deceleration	0.250
	Sideward Flight	
13	To the right	0.250
14	To the left	0.250
15	Rearward Flight	0.250
16	Full Power Climb	4.000
	Forward Level Flt.	
17	0.2 Vne	1.000
18	0.3	1.000
19	0.4	2.000
20	0.5	3.000
21	0.6	7.000
22	0.7	8.000
23	0.8	15.000
24	0.9 Vne	25.000
25	Vne	15.000
26	Part-Power Descent	1.000
	Right Turns	
27	0.3 V_H	0.500
28	0.6 V_H	1.000
29	0.9 V_H	0.500
	Left Turns	
30	0.3 V_H	0.500
31	0.6 V_H	1.000
32	0.9 V_H	0.500

TABLE A-1 - Concluded

Flight Condition Number	Flight Condition	Percent of Flight Time
	Power-on Flight (cont'd)	
	Cyclic Pull-Ups	
33	0.6 V_H	0.200
34	0.9 V_H	0.050
	Collective Pull-Ups	
35	0.6 V_H	0.200
36	0.9 V_H	0.050
	0.9 V_H Control Rev.	
37	Longitudinal	0.050
38	Lateral	0.050
39	Rudder	0.050
	Normal Landing	
40	6500 lb Gross Weight	0.100
41	7500 lb Gross Weight	0.300
42	8500 lb Gross Weight	0.450
43	9500 lb Gross Weight	0.150
	Transitions	
	Power to Auto.	
44	0.3 V_H	0.100
45	0.6 V_H	0.200
46	0.9 V_H	0.050
	Auto. to Power	
47	0.4 V_H	0.100
48	0.6 V_H	0.200
49	0.8 V_H	0.050
	Autorotation	
	Steady Forward Flight	
50	0.4 V_H	0.800
51	0.6 V_H	1.000
52	0.8 V_H	0.200
	60 Kt. Control Rev.	
53	Longitudinal	0.010
54	Lateral	0.010
55	Rudder	0.010
	Right Turns	
56	0.4 V_H	0.200
57	0.6 V_H	0.250
58	0.8 V_H	0.050
	Left Turns	
59	0.4 V_H	0.200
60	0.6 V_H	0.250
61	0.8 V_H	0.050
	Auto Landing Appr. W/Power Recovery IGE	
62	0.4 V_H	0.080
63	0.6 V_H	0.100
64	0.8 V_H	0.020
65	Full Auto Landing	0.250

TABLE A-2. FLIGHT CONDITIONS FOR CH-47C HELICOPTER

Flight Condition Number	Flight Condition	Percent of Flight Time	Alt/Gross Wt.
1	Hover	1.980	0-6000/27000
2	Transition	2.970	"
3	70% Vne	4.950	"
4	90% Vne	3.960	"
5	100% Vne	3.960	"
6	Exceed Vne	1.980	"
7	Landing Flare	1.320	"
8	Left Turn	1.610	"
9	Right Turn	1.610	"
10	Collective Pull-Up	.120	"
11	Cyclic Pull-Up	.040	"
12	Longitudinal Reversal	.170	"
13	Lateral Reversal	.180	"
14	Directional Reversal	.140	"
15	Hover	1.670	6000-10000/27000
16	Transition	2.510	"
17	70% Vne	4.180	"
18	90% Vne	3.350	"
19	100% Vne	3.350	"
20	Exceed Vne	1.670	"
21	Landing Flare	0.000	"
22	Left Turn	1.360	"
23	Right Turn	1.360	"
24	Collective Pull-Up	.100	"
25	Cyclic Pull-Up	.030	"
26	Longitudinal Reversal	.140	"
27	Lateral Reversal	.150	"
28	Directional Reversal	.120	"
29	Hover	.420	10000-above/27000
30	Transition	.630	"
31	70% Vne	1.050	"
32	90% Vne	.840	"
33	100% Vne	.840	"
34	Exceed Vne	.420	"
35	Landing Flare	0.000	"
36	Left Turn	.340	"
37	Right Turn	.340	"
38	Collective Pull-Up	.020	"
39	Cyclic Pull-Up	.010	"
40	Longitudinal Reversal	.030	"
41	Lateral Reversal	.040	"
42	Directional Reversal	.030	"
43	Hover	.990	0-6000/33000
44	Transition	1.490	"
45	70% Vne	2.430	"
46	90% Vne	1.930	"
47	100% Vne	1.980	"
48	Exceed Vne	.990	"
49	Landing Flare	.660	"
50	Left Turn	.810	"
51	Right Turn	.810	"
52	Collective Pull-Up	.060	"
53	Cyclic Pull-Up	.020	"
54	Longitudinal Reversal	.080	"
55	Lateral Reversal	.090	"
56	Directional Reversal	.070	"

TABLE A-2 - Concluded

Flight Condition Number	Flight Conditions	Percent of Flight Time	Alt/Gross Wt.
57	Hover	.840	6000-10000/33000
58	Transition	1.260	"
59	70% Vne	2.090	"
60	90% Vne	1.670	"
61	100% Vne	1.670	"
62	Exceed Vne	.840	"
63	Landing Flare	0.000	"
64	Left Turn	.680	"
65	Right Turn	.680	"
66	Collective Pull-Up	.050	"
67	Cyclic Pull-Up	.020	"
68	Longitudinal Reversal	.070	"
69	Lateral Reversal	.070	"
70	Directional Reversal	.060	"
71	Hover	.210	10000-above/33000
72	Transition	.310	"
73	70% Vne	.520	"
74	90% Vne	.420	"
75	100% Vne	.420	"
76	Exceed Vne	.210	"
77	Landing Flare	0.000	"
78	Left Turn	.170	"
79	Right Turn	.170	"
80	Collective Pull-Up	.010	"
81	Cyclic Pull-Up	.004	"
82	Longitudinal Reversal	.020	"
83	Lateral Reversal	.020	"
84	Directional Reversal	.010	"
85	Hover	1.010	0-6000/46000
86	Transition	1.520	"
87	70% Vne	2.530	"
88	90% Vne	2.030	"
89	100% Vne	2.030	"
90	Exceed Vne	1.010	"
91	Landing Flare	.390	"
92	Left Turn	.820	"
93	Right Turn	.820	"
94	Collective Pull-Up	.060	"
95	Cyclic Pull-Up	.020	"
96	Longitudinal Reversal	.080	"
97	Lateral Reversal	.090	"
98	Directional Reversal	.070	"
99	Hover	1.050	6000-above/46000
100	Transition	1.570	"
101	70% Vne	1.570	"
102	90% Vne	2.090	"
103	100% Vne	2.090	"
104	Exceed Vne	1.050	"
106	Left Turn	.850	"
107	Right Turn	.850	"
108	Collective Pull-Up	.060	"
109	Cyclic Pull-Up	.020	"
110	Longitudinal Reversal	.090	"
111	Lateral Reversal	.090	"
112	Directional Reversal	.070	"
113	Rotor Start/Stop	.250	

TABLE A-3. CH-47C FLIGHT CONDITIONS BY GROSS WEIGHT

Flight Condition Number	Flight Condition	Gross Weight (lb)
1	Hover	27000
2	Transition	27000
3	70% Vne	27000
4	90% Vne	27000
5	100% Vne	27000
6	Exceed Vne	27000
7	Landing Flare	27000
8	Left Turn	27000
9	Right Turn	27000
10	Longitudinal Pull-Up	27000
11	Collective Pull-Up	27000
12	Longitudinal Reversal	27000
13	Lateral Reversal	27000
14	Directional Reversal	27000
15	Hover	33000
16	Transition	33000
17	70% Vne	33000
18	90% Vne	33000
19	100% Vne	33000
20	Exceed Vne	33000
21	Landing Flare	33000
22	Left Turn	33000
23	Right Turn	33000
24	Longitudinal Pull-Up	33000
25	Collective Pull-Up	33000
26	Longitudinal Reversal	33000
27	Lateral Reversal	33000
28	Directional Reversal	33000
29	Hover	46000
30	Transition	46000
31	70% Vne	46000
32	90% Vne	46000
33	100% Vne	46000
34	Exceed Vne	46000
35	Landing Flare	46000
36	Left Turn	46000
37	Right Turn	46000
38	Longitudinal Pull-Up	46000
39	Collective Pull-Up	46000
40	Longitudinal Reversal	46000
41	Lateral Reversal	46000
42	Directional Reversal	46000
43	Rotor Start/Stop	

TABLE A-4. CH-47C FLIGHT CONDITIONS BY ALTITUDE

Flight Condition Number	Flight Condition	Altitude (feet)
1	Hover	0-5000
2	Transition	0-5000
3	60-70% Vne	0-5000
4	90% Vne	0-5000
5	100% Vne	0-5000
6	Exceed Vne	0-5000
7	Landing Flare	0-5000
8	Left Turn	0-5000
9	Right Turn	0-5000
10	Collective Pull-Up	0-5000
11	Longitudinal Pull-Up	0-5000
12	Longitudinal Reversal	0-5000
13	Lateral Reversal	0-5000
14	Directional Reversal	0-5000
15	Hover	5000-9000
16	Transition	5000-9000
17	60-70% Vne	5000-9000
18	90% Vne	5000-9000
19	100% Vne	5000-9000
20	Exceed Vne	5000-9000
21	Landing Flare	5000-9000
22	Left Turn	5000-9000
23	Right Turn	5000-9000
24	Collective Pull-Up	5000-9000
25	Longitudinal Pull-Up	5000-9000
26	Longitudinal Reversal	5000-9000
27	Lateral Reversal	5000-9000
29	Directional Reversal	5000-9000
29	Hover	9000 and Above
30	Transition	9000 and Above
31	60-70% Vne	9000 and Above
32	90% Vne	9000 and Above
33	100% Vne	9000 and Above
34	Exceed Vne	9000 and Above
35	Landing Flare	9000 and Above
36	Left Turn	9000 and Above
37	Right Turn	9000 and Above
38	Collective Pull-Up	9000 and Above
39	Longitudinal Pull-Up	9000 and Above
40	Longitudinal Reversal	9000 and Above
41	Lateral Reversal	9000 and Above
42	Directional Reversal	9000 and Above
43	Rotor Start/Stop Cycles	

TABLE A-5. RANKED FLIGHT CONDITIONS BY GROSS WEIGHT FOR THE CH-47C

Rank	Flight Condition	Gross Weight (lb)	Percent of Flight Time
1	Cyclic Pull-Up	33000	.147
2	Longitudinal Reversal	27000	.416
3	Landing Flare	46000	.830
4	Longitudinal Reversal	33000	.207
5	Collective Pull-Up	33000	.049
6	Cyclic Pull-Up	27000	.294
7	Collective Pull-Up	46000	.049
8	Lateral Reversal	46000	.221
9	Lateral Reversal	27000	.443
10	Transition	46000	2.895
11	Exceed V_{ne}	46000	1.930
12	Exceed V_{ne}	33000	1.930
13	Cyclic Pull-Up	46000	.147
14	Lateral Reversal	33000	.221
15	Left Turn	46000	2.038
16	Longitudinal Reversal	46000	.207
17	Directional Reversal	33000	.170
18	Right Turn	46000	2.038
19	Directional Reversal	27000	.341
20	Left Turn	33000	2.038
21	Right Turn	33000	2.038
22	Left Turn	27000	4.075
23	Rotor Start/Stop	--	.250
24	Right Turn	27000	4.075

TABLE A-6. RANKED FLIGHT CONDITIONS BY ALTITUDE FOR THE CH-47C

Rank	Flight Condition	Altitude	Percent of Flight Time
1	Cyclic Pull-Up	0-6000 ft	.094
2	Longitudinal Reversal	10000 ft-above	.052
3	Exceed V_{ne}	10000 ft-above	6.278
4	Longitudinal Reversal	0-6000 ft	.396
5	Cyclic Pull-Up	6000-10000 ft	.055
6	Longitudinal Reversal	6000-10000 ft	.231
7	Landing Flare	0-6000 ft	2.658
8	Collective Pull-Up	0-6000 ft	.281
9	Cyclic Pull-Up	10000 ft-above	.012
10	Collective Pull-Up	6000-10000 ft	.164
11	Lateral Reversal	6000-10000 ft	.246
12	Lateral Reversal	0-6000 ft	.422
13	Transition	0-6000 ft	11.961
14	Left Turn	6000-10000 ft	2.253
15	Left Turn	10000 ft-above	.510
16	Exceed V_{ne}	0-6000 ft	7.973
17	Directional Reversal	0-6000 ft	.338
18	Directional Reversal	6000-10000 ft	.197
19	70% V_{ne}	6000-10000 ft	20.926
20	70% V_{ne}	0-6000 ft	19.934
21	Lateral Reversal	10000 ft-above	.056
22	Right Turn	0-6000 ft	3.857
23	Exceed V_{ne}	6000-10000 ft	8.370
24	Rotor Start/Stop	--	.250
25	Left Turn	0-6000 ft	3.857
26	Right Turn	6000-10000 ft	2.253
27	Right Turn	10000 ft-above	.510

TABLE A-7. SYSTEM 1B

Flight Condition Category	Parameters	Thresholds (& Tolerance)	Flight Conditions Included
0	Clock time	--	2, 3, 4, 5, 6*, 7, 8, 11, 12*, 13*, 14, 15, 16, 17*, 18*, 19, 20, 26, 27, 30, 44, 47, 50, 53, 54, 55, 56, 59, 62*, 63, 64, 45, 46
1	Landing gear touchdown	--	40, 41*, 42*, 43*, 65*
2	Rotor rpm	100 rpm ±10 rpm	1*
3	A/S above threshold Vertical accel above threshold	80 kt ±3 kt 1.2 g ±.0375 g	29*, 32*, 34*, 36*, 37*
4	A/S between threshold Vertical accel above threshold	55-80 kt 1.2 g ±.0375 g	28*, 31*, 33, 35* 48*, 49*
5	A/S above threshold Vertical accel betw. "g" threshold	80 kt 3 kt .8 g < Nz < 1.2 g	24, 25, 38*, 39
6	A/S between threshold Vertical accel betw. "g" threshold	55-80 kt .8 g < Nz < 1.2 g	9, 10*, 21, 22, 23 51, 52, 57, 58, 60, 61

* Damaging flight conditions; flight condition numbers correlate with those in Table A-1.

TABLE A-8. SYSTEM 2C

Flight Condition Category	Parameters	Thresholds (& Tolerance)	Flight Conditions Included
0	Clock time	--	2, 3, 4, 5, 6*, 7, 8, 11, 12*, 13*, 14, 15, 16, 17*, 18*, 19, 20, 26, 27, 30, 44, 47, 50, 53, 54, 55, 56, 59, 62*, 63, 64, 45, 46
1	Landing gear touchdown	--	40, 41*, 42*, 43*, 65*
2	Rotor rpm	100 rpm ±10 rpm	1*
3	A/S above threshold Vertical accel above threshold Pitch rate above threshold	80 kt ±3 kt 1.2 g ±.0375 g 10°/sec ±.5°/sec	34*, 36*, 37*
4	A/S above threshold Vertical accel above threshold Pitch rate below threshold	80 kt ±3 kt 1.2 g ±.0375 g 10°/sec ±.5°/sec	29*, 32*
5	A/S between threshold Vertical accel above threshold Pitch rate above threshold	55-80 kt 1.2 g ±.0375 g 10°/sec ±.5°/sec	33, 35*
6	A/S between threshold Vertical accel above threshold Pitch rate below threshold	55-80 kt 1.2 g ±.0375 g 10°/sec ±.5°/sec	28, 31*, 48*, 49*
7	A/S above threshold Vertical accel betw. "g" threshold	80 kt ±3 kt .8 g < Nz < 1.2 g	24, 25, 38*, 39
8	A/S between threshold Vertical accel betw. "g" threshold	55-80 kt .8 g < Nz < 1.2 g	9, 10, 21, 22, 23 51, 52, 57, 58, 60, 61

* Damaging flight conditions; flight condition numbers correlate with those in Table A-1.

TABLE A-9. SYSTEM 3A

Flight Condition Category	Parameters	Thresholds (& Tolerance)	Flight Conditions Included
0	Clock time	--	2, 3, 4, 5, 6*, 7, 8, 11, 12*, 13*, 14, 15, 16, 17*, 18*, 19, 20, 26, 27, 30, 44, 46, 47, 55, 50, 53, 54, 56, 59, 62*, 63, 64, 45
1	Landing gear touchdown	--	40, 41*, 42*, 43*
2	Power buss and landing gear	--	65*
3	Rotor rpm	100 rpm ±10 rpm	1*
4	A/S between thresholds	55-80 kt	9. 10*, 21, 22, 23, 51, 52, 57, 58, 60, 61
5	A/S above threshold	80 kt ±3 kt	24, 25
6	A/S between thresholds Roll rate above threshold Yaw rate above threshold	55-80 kt 5°/sec ±.1°/sec 5°/sec ±.1°/sec	28*
7	A/S above threshold Roll rate above threshold Yaw rate above threshold	80 kt ±3 kt 5°/sec ±.1°/sec 5°/sec ±.1°/sec	29*
8	A/S between thresholds Roll rate above threshold Yaw rate above threshold	55-80 kt 5°/sec ±.1°/sec 5°/sec ±.1°/sec	31*
9	A/S above threshold Roll rate above threshold Yaw rate above threshold	80 kt ±3 kt 5°/sec ±.1°/sec 5°/sec ±.1°/sec	32*
10	Pitch rate above threshold A/S between threshold	10°/sec ±.5°/sec 55-80 kt	33, 35*
11	Pitch rate above threshold A/S above threshold	10°/sec ±.5°/sec 80 kts ±3 kts	34*, 36*, 37*
12	Pitch rate below threshold A/S between threshold	10°/sec ±.5°/sec 55-80 kts	48*, 49*
13	Roll rate above threshold A/S above threshold A/S above threshold	5°/sec ±.1°/sec 80 kts 80 kts ±3 kts	38*
14	Yaw rate above threshold A/S above threshold	5°/sec ±.1°/sec 80 kts ±3 kts	39

* Damaging flight conditions; flight condition numbers correlate with those in Table A-1.

TABLE A-10. SYSTEM I

Flight Condition Category	Parameters	Thresholds (& Tolerance)	Flight Conditions Included
0	Clock time	--	1(.985), 2, 12*, 13*, 14*, 15(.985), 16, 26*, 27*, 28, 29(.985), 30*, 40*, 41*, 42
1	Power buss & landing gear	--	7, 21, 35*
2	Rotor rpm	100 rpm ±10 rpm	43*
3	Vertical accel above threshold	1.2 g ±.0375 g	10*, 11*, 24*, 25*, 38*, 39*
4	Airspeed LCST position	V < 60 kt Extended	1, 15, 29
5	Airspeed	84 kt < V < 140 kt	3(.985), 4(.985), 8*(.900), 9*(.900), 17(.985), 18(.985), 19(.985), 22*(.900), 23*(.900), 31*(.985), 32(.985), 33(.985), 36*(.900), 37*(.900)
6	Airspeed	V > 140 kt	6(.985), 8*(.100), 9*(.100), 20*(.985), 22*(.100), 23*(.100), 34*(.985), 36*(.100), 37*(.100)
7	Airspeed LCST position	V > 80 kt Retracted	3(.015), 4(.015), 5(.015), 6(.015), 17(.015), 18(.015), 19(.015), 20*(.015), 31*(.015), 32(.015), 33(.015), 34*(.015)

* Damaging flight condition; flight condition numbers correlate with those in Table A-3; decimals within parentheses represent fraction of time of flight condition in corresponding flight condition category.

TABLE A-11. SYSTEM II

Flight Condition Category	Parameters	Thresholds (& Tolerance)	Flight Conditions Included
0	Clock time	--	--
1	Landing gear touchdowns	--	7, 21, 35*
2	Rotor rpm	100 rpm ±10 rpm	43*
3	Vertical accel above threshold	1.2 g ±.0375 g	10*, 11, 12*, 24*, 25*, 26*, 38*, 39*, 40*
4	Airspeed LCST position	V < 60 kt Extended	1(.015), 15(.015), 29(.015)
5	Airspeed LCST position Gross Weight	V < 84 kt Retracted GW < 33000	1(.985)
6	Airspeed LCST position Gross Weight	V < 84 kt Retracted 33000 < V < 40000	15(.985)
7	Airspeed LCST position Gross Weight	V < 84 kt Retracted 40000 < V < 46000	29(.492)
8	Airspeed LCST position Gross Weight	V < 84 kt Retracted GW > 46000	29(.493)
9	Airspeed LCST position Gross Weight	84 kt < V < 140 kt Extended GW < 33000	2, 3(.985), 4(.985), 5(.985) 8*, 9*, 13*, 14*
10	Airspeed LCST position Gross Weight	84 kt < V < 140 kt Extended 33000 < GW < 40000	16, 17(.985), 18(.985), 19(.985), 22*, 23*, 27*, 28

* Damaging flight condition; flight condition numbers correlate with those in Table A-3; decimals within parentheses represent fraction of time of flight condition in corresponding flight condition category

TABLE A-11 - Concluded

Flight Condition Category	Parameters	Thresholds (& Tolerance)	Flight Conditions Included
11	Airspeed LCST position Gross Weight	84 kt < V < 140 kt Extended 40000 < GW < 46000	31*(.492), 32(.492), 33(.492)
12	Airspeed LCST position Gross Weight	84 kt < V < 140 kt Extended GW > 46000	30*, 31*(.492), 32(.493), 33(.493), 36*, 37*, 41*, 42
13	Airspeed LCST position Gross Weight	V > 140 kt Extended GW < 33000	6(.985)
14	Airspeed LCST position Gross Weight	V > 140 kt Extended 33000 < GW < 40000	20*(.985)
15	Airspeed LCST position Gross Weight	V > 140 kt Extended 40000 < GW < 46000	34*(.492)
16	Airspeed LCST position Gross Weight	V > 140 kt Extended GW > 46000	34*(.493)
17	Airspeed LCST position Gross Weight	V > 76 kt Retracted GW < 33000	3(.015), 4(.015), 5(.015), 6(.015)
18	Airspeed LCST position Gross Weight	V > 88 kt Retracted 33000 < GW < 40000	17(.015), 18(.015), 19(.015), 20*(.015)
19	Airspeed LCST position Gross Weight	V > 96 kt Retracted GW > 46000	31*(.015), 32(.015), 33(.015), 34*(.015)

* Damaging flight condition; flight condition numbers correlate with those in Table A-3; decimals within parentheses represent fraction of time of flight condition in corresponding flight condition category.

TABLE A-12. SYSTEM IIA

Flight Condition Category	Parameters	Thresholds (& Tolerance)	Flight Conditions Included
0	Clock time	--	1(.015), 2, 3(.985), 4(.985), 5(.985), 6(.985), 13*, 14*, 15(.015), 16, 17(.985), 18(.985), 19(.985), 20*(.985), 27*, 28, 29(.015), 30*, 31*(.985), 32(.985), 33(.985), 34*(.985), 41*, 42
1	Landing gear touchdowns Gross Weight	-- GW > 46000	35*
2	Rotor rpm	100 rpm ±10 rpm	43*
3	Vertical accel above threshold Gross Weight	1.2 g ±.0375 g GW > 46000	38*, 39*, 40*
4	Vertical accel above threshold Gross Weight	1.2 g ±.0375 g 40000 < GW < 46000	--
5	Vertical accel above threshold Gross Weight	1.2 g ±.0375 g 33000 < GW < 40000	21, 24*, 25*, 26*
6	Vertical accel above threshold Gross Weight	1.2 g ±.0375 g GW < 33000	7, 10*, 11, 12*
7	Airspeed LCST position	V < 84 kt Programmed	1(.985), 15(.985), 29(.985)
8	Airspeed LCST position Gross Weight	84 kt < V < 140 kt Programmed GW > 46000	--
9	Airspeed LCST position Gross Weight	V > 76 kt Retracted GW < 33000	3(.015), 4(.015), 5(,015), 6(.015)
10	Airspeed LCST position Gross Weight	V > 88 kt Retracted 33000 < GW < 40000	17(.015), 18(.015), 19(.015), 20*(.015)
11	Airspeed LCST position Gross Weight	V > 96 kt Retracted GW > 40000	31*(.015), 32(.015), 33(.015), 34*(.015)
12	Roll rate above threshold Yaw rate above threshold	5°/sec ±.1°/sec 5°/sec ±.1°/sec	8*, 9*, 22*, 23*, 36*, 37*

* Damaging flight condition; flight condition numbers correlate with those in Table A-3; decimals within parentheses represent fraction of time of flight condition in corresponding flight condition category.

TABLE A-13. SYSTEM IIIA

Flight Condition Category	Parameters	Thresholds (& Tolerance)	Flight Conditions Included
0	Clock time	--	1(.985), 2, 3(.985), 4(.985), 5(.985), 13*, 14*, 15(.985), 16, 17(.985), 18(.985), 19(.985), 27*, 28, 29(.985), 30*, 31*(.985), 32(.985), 33(.985), 41*, 42
1	Landing gear touchdowns	--	7, 21, 35*
2	Rotor rpm	100 rpm ±10 rpm	43*
3	Airspeed LCST position	V < 60 kt Extended	1(.015), 15(.015), 29(.015)
4	Airspeed LCST position Gross Weight	V > 76 kt Retracted GW < 33000	3(.015), 4(.015), 5(.015), 6(.015)
5	Airspeed LCST position Gross Weight	V > 88 kt Retracted 33000 < GW < 40000	17(.015), 18(.015), 19(.015), 20*(.015)
6	Airspeed LCST position Gross Weight	V > 96 kt Retracted GW > 40000	31*(.015), 32(.015), 33(.015), 34*(.015)
7	Airspeed Gross Weight	84 kt < V < 140 kt GW > 46000	--
8	Airspeed Gross Weight	V > 140 kt GW > 46000	--
9	Airspeed Gross Weight	V > 140 kt 40000 < V < 46000	10*(.985)

* Damaging flight condition; flight condition numbers correlate with those in Table A-3; decimals within parentheses represent fraction of time of flight condition in corresponding flight condition category.

TABLE A-13 - Continued

Flight Condition Category	Parameters	Thresholds (& Tolerance)	Flight Conditions Included
10	Airspeed Gross Weight	V > 140 kt 33000 < V < 40000	20*(.985)
11	Airspeed Gross Weight	V > 140 kt GW < 33000	6(.985)
12	Airspeed Vertical accel above threshold Gross Weight	84 kt < V < 112 kt 1.2 g ±.0375 g GW > 46000	--
13	Airspeed Vertical accel above threshold Gross Weight	84 kt < V < 112 kt 1.2 g ±.0375 g 40000 < GW < 46000	39*(.500)
14	Airspeed Vertical accel above threshold Gross Weight	84 kt < V < 112 kt 1.2 g ±.0375 g 33000 < GW < 40000	25*(.500)
15	Airspeed Vertical accel above threshold Gross Weight	84 kt < V < 112 kt 1.2 g ±.0375 g GW < 33000	11(.500)
16	Airspeed Vertical accel above threshold Gross Weight	112 kt < V < 140 kt 1.2 g ±.0375 g GW > 46000	--
17	Airspeed Vertical accel above threshold Gross Weight	112 kt < V < 140 kt 1.2 g ±.0375 g 40000 < GW < 46000	--
18	Airspeed Vertical accel above threshold Gross Weight	112 kt < V < 140 kt 1.2 g ±.0375 g 33000 < GW < 40000	25*(.500)

* Damaging flight condition; flight condition numbers correlate with those in Table A-3; decimals within parentheses represent fraction of time of flight condition in corresponding flight condition category.

TABLE A-13 - Concluded

Flight Condition Category	Parameters	Thresholds (& Tolerance)	Flight Conditions Included
19	Airspeed Vertical accel above threshold Gross Weight	112 kt < V < 140 kt 1.2 g ±.0375 g GW < 33000	11(.500)
20	Airspeed Pitch rate above threshold Gross Weight	84 kt < V < 112 kt 10°/sec ±.5°/sec GW > 46000	--
21	Airspeed Pitch rate above threshold Gross Weight	84 kt < V < 112 kt 10°/sec ±.5°/sec 40000< GW < 46000	--
22	Airspeed Pitch rate above threshold Gross Weight	84 kt < V < 112 kt 10°/sec ±.5°/sec 33000 < GW < 40000	22*(.500), 23*(.500), 24*(.500), 26*(.500)
23	Airspeed Pitch rate above threshold Gross Weight	84 kt < Vne < 112 kt 10°/sec ±.5°/sec GW < 33000	8*(.500), 9*(.500), 10*(.500), 12*(.500)
24	Airspeed Pitch rate above threshold Gross Weight	112 kt < V < 140 kt 10°/sec ±.5°/sec GW > 46000	--
25	Airspeed Pitch rate above threshold Gross Weight	112 kt < V < 140 kt 10°/sec ±.5°/sec 40000 < GW < 46000	36*(.500), 37*(.500), 38*(.500), 40*(.500)
26	Airspeed Pitch rate above threshold Gross Weight	112 kt < V < 140 kt 10°/sec ±.5°/sec 33000 < GW < 40000	22*(.500), 23*(.500), 24*(.500), 26*(.500)
27	Airspeed Pitch rate above threshold Gross Weight	112 kt < V < 140 kt 10°/sec ±.5°/sec GW < 33000	8*(.500), 9*(.500), 10*(.500), 12*(.500)

* Damaging flight condition; flight condition numbers correlate with those in Table A-3; decimals within parentheses represent fraction of time of flight condition in corresponding flight condition category.

TABLE A-14. SYSTEM IVA

Flight Condition Category	Parameters	Thresholds (& Tolerance)	Flight Conditions Included
0	Clock time	--	1(.985), 2*, 3*(.985), 4(.985), 5(.985), 13*, 14*, 15(.985), 16, 17*(.985), 18(.985), 19(.985), 27*, 28*, 29(.985), 30, 31*(.985), 32(.985), 33(.985), 41*, 42
1	Landing gear touchdowns	--	7*, 21, 35
2	Rotor rpm	100 rpm ±10 rpm	43*
3	Vertical accel above threshold	1.2 g ±.0375 g	--
4	Altitude Airspeed Vertical accel above threshold	0 < ALT < 5000 84 kt < V < 112 kt 1.2 g ±.0375 g	10*(.500), 11*(.500), 12*(.500)
5	Altitude Airspeed Vertical accel above threshold	0 < ALT < 5000 112 kt < V < 140 kt 1.2 g ±.0375 g	10*(.500), 11*(.500), 12*(.500)
6	Altitude Airspeed	0 < ALT < 5000 V > 150 kt	6*(.985)
7	Altitude Airspeed Pitch rate above threshold	0 < ALT < 5000 84 kt < V < 112 kt 10°/sec ±.5°/sec	8*(.500), 9*(.500)
8	Altitude Airspeed Pitch rate above threshold	0 < ALT < 5000 112 kt < V < 140 kt 10°/sec ±.5°/sec	8*(.500), 9*(.500)
9	Altitude Airspeed Vertical accel above threshold	5000 < ALT < 9000 84 kt < Vne < 112 kt 1.2 g ±.0375 g	24*(.250), 25*(.250), 26*(.250)
10	Altitude Airspeed Vertical accel above threshold	5000 < ALT < 9000 112 kt < V < 140 kt 1.2 g ±.0375 g	24*(.750), 25*(.750), 26*(.750)
11	Altitude Airspeed	5000 < ALT < 9000 V > 140 kt	20*(.985)

* Damaging flight condition; flight condition numbers correlate with those in Table A-4; decimals within parentheses represent fraction of time of flight condition in corresponding flight condition category.

TABLE A-14 - Concluded

Flight Condition Category	Parameters	Thresholds (& Tolerance)	Flight Conditions Included
12	Altitude Airspeed Pitch rate above threshold	5000 < ALT < 9000 84 kt < V < 112 kt 10°/sec ±.5°/sec	22*(.250), 23*(.250)
13	Altitude Airspeed Pitch rate above threshold	5000 < ALT < 9000 112 kt < V < 140 kt 10°/sec ±.5°/sec	22*(.750), 23*(.750)
14	Altitude Airspeed Vertical accel above threshold	ALT > 9000 84 kt < V < 112 kt 1.2 g ±.0375 g	38*(.200), 39*(.200), 40*(.200)
15	Altitude Airspeed Vertical accel above threshold	ALT > 9000 112 kt < V < 140 kt 1.2 g ±.0375 g	38(.800), 39*(.800), 40*(.800)
16	Altitude Airspeed	ALT > 9000 V > 140 kt	34*(.985)
17	Altitude Airspeed Pitch rate above threshold	ALT > 9000 84 kt < V < 112 kt 10°/sec ±.5°/sec	36*(.200), 37*(.200)
18	Altitude Airspeed Pitch rate above threshold	ALT > 9000 112 kt < V < 140 kt 10°/sec ±.5°/sec	36*(.800), 37*(.800)
19	Airspeed LCST position	V < 60 kt Extended	1(.015), 15(.015), 29(.015)
20	Airspeed LCST position	V > 80 kt Retracted	3*(.015), 4(.015), 5(.015), 6*(.015), 17*(.015), 18(.015), 19(.015), 20*(.015), 31*(.015), 32(.015), 33(.015), 34*(.015)

* Damaging flight condition; flight condition numbers correlate with those in Table A-4; decimals within parentheses represent fraction of time of flight condition in corresponding flight condition category.

TABLE A-15. SYSTEM VA

Flight Condition Category	Parameters	Thresholds (& Tolerance)	Flight Conditions Included
0	Clock time	--	1(.985), 8*(.500), 9*(.500), 13*, 14*, 15(.985), 22*(.500), 23*(.500), 27*, 28*, 29(.985), 31*(.200), 32(.200), 33(.300), 36*(.500), 37*(.500), 41*, 42
1	Landing gear touchdowns	--	7*, 21, 35
2	Rotor rpm	100 rpm ±10 rpm	43*
3	Vertical accel above threshold Pitch rate below threshold	1.2 g ±.0375 g 10°/sec ±.5°/sec	2*(.500), 10*(.500), 11*(.500), 12*(.500), 16(.500), 24*(.500), 25*(.500), 26*(.500), 30(.500), 38*(.500), 39*(.500), 40*(.500)
4	Vertical accel above threshold Pitch rate above threshold	1.2 g ±.0375 g 10°/sec ±.5°/sec	2*(.500), 8*(.500), 9*(.500), 10*(.500), 11*(.500), 12*(.500), 16(.500), 22*(.500), 23*(.500), 24*(.500), 25*(.500), 26*(.500), 30(.500), 37*(.500), 38*(.500), 39*(.500), 40*(.500)
5	Airspeed LCST position	V < 60 kt Extended	1(.015), 15(.015), 29(.015)
6	Airspeed LCST position	V > 80 kt Retracted	3*(.015), 4(.015), 5(.015), 6*(.015), 17*(.015), 18(.015), 19(.015), 31*(.015), 32(.015), 33(.015)
7	Airspeed Altitude	60 kt < V < 110 kt ALT < 5000	3*(.200), 4(.150), 5(.100)
8	Airspeed Altitude	110 kt < V < 170 kt ALT < 5000	3*(.785), 4(.835), 5(.835)

* Damaging flight condition; flight condition numbers correlate with those in Table A-4; decimals within parentheses represent fraction of time of flight condition in corresponding flight condition category.

TABLE A-15 - Concluded

Flight Condition Category	Parameters	Thresholds (& Tolerance)	Flight Conditions Included
9	Airspeed Altitude	V > 170 kt ALT < 5000	5(.050)
10	Airspeed Altitude	60 kt < V < 140 kt 5000 < ALT < 9000	17*(.985), 18(.350), 19(.300)
11	Airspeed Altitude	140 kt < V < 170 kt 5000 < ALT < 9000	18(.635), 19(.685)
12	Airspeed Altitude	60 kt < V < 100 kt ALT > 9000	31*(.785(, 32(.400), 33(.400)
13	Airspeed Altitude	100 kt < V < 125 kt ALT > 9000	32(.385), 33(.285)
14	Airspeed	V > Vne	6*(.985), 20*, 34*

* Damaging flight condition; flight condition numbers correlate with those in Table A-4; decimals within parentheses represent fraction of time of flight condition in corresponding flight condition category.

TABLE A-16. SYSTEM VI

Flight Condition Category	Parameters	Thresholds	Flight Conditions Included
0	Clock time	--	1, 2*, 3*, 4, 5, 14*, 16, 17*, 18, 19, 21, 28*, 29, 30, 31*, 32, 33, 35, 42
1	Landing gear touchdown	--	7
2	Rotor rpm	Start/stop cycles	43*
3	Vertical accel above threshold	1.2 g ±.0375 g	10*, 11*, 24*, 25*, 38*, 39*
4	Pitch rate	P > 10°/sec ±.5°/sec	12*, 26*, 40*
5	Roll rate	R > 5°/sec ±.1°/sec	8*, 9*, 13*, 22*, 23*, 27*, 36*, 37*, 41*
6	Altitude Airspeed	0 < ALT < 5000 V > 145 kt	6*
7	Altitude Airspeed	5000 < ALT < 9000 V > 125 kt	20*
8	Altitude Airspeed	ALT > 9000 V > 100 kt	34*
9	Airspeed LCST position	V < 60 kt Extended	--
10	Airspeed LCST position	V > 80 kt Retracted	--

* Damaging flight condition; flight condition numbers correlate with those in Table A-4; decimals within parentheses represent fraction of time of flight condition in corresponding flight condition category.

TABLE A-17. FDAM CONSTANTS, C_{ij}, FOR UH-1H FCM SYSTEM 1B

*FLIGHT CONDITION CATEGORY	COMPONENT(i)									
	1	2	3	4	5	6	7	8	9	10
	MAIN ROTOR RETENTION STRAP	MAIN ROTOR YOKE	STABILIZER BAR	MAIN ROTOR DRAG BRACE	SWASHPLATE SUPPORT	COLLECTIVE LEVER	MAIN ROTOR PITCH HORN	MAIN ROTOR SCISSORS	MAIN ROTOR GRIP	MAIN ROTOR BLADE
0	0.	0.	0.	.5370E-04	0.	0.	.2490E-05	.3850E-05	.7430E-06	.6180E-03
1	0.	0.	.2770E-01	0.	.7030E-02	.5000E-02	0.	.2740E-03	.2830E-03	.7790E-02
2	.3280E-01	0.	0.	0.	0.	0.	0.	0.	0.	0.
3	0.	.7190E-02	0.	.2220E-01	.1540E-01	.1330E-01	.1500E-01	.2840E-01	.1730E-02	.5100E-02
4	0.	0.	0.	0.	.2050E-02	.2230E-02	.5120E-03	.2380E-03	.2060E-03	.4030E-02
5	0.	0.	0.	.1320E-03	.5410E-05	.4300E-05	.1720E-05	.3690E-05	.3920E-05	.1410E-04
6	0.	0.	0.	0.	0.	0.	0.	.5120E-05	0.	.1980E-04

*FLIGHT CONDITION CATEGORY

0 Total flight time not recorded in categories 3-8
1 Number of landing gear touchdowns
2 Number of rotor shutdowns
3 Time at V > 80 kt, n_z > 1.2 g
4 Time at 55 kt < V < 80 kt, n_z > 1.2 g
5 Time at V > 80 kt, .8 g < n_z < 1.2 g
6 Time at 55 kt < V < 80 kt, .8 g < n_z < 1.2 g

TABLE A-18. FDAM CONSTANTS, C_{ij}, FOR UH-1H FCM SYSTEM 2C

*FLIGHT CONDITION CATEGORY	COMPONENT(i)									
	1	2	3	4	5	6	7	8	9	10
	MAIN ROTOR RETENTION STRAP	MAIN ROTOR YOKE	STABILIZER BAR	MAIN ROTOR DRAG BRACE	SWASHPLATE SUPPORT	COLLECTIVE LEVER	MAIN ROTOR PITCH HORN	MAIN ROTOR SCISSORS	MAIN ROTOR GRIP	MAIN ROTOR BLADE
0	0.	0.	0.	.5370E-04	0.	0.	.1490E-05	.3890E-05	.7450E-06	.6150E-03
1	0.	0.	.8170E-01	0.	.7090E-03	.6[illegible]E-03	0.	.1740E-03	.2830E-03	.7730E-02
2	.3290E-01	0.	0.	0.	0.	0.	0.	0.	0.	0.
3	0.	.9510E-01	0.	.1700E+00	.3930E-01	.7210E-1	.3200E-01	.6710E-01	.1330E-01	.2740E-01
4	0.	0.	0.	0.	.4680E-03	.1020E-[illegible]	.1300E-01	.3030E-01	0.	.1760E-02
5	0.	0.	0.	0.	.2070E-03	.2050E-03	.1[illegible]07E-02	.1590E-02	.1360E-03	.8420E-02
6	0.	0.	0.	0.	.2[illegible]0E-01	.2[illegible]E-03	.5[illegible]0E-04	.7470E-04	0.	.4310E-02
7	0.	0.	0.	.1220E-03	.5410E-[illegible]	.4[illegible]0E-[illegible]	.1730E-05	.3[illegible]90E-05	.3920E-05	.1410E-04
8	0.	0.	0.	0.	0.	0.	0.	.5130E-05	0.	.1430E-04

*FLIGHT CONDITION CATEGORY

0 Total flight time not recorded in categories 3-10
1 Number of landing gear touchdowns
2 Number of rotor shutdowns
3 Time at V > 80 kt, n_z > 1.2 g, P > PT
4 Time at V > 80 kt, n_z > 1.2 g, P < PT
5 Time at 55 kt < V < 80 kt, n_z > 1.2 g, P > PT
6 Time at 55 kt < V < 80 kt, n_z > 1.2 g, P < PT
7 Time at V > 80 kt, .8 g < n_z < 1.2 g
8 Time at 55 kt < V < 80 kt, .8 g < n_z < 1.2 g

TABLE A-19. FDAM CONSTANTS, C_{ij}, FOR UH-1H FCM SYSTEM 3A

*FLIGHT CONDITION CATEGORY	COMPONENT(i)									
	1	2	3	4	5	6	7	8	9	10
	MAIN ROTOR RETENTION STRAP	MAIN ROTOR YOKE	STABILIZER BAR	MAIN ROTOR DRAG BRACE	SWASHPLATE SUPPORT	COLLECTIVE LEVER	MAIN ROTOR PITCH HORN	MAIN ROTOR SCISSORS	MAIN ROTOR GRIP	MAIN ROTOR BLADE
0	0.	0.	0.	.5370E-04	0.	0.	.2490E-05	.3890E-05	.7480E-06	.6180E-03
1	0.	0.	0.	0.	0.	0.	0.	0.	.3530E-03	.9540E-02
2	0.	0.	.1190E+00	0.	.2540E-01	.3000E-01	0.	.1370E-02	0.	.8200E-03
3	.3280E-01	0.	0.	0.	0.	0.	0.	0.	0.	0.
4	0.	0.	0.	0.	0.	0.	0.	.5120E-05	0.	.1980E-04
5	0.	0.	0.	0.	0.	0.	0.	0.	0.	0.
6	0.	0.	0.	0.	0.	0.	0.	0.	0.	.3400E-03
7	0.	0.	0.	0.	.8560E-02	.7110E-02	.1250E-01	.2610E-01	0.	.8220E-03
8	0.	0.	0.	0.	0.	0.	0.	0.	0.	.4320E-02
9	0.	0.	0.	0.	0.	0.	.1480E-01	.1450E-01	0.	.2690E-02
10	0.	0.	0.	0.	.3070E-03	.2050E-03	.3070E-02	.1560E-02	.1360E-02	.2420E-02
11	0.	.5510E-01	0.	.1700E+00	.8920E-01	.7810E-01	.3200E-01	.6710E-01	.1330E-01	.2740E-01
12	0.	0.	0.	0.	.2760E-02	.2720E-02	.5200E-03	.6720E-03	0.	.2020E-01
13	0.	0.	0.	.9770E-01	.4340E-02	.3500E-02	.1380E-02	.2960E-02	.3140E-02	.1130E-01
14	0.	0.	0.	0.	0.	0.	0.	0.	0.	0.

*FLIGHT CONDITION CATEGORY

0 Total flight time not recorded in categories 4-14
1 Number of landing gear touchdowns
2 Number of full autorotative landings
3 Number of rotor shutdowns
4 Time in level flight at 55 kt < V < 80 kt
5 Time in level flight at V > 80 kt
6 Time in right, nonsymmetric conditions at 55 kt < V < 80 kt
7 Time in right, nonsymmetric conditions at V > 80 kt
8 Time in left, nonsymmetric conditions at 55 kt < V < 80 kt
9 Time in left, nonsymmetric conditions at V > 80 kt
10 Time in symmetric conditions, P > PT, 55 kt < V < 80 kt
11 Time in symmetric conditions, P > PT, V > 80 kt
12 Time in symmetric conditions, P < PT, 55 kt < V < 80 kt
13 Time in level conditions, R > RT, V > 80 kt
14 Time in level conditions, Y > YT, V > 80 kt

TABLE A-20. FDAM CONSTANTS, C_{ij}, FOR CH-47C FCM SYSTEM I

*FLIGHT CONDITION CATEGORY	COMPONENT(i)									
	1	2	3	4	5	6	7	8	9	10
	AFT ROTOR SHAFT P/N	AFT ROTOR PITCH SHAFT	FWD ROTOR PITCH SHAFT	AFT HUB	AFT HORIZ HINGE PIN	AFT ROTOR BLADE	AFT ROTOR BLADE SOCKET	FWD ROTOR BLADE SOCKET	AFT TIE BAR	FWD TIE BAR
0	.5630E-03	.7820E-03	.6270E-03	.3140E-03	.3140E-03	.6560E-03	.7130E-03	.6360E-03	0.	0.
1	0.	0.	.3600E-03	0.	0.	.3530E-02	.5070E-05	.4350E-03	0.	0.
2	0.	0.	0.	0.	0.	0.	0.	0.	.2130E-02	.2130E-02
3	.3830E-02	.9930E-02	.5710E-03	.7580E-02	.7580E-02	.8240E-02	.5740E-02	.1430E-02	0.	0.
4	0.	0.	0.	0.	0.	0.	0.	0.	0.	0.
5	.2920E-04	.3050E-04	0.	.4250E-04	.4250E-04	.5340E-04	.1050E-03	.3280E-04	0.	0.
6	.2470E-02	.1040E-02	0.	.5830E-04	.5830E-04	.5130E-03	.1170E-03	.8500E-04	0.	0.
7	.3800E-03	.1530E-03	0.	0.	0.	.1270E-03	.6230E-05	0.	0.	0.

*FLIGHT CONDITION CATEGORY

0 Total flight time not recorded in categories 1-7
1 Number of landing gear touchdowns
2 Number of rotor shutdowns
3 Number of n_z peaks
4 Time at V < 60 kt, LCST extended
5 Time at 84 kt < V < 140 kt
6 Time at V > 140 kt
7 Time at V > 80 kt, LCST retracted

TABLE A-21. FDAM CONSTANTS, C_{ij}, FOR CH-47C FCM SYSTEM II

*FLIGHT CONDITION CATEGORY	COMPONENT(i)									
	1	2	3	4	5	6	7	8	9	10
	AFT ROTOR SHAFT P/N	AFT ROTOR PITCH SHAFT	FWD ROTOR PITCH SHAFT	AFT HUB	AFT HORIZ HINGE PIN	AFT ROTOR BLADE	AFT ROTOR BLADE SOCKET	FWD ROTOR BLADE SOCKET	AFT TIE BAR	FWD TIE BAR
0	0.	0.	0.	0.	0.	0.	0.	0.	0.	0.
1	0.	0.	.3600E-03	0.	0.	.2580E-02	.5070E-05	.4350E-03	0.	0.
2	0.	0.	0.	0.	0.	0.	0.	0.	.2130E-02	.2130E-02
3	.7160E-02	.1210E-01	.1020E-01	.7030E-02	.7030E-02	.4320E-02	.4090E-02	.7510E-02	0.	0.
4	0.	0.	0.	0.	0.	0.	0.	0.	0.	0.
5	0.	0.	0.	0.	0.	0.	0.	0.	0.	0.
6	0.	0.	0.	0.	0.	0.	0.	0.	0.	0.
7	0.	0.	0.	0.	0.	0.	0.	0.	0.	0.
8	0.	0.	0.	0.	0.	0.	0.	0.	0.	0.
9	.1090E-03	.6200E-04	0.	0.	0.	0.	.1330E-03	.3840E-04	0.	0.
10	.1080E-03	.3360E-04	.1160E-04	.4330E-05	.4330E-05	.1340E-04	.1190E-03	.1400E-03	0.	0.
11	0.	0.	0.	0.	0.	.6200E-03	0.	0.	0.	0.
12	.6260E-04	.7110E-03	.7640E-05	.3820E-03	.3820E-03	.3440E-03	.6280E-03	.6420E-04	0.	0.
13	0.	0.	0.	0.	0.	0.	0.	0.	0.	0.
14	.8380E-02	.2410E-02	0.	0.	0.	.2260E-02	.1530E-03	0.	0.	0.
15	.3000E-02	.2160E-02	0.	0.	0.	.1140E-03	.2230E-04	0.	0.	0.
16	.3000E-02	.2160E-02	0.	0.	0.	.1140E-03	.2230E-04	0.	0.	0.
17	0.	0.	0.	0.	0.	0.	0.	0.	0.	0.
18	.1120E-02	.3210E-03	0.	0.	0.	.3010E-02	.2200E-04	0.	0.	0.
19	.4010E-03	.2880E-03	0.	0.	0.	.2050E-03	.2430E-05	0.	0.	0.

*FLIGHT CONDITION CATEGORY

0 Total flight time not recorded in categories 4-19
1 Number of landing gear touchdowns
2 Number of rotor shutdowns
3 Number of n_z peaks
4 Time at V<60 kt, LCST extended
5 Time at V<80 kt, LCST retracted, GW<33000
6 Time at V<84 kt, LCST retracted, 33000<GW<40000
7 Time at V<84 kt, LCST retracted, 40000<GW<46000
8 Time at V<84 kt, LCST retracted, GW>46000
9 Time at 84 kt<V<140 kt, LCST extended, GW<33000
10 Time at 84 kt<V<140 kt, LCST extended, 33000<GW<40000
11 Time at 84 kt<V<140 kt, LCST extended, 40000<GW<46000
12 Time at 84 kt<V<140 kt, LCST extended, GW>46000
13 Time at V>140 kt, LCST extended, GW<33000
14 Time at V>140 kt, LCST extended, 33000<GW<40000
15 Time at V>140 kt, LCST extended, 40000<GW<46000
16 Time at V>140 kt, LCST extended, GW>46000
17 Time at V>76 kt, LCST extended, GW<33000
18 Time at V>88 kt, LCST retracted, 33000<GW<40000
19 Time at V>96 kt, LCST retracted, GW>40000

TABLE A-22. FDAM CONSTANTS, C_{ij}, FOR CH-47C FCM SYSTEM IIA

*FLIGHT CONDITION CATEGORY	COMPONENT(i)									
	1	2	3	4	5	6	7	8	9	10
	AFT ROTOR SHAFT P/N	AFT ROTOR PITCH SHAFT	FWD ROTOR PITCH SHAFT	AFT HUB	AFT HORIZ HINGE PIN	AFT ROTOR BLADE	AFT ROTOR BLADE SOCKET	FWD ROTOR BLADE SOCKET	AFT TIE BAR	FWD TIE BAR
0	.3800E-03	.2220E-03	.4470E-05	.3040E-04	.3040E-04	.2210E-03	.1200E-03	.6450E-04	0.	0.
1	0.	0.	.8210E-02	0.	0.	.1580E-01	.3110E-04	.2670E-02	0.	0.
2	0.	0.	0.	0.	0.	0.	0.	0.	.2130E-02	.2130E-02
3	.2480E-02	.5760E-02	.5560E-03	.3850E-03	.3850E-02	.2020E-02	.6410E-02	.5220E-03	0.	0.
4	0.	0.	0.	0.	0.	0.	0.	0.	0.	0.
5	.3140E-02	.7180E-02	.3630E-02	.5750E-02	.5750E-02	.1650E-02	.2930E-02	.3720E-02	0.	0.
6	.3300E-02	.3740E-02	.5040E-02	.1880E-02	.1880E-02	.2130E-02	.2980E-02	.3200E-02	0.	0.
7	0.	0.	0.	0.	0.	0.	0.	0.	0.	0.
8	0.	0.	0.	0.	0.	0.	0.	0.	0.	0.
9	0.	0.	0.	0.	0.	0.	0.	0.	0.	0.
10	.1120E-02	.3210E-03	0.	0.	0.	.3010E-03	.2200E-04	0.	0.	0.
11	.4010E-03	.2380E-03	0.	0.	0.	.2050E-03	.2980E-05	0.	0.	0.
12	.1570E-03	.4330E-03	0.	.2230E-03	.2230E-03	.4420E-04	.5620E-03	.1760E-03	0.	0.

*FLIGHT CONDITION CATEGORY

0 Total flight time not recorded in categories 3-12
1 Number of landing gear touchdowns at GW > 46000
2 Number of rotor shutdowns
3 Time at n_z > 1.2 g, GW > 46000
4 Time at n_z > 1.2 g, 40000 < GW < 46000
5 Time at n_z > 1.2 g, 33000 < GW < 40000
6 Time at n_z > 1.2 g, GW < 33000
7 Time at V < 84 kt, LCST programmed
8 Time at 84 kt < V < 140 kt, LCST programmed, GW > 46000
9 Time at V > 76 kt, LCST retracted, GW < 33000
10 Time at V > 88 kt, LCST retracted, 33000 < GW < 40000
11 Time at V > 96 kt, LCST retracted, GW > 40000
12 Time at R > RT, Y > YT

TABLE A-23. FDAM CONSTANTS, C_{ij}, FOR CH-47C FCM SYSTEM IIIA

*FLIGHT CONDITION CATEGORY	COMPONENT (i)									
	1	2	3	4	5	6	7	8	9	10
	AFT ROTOR SHAFT P/N	AFT ROTOR PITCH SHAFT	FWD ROTOR PITCH SHAFT	AFT HUB	AFT HORIZ HINGE PIN	AFT ROTOR BLADE	AFT ROTOR BLADE SOCKET	FWD ROTOR BLADE SOCKET	AFT TIE BAR	FWD TIE BAR
0	.7030E-04	.3740E-04	.4430E-05	.3050E-04	.3050E-04	.1670E-03	.1150E-03	.6460E-04	0.	0.
1	0.	0.	.3600E-03	0.	0.	.2580E-02	.5070E-05	.4350E-03	0.	0.
2	0.	0.	0.	0.	0.	0.	0.	0.	.2130E-02	.2130E-02
3	0.	0.	0.	0.	0.	0.	0.	0.	0.	0.
4	0.	0.	0.	0.	0.	0.	0.	0.	0.	0.
5	.1120E-02	.3210E-03	0.	0.	0.	.2010E-03	.2200E-04	0.	0.	0.
6	.4010E-03	.2880E-03	0.	0.	0.	.2050E-03	.2960E-05	0.	0.	0.
7	0.	0.	0.	0.	0.	0.	0.	0.	0.	0.
8	0.	0.	0.	0.	0.	0.	0.	0.	0.	0.
9	.3000E-02	.2160E-02	0.	0.	0.	.1060E-03	.2230E-04	0.	0.	0.
10	.8380E-02	.2410E-02	0.	0.	0.	.2260E-02	.1530E-03	0.	0.	0.
11	0.	0.	0.	0.	0.	0.	0.	0.	0.	0.
12	0.	0.	0.	0.	0.	0.	0.	0.	0.	0.
13	0.	.6400E-02	0.	0.	0.	.2520E-02	.1130E-01	0.	0.	0.
14	.2540E-01	.5730E-01	.2130E-02	.6200E-01	.6200E-01	.9330E-02	.2370E-01	.9790E-02	0.	0.
15	.3300E-02	.4360E-02	0.	.3640E-03	.3640E-03	.5360E-03	.4360E-02	0.	0.	0.
16	0.	0.	0.	0.	0.	0.	0.	0.	0.	0.
17	0.	.6400E-02	0.	0.	0.	.2520E-02	.1130E-01	0.	0.	0.
18	.2540E-01	.5790E-01	.2130E-02	.6200E-01	.6200E-01	.9330E-02	.2370E-01	.9790E-02	0.	0.
19	.3300E-02	.4360E-02	0.	.3640E-03	.3640E-03	.5360E-03	.4360E-02	0.	0.	0.
20	0.	0.	0.	0.	0.	0.	0.	0.	0.	0.
21	.2520E-03	.1890E-02	.5280E-04	.8160E-03	.8160E-03	.2580E-03	.1930E-02	.1830E-03	0.	0.
22	.9240E-03	.1410E-02	.1000E-02	.9290E-03	.9290E-03	.4170E-03	.8760E-03	.1170E-02	0.	0.
23	.8790E-03	.1030E-02	.1400E-02	.5120E-03	.5120E-03	.5870E-03	.8950E-03	.1020E-02	0.	0.
24	0.	0.	0.	0.	0.	0.	0.	0.	0.	0.
25	.2520E-03	.1890E-02	.5280E-04	.8160E-03	.8160E-03	.2580E-03	.1930E-02	.1830E-03	0.	0.
26	.9240E-03	.1410E-02	.1000E-02	.9290E-03	.9290E-03	.4170E-03	.8760E-03	.1170E-02	0.	0.
27	.8790E-03	.1030E-02	.1400E-02	.5120E-03	.5120E-03	.5870E-03	.8950E-03	.1020E-02	0.	0.

*FLIGHT CONDITION CATEGORY

0 Total flight time not recorded in categories 3-27
1 Number of landing gear touchdowns
2 Number of rotor shutdowns
3 Time at V < 60 kt, LCST extended
4 Time at V > 76 kt, LCST retracted, GW < 33000
5 Time at V > 88 kt, LCST retracted, 33000 < GW < 40000
6 Time at V > 96 kt, LCST retracted, GW > 40000
7 Time at 84 kt < V < 140 kt, GW > 46000
8 Time at V > 140 kt, GW > 46000
9 Time at V > 140 kt, 40000 < GW < 46000
10 Time at V > 140 kt, 33000 < GW < 40000
11 Time at V > 140 kt, GW < 33000
12 Time at 84 kt < V < 112 kt, GW > 46000, n_z > 1.2g
13 Time at 84 kt < V < 112 kt, 40000 < GW < 46000, n_z > 1.2g
14 Time at 84 kt < V < 112 kt, 33000 < GW < 40000, n_z > 1.2 g
15 Time at 84 kt < V < 112 kt, GW < 33000, n_z > 1.2 g
16 Time at 112 kt < V < 140 kt, GW > 46000, n_z > 1.2 g
17 Time at 112 kt < V < 140 kt, 40000 < GW < 46000, n_z > 1.2 g
18 Time at 112 kt < V < 140 kt, 33000 < GW < 40000, n_z > 1.2 g
19 Time at 112 kt < V < 140 kt, GW < 33000, n_z > 1.2 g
20 Time at 84 kt < V < 112 kt, GW > 46000, P > PT
21 Time at 84 kt < V < 112 kt, 40000 < GW < 46000, P > PT
22 Time at 84 kt < V < 112 kt, 33000 < GW < 40000, P > PT
23 Time at 84 kt < V < 112 kt, GW < 33000, P > PT
24 Time at 112 kt < V < 140 kt, GW > 46000, P > PT
25 Time at 112 kt < V < 140 kt, 40000 < GW < 46000, P > PT
26 Time at 112 kt < V < 140 kt, 33000 < GW < 40000, P > PT
27 Time at 112 kt < V < 140 kt, GW < 33000, P > PT

TABLE A-24. FDAM CONSTANTS, C_{ij}, FOR CH-47C FCM SYSTEM IVA

*FLIGHT CONDITION CATEGORY	COMPONENT(i)									
	1	2	3	4	5	6	7	8	9	10
	AFT ROTOR SHAFT P/N	AFT ROTOR PITCH SHAFT	FWD ROTOR PITCH SHAFT	AFT HUB	AFT HORIZ HINGE PIN	AFT ROTOR BLADE	AFT ROTOR BLADE SOCKET	FWD ROTOR BLADE SOCKET	AFT TIE BAR	FWD TIE BAR
0	.7930E-04	.9680E-04	.4490E-05	.2730E-04	.2730E-04	.1270E-03	.1200E-03	.6590E-04	0.	0.
1	0.	0.	.4120E-03	0.	0.	.2450E-02	.5070E-05	.4980E-03	0.	0.
2	0.	0.	0.	0.	0.	0.	0.	0.	.2130E-02	.2130E-02
3	0.	0.	0.	0.	0.	0.	0.	0.	0.	0.
4	.8220E-02	.1170E-01	.1080E-01	.9100E-02	.9100E-02	.5580E-02	.1050E-01	.9220E-02	0.	0.
5	.8220E-02	.1170E-01	.1080E-01	.9100E-02	.9100E-02	.5580E-02	.1050E-01	.9220E-02	0.	0.
6	.1460E-02	.1050E-02	0.	0.	0.	.5490E-04	.5870E-04	0.	0.	0.
7	.1260E-03	.5930E-04	0.	.2900E-04	.2900E-04	.7870E-04	.2390E-03	.2720E-03	0.	0.
8	.1260E-03	.5930E-04	0.	.2900E-04	.2900E-04	.7870E-04	.2390E-03	.2720E-03	0.	0.
9	.7620E-02	.1130E-01	.9740E-02	.8850E-02	.8850E-02	.5840E-02	.9430E-02	.8360E-02	0.	0.
10	.7620E-02	.1130E-01	.9740E-02	.8850E-02	.8850E-02	.5840E-02	.9430E-02	.8360E-02	0.	0.
11	0.	0.	0.	0.	0.	0.	.3400E-04	0.	0.	0.
12	.1280E-03	.6510E-03	0.	.3450E-03	.3450E-03	.2770E-05	.4670E-03	.1070E-03	0.	0.
13	.1280E-03	.6510E-03	0.	.3450E-03	.3450E-03	.2770E-05	.4670E-03	.1070E-03	0.	0.
14	.1270E-01	.1240E-01	.2760E-01	.5090E-02	.5090E-02	.4550E-02	.4400E-02	.3000E-02	0.	0.
15	.1270E-01	.1240E-01	.2760E-01	.5090E-02	.5090E-02	.4550E-02	.4400E-02	.3000E-02	0.	0.
16	.3400E-01	.9770E-02	0.	0.	0.	.9160E-02	.4780E-05	0.	0.	0.
17	.5250E-03	.5570E-03	0.	.1800E-03	.1800E-03	.1030E-03	.1120E-02	.2500E-03	0.	0.
18	.5250E-03	.5570E-03	0.	.1800E-03	.1800E-03	.1030E-03	.1120E-02	.2500E-03	0.	0.
19	0.	0.	0.	0.	0.	0.	0.	0.	0.	0.
20	.4430E-03	.1680E-03	0.	0.	0.	.1260E-03	.6230E-05	0.	0.	0.

*FLIGHT CONDITION CATEGORY

0 Total flight time not recorded in classes 4-20
1 Number of landing gear touchdowns
2 Number of rotor shutdowns
3 Number of maneuver n_z peaks
4 Time at 0 < ALT < 5000, 84 kt < V < 112 kt, n_z > 1.2 g
5 Time at 0 < ALT < 5000, 112 kt < V < 140 kt, n_z > 1.2 g
6 Time at 0 < ALT < 5000, V > 140 kt
7 Time at 0 < ALT < 5000, 84 kt < V < 112 kt, P > PT
8 Time at 0 < ALT < 5000, 112 kt < V < 140 kt, P > PT
9 Time at 5000 < ALT < 9000, 84 kt < V < 112 kt, n_z > 1.2 g
10 Time at 5000 < ALT < 9000, 112 kt < V < 140 kt, n_z > 1.2 g
11 Time at 5000 < ALT < 9000, V > 140 kt
12 Time at 5000 < ALT < 9000, 84 kt < V < 112 kt, P > PT
13 Time at 5000 < ALT < 9000, 112 kt < V < 140 kt, P > PT
14 Time at ALT > 9000, 84 kt < V < 112 kt, n_z > 1.2 g
15 Time at ALT > 9000, 112 kt < V < 140 kt, n_z > 1.2 g
16 Time at ALT > 9000, V > 140 kt
17 Time at ALT > 9000, 84 kt < V < 112 kt, P > PT
18 Time at ALT > 9000, 112 kt < V < 140 kt, P > PT
19 Time at 0 < V < 60 kt, LCST extended
20 Time at V > 80 kt, LCST retracted

TABLE A-25. FDAM CONSTANTS, C_{ij}, FOR CH-47C FCM SYSTEM VA

*FLIGHT CONDITION CATEGORY	COMPONENT(i)									
	1	2	3	4	5	6	7	8	9	10
	AFT ROTOR SHAFT P/N	AFT ROTOR PITCH SHAFT	FWD ROTOR PITCH SHAFT	AFT HUB	AFT HORIZ HINGE PIN	AFT ROTOR BLADE	AFT ROTOR BLADE SOCKET	FWD ROTOR BLADE SOCKET	AFT TIE BAR	FWD TIE BAR
0	.4040E-02	.5630E-02	.1360E-04	.1320E-03	.1320E-03	.1750E-04	.6820E-03	.3660E-03	0.	0.
1	0.	0.	.4120E-03	0.	0.	.2950E-02	.5070E-05	.4980E-03	0.	0.
2	0.	0.	0.	0.	0.	0.	0.	0.	.2130E-02	.2130E-02
3	.2380E-03	.1170E-02	.1150E-02	.8770E-03	.8770E-03	.1130E-02	.3650E-03	.8420E-03	0.	0.
4	.5020E-03	.7490E-03	.5460E-03	.5320E-03	.5320E-03	.5950E-03	.6890E-03	.5250E-03	0.	0.
5	0.	0.	0.	0.	0.	0.	0.	0.	0.	0.
6	.1020E-03	.7210E-04	0.	0.	0.	.3440E-04	.4520E-05	0.	0.	0.
7	0.	0.	0.	0.	0.	.3940E-04	0.	0.	0.	0.
8	0.	0.	0.	0.	0.	.2920E-04	0.	0.	0.	0.
9	0.	0.	0.	0.	0.	0.	0.	0.	0.	0.
10	0.	0.	0.	0.	0.	.7050E-04	.5380E-06	0.	0.	0.
11	0.	0.	0.	0.	0.	0.	.1750E-05	0.	0.	0.
12	0.	0.	0.	0.	0.	0.	0.	0.	0.	0.
13	0.	0.	0.	0.	0.	0.	0.	0.	0.	0.
14	.3340E-02	.1260E-02	0.	0.	0.	.7360E-03	.4370E-04	0.	0.	0.

*FLIGHT CONDITION CATEGORY

0 Total flight time not recorded in classes 5-14
1 Number of landing gear touchdowns
2 Number of rotor shutdowns
3 Number of n_z peaks with P < PT
4 Number of n_z peaks with P > PT
5 Time at V < 60 kt, LCST extended
6 Time at V > 80 kt, LCST retracted
7 Time at 60 kt < V < 110 kt, 0 < ALT < 5000
8 Time at 110 kt < V < 170 kt, 0 < ALT < 5000
9 Time at V > 170 kt, 0 < ALT < 5000
10 Time at 60 kt < V < 140 kt, 5000 < ALT < 9000
11 Time at 140 kt < V < 170 kt, 5000 < ALT < 9000
12 Time at 60 kt < V < 100 kt, ALT > 9000
13 Time at 100 kt < V < 125 kt, ALT > 9000
14 Time at V > 140 kt

TABLE A-26. FDAM CONSTANTS, C_{ij}, FOR CH-47C FCM SYSTEM VI

*FLIGHT CONDITION CATEGORY	COMPONENT(i)									
	1	2	3	4	5	6	7	8	9	10
	AFT ROTOR SHAFT P/N	AFT ROTOR PITCH SHAFT	FWD ROTOR PITCH SHAFT	AFT HUB	AFT HORIZ HINGE PIN	AFT ROTOR BLADE	AFT ROTOR BLADE SOCKET	FWD ROTOR BLADE SOCKET	AFT TIE BAR	FWD TIE BAR
0	0.	0.	.5530E-05	0.	0.	.2230E-03	.3710E-04	.2480E-04	0.	0.
1	0.	0.	.4120E-03	0.	0.	.2950E-02	.5070E-05	.4980E-03	0.	0.
2	0.	0.	0.	0.	0.	0.	0.	0.	.2130E-02	.2130E-02
3	.3830E-02	.6510E-02	.5710E-03	.1020E-01	.1020E-01	.2240E-02	.5750E-02	.1430E-02	0.	0.
4	.1230E-01	.1620E-01	.2160E-01	.7310E-02	.7310E-02	.8600E-02	.1300E-01	.1450E-01	0.	0.
5	.5640E-03	.8500E-03	.7310E-05	.3170E-03	.3170E-03	.4240E-04	.3080E-03	.4630E-03	0.	0.
6	.2910E-03	.2090E-03	0.	0.	0.	.1100E-04	.1170E-04	0.	0.	0.
7	0.	0.	0.	0.	0.	0.	.3150E-05	0.	0.	0.
8	.6800E-02	.1350E-02	0.	0.	0.	.1330E-02	.9550E-06	0.	0.	0.
9	0.	0.	0.	0.	0.	0.	0.	0.	0.	0.
10	0.	0.	0.	0.	0.	0.	0.	0.	0.	0.

*FLIGHT CONDITION CATEGORY

0 Total flight time not recorded in classes 1-10
1 Number of landing gear touchdowns
2 Number of rotor shutdowns
3 Time at n_z > 1.2 g
4 Time at P > PT
5 Time at R < RT
6 Time at 0 < ALT < 5000, V > 145 kt
7 Time at 5000 < ALT < 9000, V > 125 kt
8 Time at ALT > 9000, V > 100 kt
9 Time at V < 60 kt, LCST extended
10 Time at V > 80 kt, LCST retracted

DIRECT MONITORING

INTRODUCTION

The problem of fatigue and structural reliability has continually grown in importance as demands for extended helicopter service life and the severity of operating conditions have increased. There is a strong need for development of a reliable fatigue life indicator to assess the fatigue damage experienced by an individual aircraft and its components. Determination of component retirement lives by individual aircraft usage rather than by fleet usage would improve fleet reliability and decrease component failures prior to replacement time. There would also be an economy of operation due to increased component service life on aircraft experiencing a milder usage than that of the rest of the fleet.

Two fundamental obstacles hamper the development of the fatigue indicator. First, no single generalized fatigue mechanism exists which is applicable to materials of different metallurgical structures. Second, the degree of "fatigue damage" is not established or defined in terms of exact quantities, i.e., the changes in metallurgical structure prior to crack initiation, number of crack initiations, and crack length as a function of cycles of loading to the expected life.

While a measure of "fatigue damage" has not been explicitly defined, there do exist material phenomena which can be empirically related to the fatigue life expectancy of the material. Three methods for measuring these related phenomena were investigated during this program. Called "direct fatigue monitoring concepts," they are:

1) acoustic emission
2) inductance sensing
3) foil gage

Acoustic emission and inductance testing monitor phenomena generally acknowledged to be directly related to the fatigue failure mechanism. The foil gage is a less direct method as it implies damage to the structure of interest via strain induced damage to the gage. This investigation surveyed the three concepts and assessed their applicability to helicopters.

ACOUSTIC EMISSION

Theory

Acoustic emission is the spontaneous generation of elastic waves caused by localized movement in a material under stress.

These movements can occur at both the microscopic and macroscopic levels. At the microscopic level acoustic emission in metals is generally associated with the accumulation and breakaway of dislocations. At the macroscopic level acoustic emission is attributed to crack growth.

Flawed and unflawed metals demonstrate different acoustic emission behavior. Acoustic emission from initially flaw-free metal is low-level and continuous in nature. On an oscilloscope, it appears very much like background electrical noise. It is associated with plastic deformation occurring at relatively small plastic strain. The emission rate reaches a maximum just above the elastic limit, and then exponentially decreases in the plastic region of the metal (see Figure A-1).

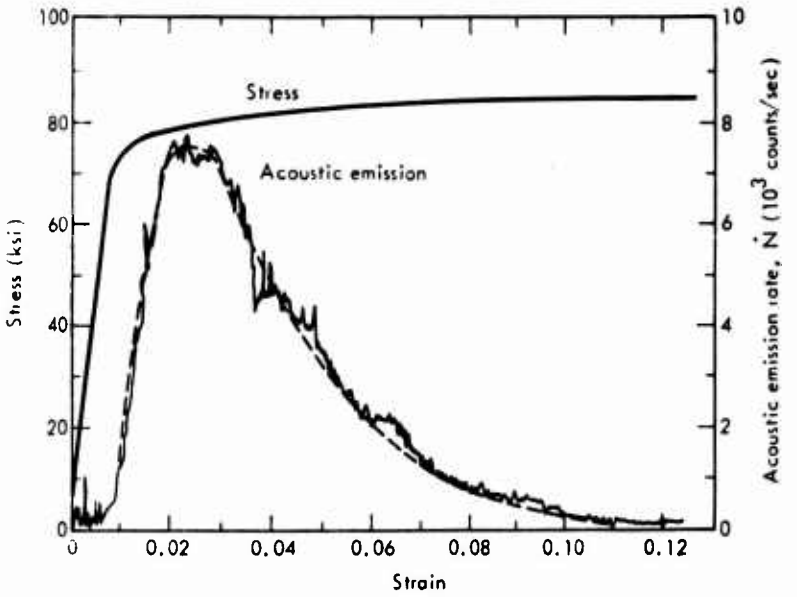

Figure A-1. Acoustic Emission and Stress vs. Strain for a 7075-T6 Aluminum Tensile Specimen.

The energy content of continuous emission is extremely low and its amplitude increases with loading and is strain-rate dependent. At or near failure, the continuous emission is replaced by burst emission (usually associated with flawed metals).

In flawed metals, anomalies act as localized stress concentrators and will grow by causing localized plastic deformation at nominal stress levels well below general yielding. The resulting acoustic emission occurs as high amplitude bursts (sudden increases in emission rate) coinciding with the irregular nature of the macroscopic flaw growth. As an anomaly grows, the acoustic emission rate will continuously increase up to the discontinuity's critical size, where complete fracture occurs (see Figure A-2).

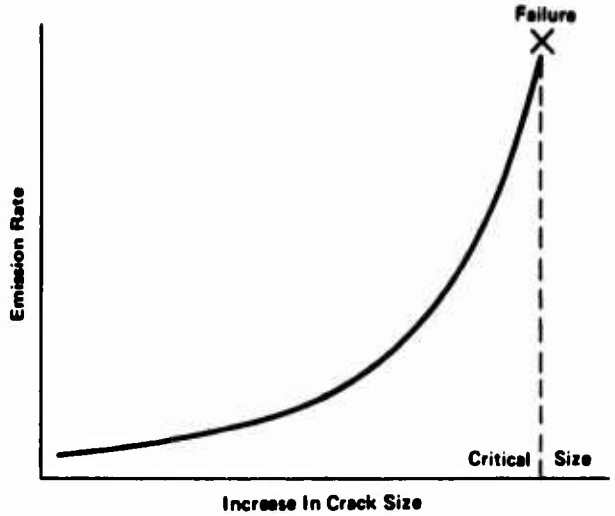

Figure A-2. Acoustic Emission During Crack Growth.

Acoustic emission is an irreversible process and this behavior is labeled the Kaiser effect. That is, once a metal has been loaded and unloaded, reloading will not cause emission until the initial maximum stress level has been exceeded.

Discussion

Theoretical analysis has shown that the plastic volume at a crack tip should vary as some power of the stress intensity factor. It has also been theoretically shown, via dislocation theory, that the summation of acoustic emission is related to the generated plastic volume. In support of this, Dunegan et al.[13],[14] obtained data which indicated that the total number N, of acoustic emission signals resulting from dislocation motion in the plastic zone near a crack tip, can be directly related to the stress intensity factor of the crack by

$$N = AK^m \qquad \text{(A-1)}$$

where

m = const. for a given material of a particular thickness
A = proportionality constant
K = stress intensity factor

[13] Dunegan, H.L., Harris, D.O., and Tatro, C.A., FRACTURE ANALYSIS BY USE OF ACOUSTIC EMISSION, Journal of Engineering Fracture Mechanics, Vol. 1, June 1968, p. 105-122.

[14] Dunegan, H.L., and Harris, D.O., ACOUSTIC EMISSION--A NEW NON-DESTRUCTIVE TESTING TOOL, Proceedings of Third Annual Symposium on Non-destructive Testing of Welds and Materials Joining, Los Angeles, California, March 1968.

Equation (A-1) suggests that acoustic emission could be applied to the detection of cracks and their subcritical growth (extension of cracks at K levels below that required for rapid crack propagation) by continuous monitoring of a structure. Gerberich et al.[15] examined this relationship during an investigation of the applicability of acoustic emission analysis to the detection of hydrogen-induced crack growth and stress corrosion cracking (see Figure A-3).

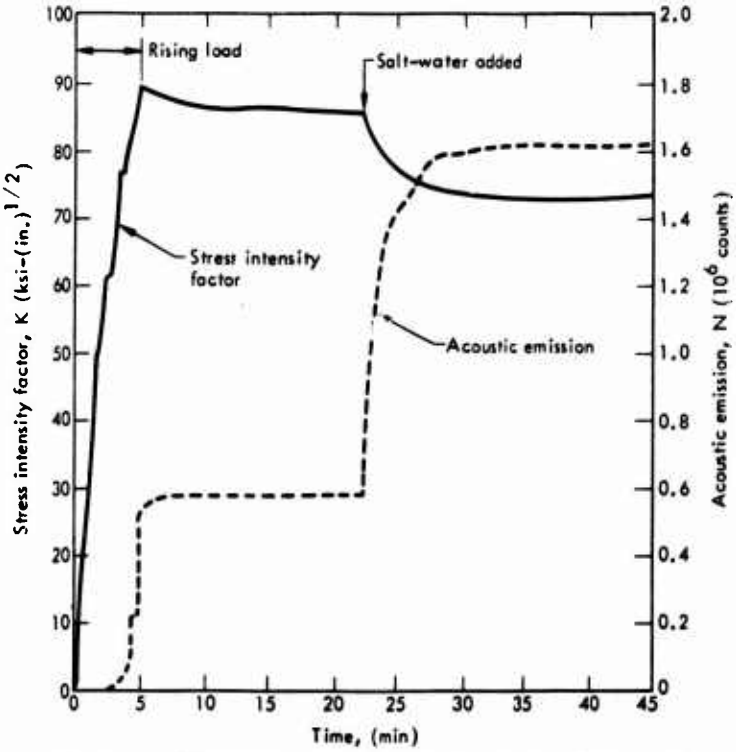

Figure A-3. Stress Intensity Factor and Acoustic Emission as a Function of Time for a Crack Propagating in a Uranium-0.3% Titanium Alloy Immersed in a 3% Salt-Water Solution.

Figure A-3 shows a relationship between N and K, while the load was increasing, as predicted by Equation (A-1). During the time from which the load was no longer increasing and prior to the addition of salt water, there was very little emission activity. Accompanying the crack extension, immediately following the addition of salt water, there is greatly increased acoustic emission activity. These results are a good indication that acoustic emission is a sensitive indicator of subcritical flaw growth.

---

[15] Gerberich, W.W., and Hartbower, C.E., MONITORING CRACK GROWTH OF HYDROGEN EMBRITTLEMENT AND STRESS CORROSION CRACKING BY ACOUSTIC EMISSION, in Proceedings of the Conference on Fundamental Aspects of Stress Corrosion Cracking (Ohio State University, Columbus, Ohio, 1967).

Hutton[16] investigated the relationship between acoustic emission and mechanical fatigue in metals (see Figure A-4). Figure A-4 summarizes acoustic emission data from low-cycle tension-compression fatigue testing of a high nickel alloy at 1000°F. Three peaks are evident in the emission curve prior to failure. The first is attributed to the Kaiser effect being extended by work hardening and the second to microcracking. The third is attributed to macrocrack formation. In another set of tests, acoustic emission data are taken during high-cycle tension-tension fatigue testing of notched aluminum panels (see Figure A-5).

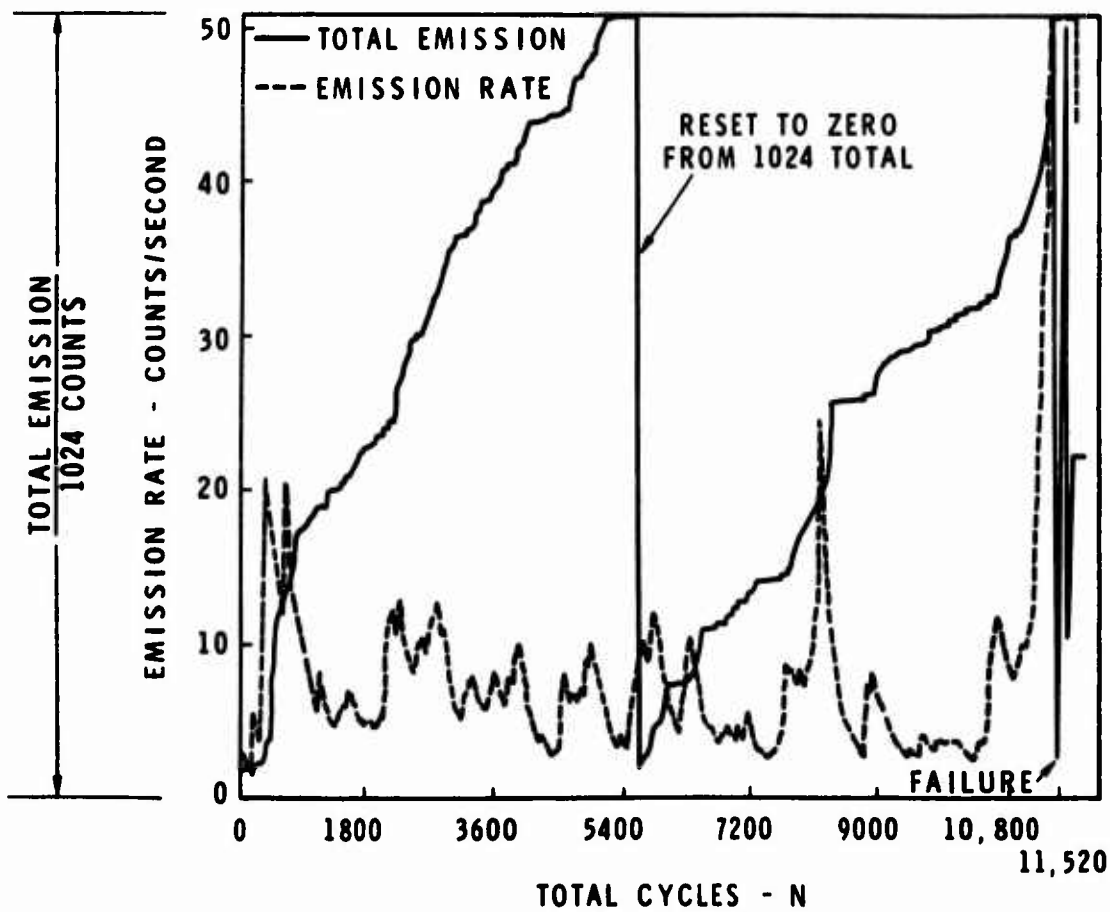

Figure A-4. Acoustic Emission Response - Fatigue of High Nickel Steel.

[16] Hutton, P.H., ACOUSTIC EMISSION APPLIED TO DETERMINATION OF STRUCTURAL INTEGRITY, for presentation at the 11th Open Meeting of the Mechanical Failures Prevention Group sponsored by the Office of Naval Research at Williamsburg, Virginia, April 7 and 8, 1970.

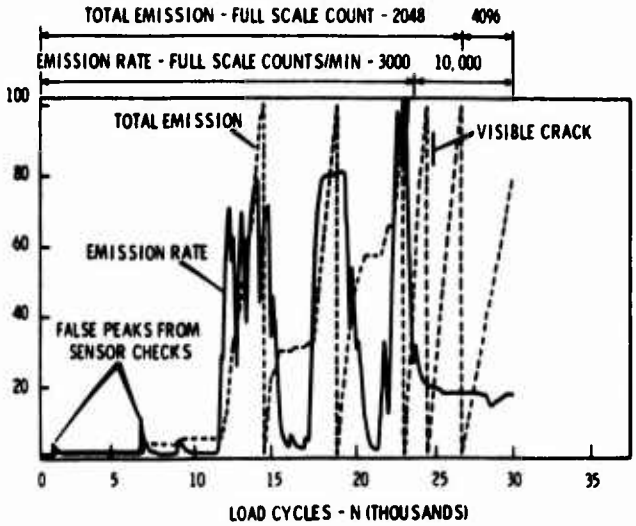

Figure A-5. Acoustic Emission from Macrocrack Formation - Fatigue Test of Center Notch Aluminum Panels.

Indication of macrocrack formation ranged from 4% to 6.5% of total life in three specimens tested similarly. The number of cycles to failure on these specimens ranged from 362,000 to 391,000. Additional data were taken with notched carbon steel specimens (see Figure A-6). The notched bar specimen was cycled in tension-tension for a total of 716,000 cycles. The characteristic sharp increase in acoustic emission occurred 11,000 cycles prior to this. Examination of the specimen revealed no surface crack, even under a microscope. Metallographic examination, however, revealed an abundance of microcracking in the vicinity of one corner of the notch. This is strong evidence that macrocrack nucleation produced the sharp increase in emission.

In all cases, both the total acoustic emission count and the count per cycle increased slowly with the increasing number of fatigue cycles and then increased rapidly just prior to failure. This suggests it may be possible to test a few specimens to failure for acoustic emission calibration and from this isolate a particular perturbation in the emission curve from which total fatigue life could be predicted.

The presence of background noise, possible damage to the sensors, the high cost of equipment, and the difficulty in monitoring dynamic systems make continuous monitoring of acoustic emission impractical in most applications. As an alternative to continuous monitoring, a procedure which takes advantage of the irreversibility of acoustic emission is examined.

If a flawed structure is loaded to a particular value of K and then unloaded, acoustic emission will not occur during reloading until the previous value of K is exceeded. Thus it is

possible to determine crack growth by periodically overstressing (proof-testing) a structure at a stress σ_p greater than the working stress σ_w. If flaws have grown since the previous overstress, then the stress intensity factor will have increased and emission will occur.

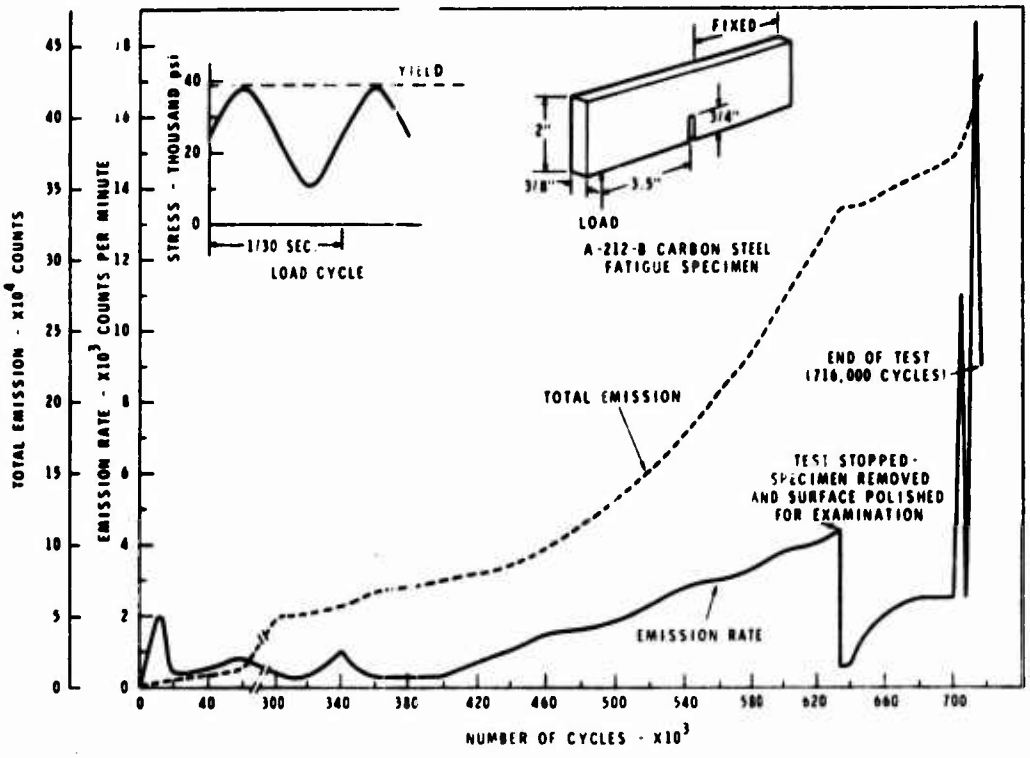

Figure A-6. Acoustic Emission from Carbon Steel Fatigue Specimen.

Dunegan et al.[17] developed a model to analytically predict the total number of emission counts N during each proof cycle as a function of the number of fatigue cycles. This model is predicated on the dependence of the crack growth rate on K[18]. Dunegan et al.[19] experimentally investigated the theoretical predictions of the model (see Figure A-7).

---

17 Dunegan, H.L., Harris, D.O., and Tetelman, A.S., DETECTION OF FATIGUE CRACK GROWTH BY ACOUSTIC EMISSION TECHNIQUES, Materials Evaluation, Vol. 28, July-December 1970.

18 Paris, P.C., THE FRACTURE MECHANICS APPROACH TO FATIGUE, Proceedings 10th Sagamore Conference, Syracuse University Press, 1965, p. 107.

19 Dunegan, H.L., Harris, D.O., and Tetelman, A.S., PREDICTION OF FATIGUE LIFETIME BY COMBINED FRACTURE MECHANICS AND ACOUSTIC EMISSION TECHNIQUES, Proceedings of the Air Force Conference on Fatigue and Fracture of Aircraft Structures and Materials, Miami Beach, Florida, 15-18 December 1969.

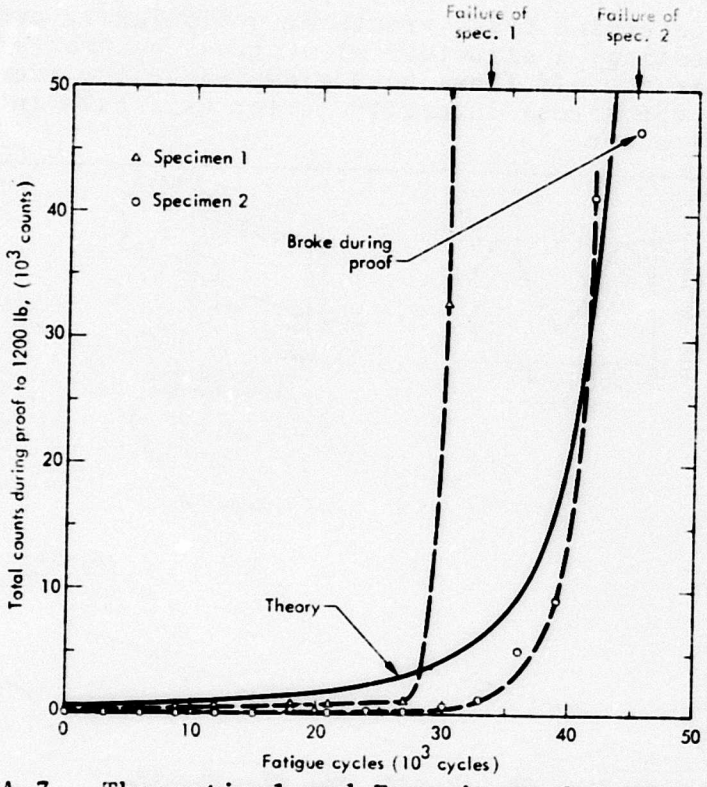

Figure A-7. Theoretical and Experimental Results of Periodic Tests with Acoustic Emission from 7075-T6 WOL Fracture Toughness Specimens.

Figure A-7 presents the results from two aluminum specimens cycled to 800 lb, and proofed to 1200 lb every 3000 cycles. This figure shows good agreement between the theoretical and experimental results. The amount of acoustic emission observed during the periodic proof increased very rapidly several thousand cycles prior to catastrophic failure, providing warning of impending failure. It was also observed during the investigation that if emission occurs while holding at the proof stress, then a crack with a K value close to critical is present, and failure is imminent.

Instrumentation

The basic information recorded in a typical acoustic emission test is the rate at which acoustic emission events occur as a function of changes in the load parameter. Proper biasing of the counting equipment is essential and must satisfy two primary requirements. The first is that the trigger of the counter can be set to a predetermined signal amplitude reliably and with small jitter. The second requirement is that the counter must contain a time interval gate, so that a rate of occurrence for acoustic emission events can be inferred.

For more sophisticated processing of acoustic emission data, on-line computers can be utilized. When testing large components where the origin of the emission is uncertain, simultaneous processing of several acoustic emission channels can be utilized to determine the location via triangulation. A typical system for detecting acoustic emission is illustrated in Figure A-8. The key, of course, to obtaining useful acoustic emission information is the sensor. The choice of sensor is essentially limited to a properly chosen piezoelectric transducer. It is still difficult to operate in any mode other than that which capitalizes on the enhanced output of the transducer at resonance. The principal limitation for the rest of the electronic portion of the system is signal-to-noise ratio. This is the major consideration in selecting the first amplifier stage following the transducer. Two important secondary considerations for a first-stage amplifier are ability to recover quickly from overloads and protection from burnout. Nakamura et al.[20] have developed a technique to eliminate high background noise. Basically, the system utilizes a few master detectors located in the area of interest and surrounded by a ring of slave transducers. Only those signals detected by all the master transducers before any slave transducer detects the event are saved for analysis. This shields against emission or noise coming from other areas. The system has a rejection ratio of 30,000 to 1, but requires a large number of transducers.

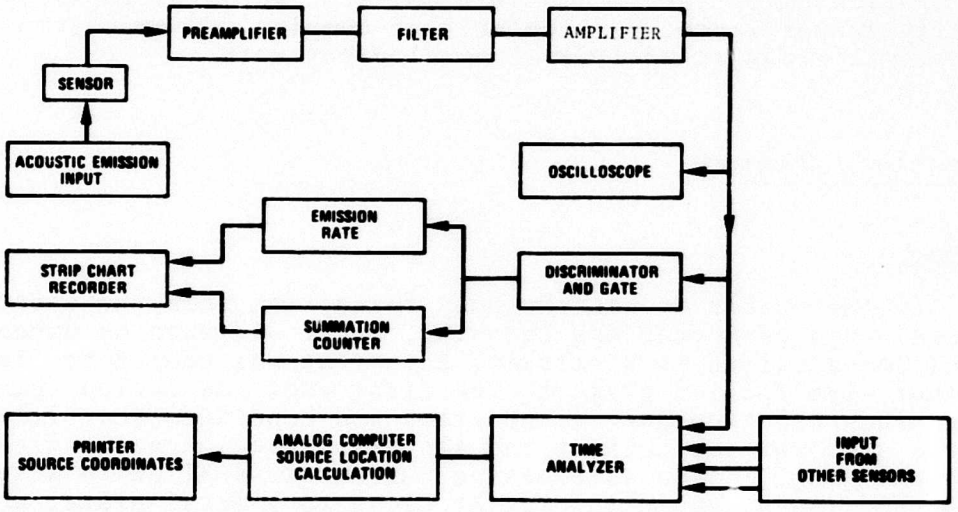

Figure A-8. Block Diagram - Acoustic Emission Monitor System.

[20] Nakamura, T., McCauley, B.O., Gardner, A.H., Redmond, J.C., Hagemeyer, J.W., and Burton, G.M., DEVELOPMENT OF AN ACOUSTIC EMISSION MONITORING SYSTEM, General Dynamics, Ft. Worth, Texas, Report ERR-FW-901 (1969).

Summary

The monitoring of acoustic emission during periodic proof stressing provides a means of detecting the presence and growth of fatigue cracks. This technique provides early warning of impending failure in materials with low-cycle fatigue lives. Good agreement has been observed between experimental results and predictions made from an analytical model relating the total number of emission counts during proof testing to the number of fatigue cycles. It still remains, however, to be determined if the model applies to the high-cycle fatigue lives encountered in helicopter components, or to a wide range of materials with different ratios of the proof to working stress, as well as for different intervals of cycles between inspections.

Additionally, adequate fixtures must be designed for application of appropriate proof loads. If dealing with a complex structure, disassembly may be required to proof test certain components.

The principal detection and analysis problem areas are:

(1) Sensor design and placement
(2) Signal analysis and characterization
(3) Noise recognition and rejection

Full utilization of acoustic emission for structural integrity surveillance, particularly of complex, dynamic structures, will require additional development work.

INDUCTANCE SENSING

Theory

In the 1830's Michael Faraday found that when the electric current in a conductor was changing, as it did when he opened or closed a switch in a circuit, a current was caused to flow in another wire located close to the first one. He called this phenomenon electromagnetic induction and concluded that it occurred whenever the current and its associated magnetic field were changing. If an alternating current is applied to a solenoid, and the solenoid is brought close to a metal plate, a current is caused to flow in a plate by electromagnetic induction. These currents that are induced to flow in closed paths perpendicular to the magnetic field are called eddy currents. The magnetic field due to the eddy currents will induce a current in the solenoid that opposes the current already flowing. Any change in the material properties (cracks, flaws or other inhomogeneities) of the plate will alter the flow of the eddy currents causing a change in the reluctance of the solenoid

flux path. Such changes can be monitored by an A.C. bridge circuit.

Discussion

To investigate the effectiveness of the inductive sensing system, vibratory beam fatigue tests[21] were conducted on 6061-T6 aluminum, 7310 steel, and Inconel X. Roll tests were conducted on 8620-H steel. Inductive scanning was performed during the tests and microanalytic techniques were applied to determine the sensitivity and applicability of the inductive sensing method.

For the beam tests eighteen samples of each material were fabricated and tested. The bar graphs in Figures A-9 and A-10 summarize the results of the tests. (Individual sample results for Inconel X not available; see discussion for average results.) The top of the black portion of a bar indicates th number of cycles at which a signal appeared. The top of the clear portion indicates the number of cycles at which failure occurred. The number at each bar indicates the percentage of life expended at the time a signal appeared. The asterisks represent a qualitative measure of the conservative treatment of data inherent in the tests. Because scanning was performed periodically, a crack could have developed considerably by the time the first scan was made. That is, had the scanning been continuous the signal could have been observed sooner and a lower percentage of fatigue life expended would have been indicated. This conservatism in the test data was indicated by an asterisk whenever a first-recorded signal of relatively high amplitude was encountered.

For the 6061-T6 aluminum, deflections for the three stress levels were set at ±0.040, ±0.050, and ±0.555 inch. The cycles to failure averaged 1.4×10^6, 0.7×10^6, and 0.43×10^6, respectively. The respective average percentages of life expended at first-signal detection were 76.7%, 74.5%, and 64.0%. The average percentage across all 18 samples was 71.7%.

For the Inconel X, deflections for the three stress levels were set at ±0.090, ±0.100, and ±0.130 inch. The cycles to failure averaged 1.4×10^6, 0.94×10^6, and 0.33×10^6, respectively. The respective average percentages of life expended at

---

[21] Moross, George G., INVESTIGATION TO DETERMINE THE FEASIBILITY OF DETECTING IMPENDING METAL FATIGUE FAILURE THROUGH USE OF AN INDUCTIVE SENSING DEVICE, Mechanical Technology Incorporated; USAAVLABS Technical Report 69-97, U.S. Army Aviation Materiel Laboratories, Fort Eustis, Virginia, February 1970, AD871155.

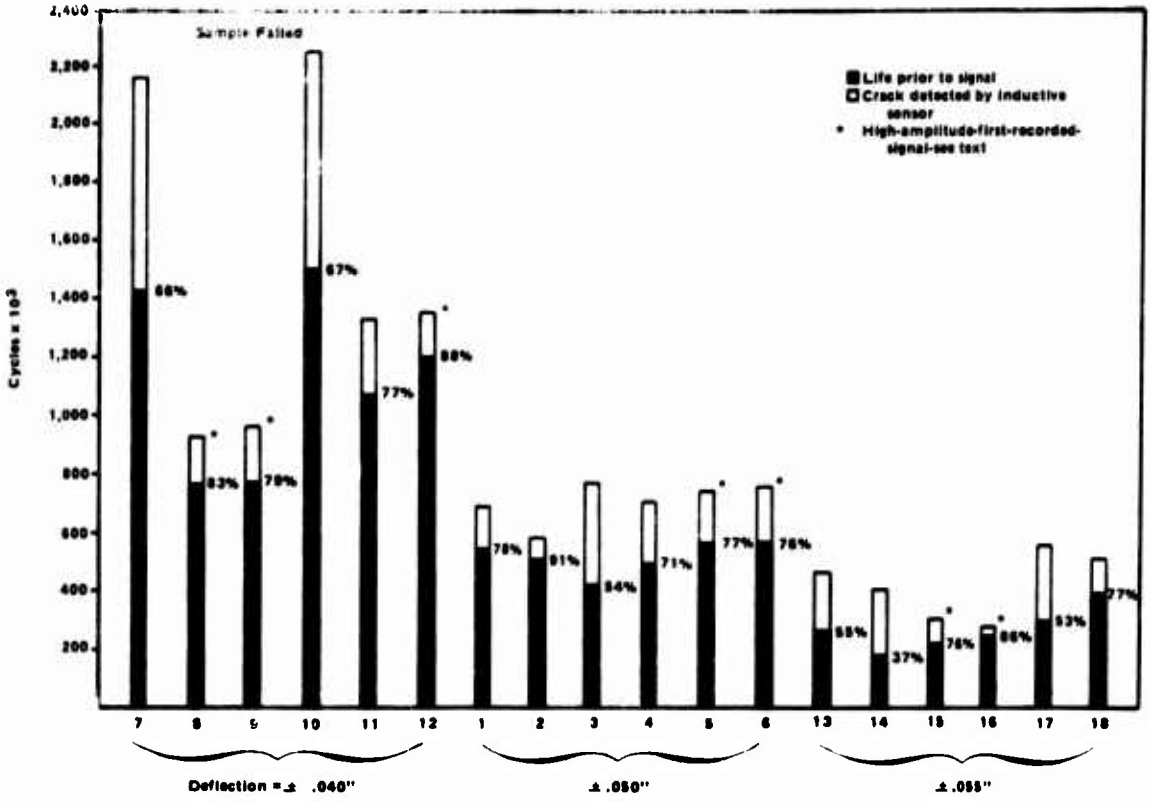

Figure A-9. Graphical Presentation of Results, Aluminum.

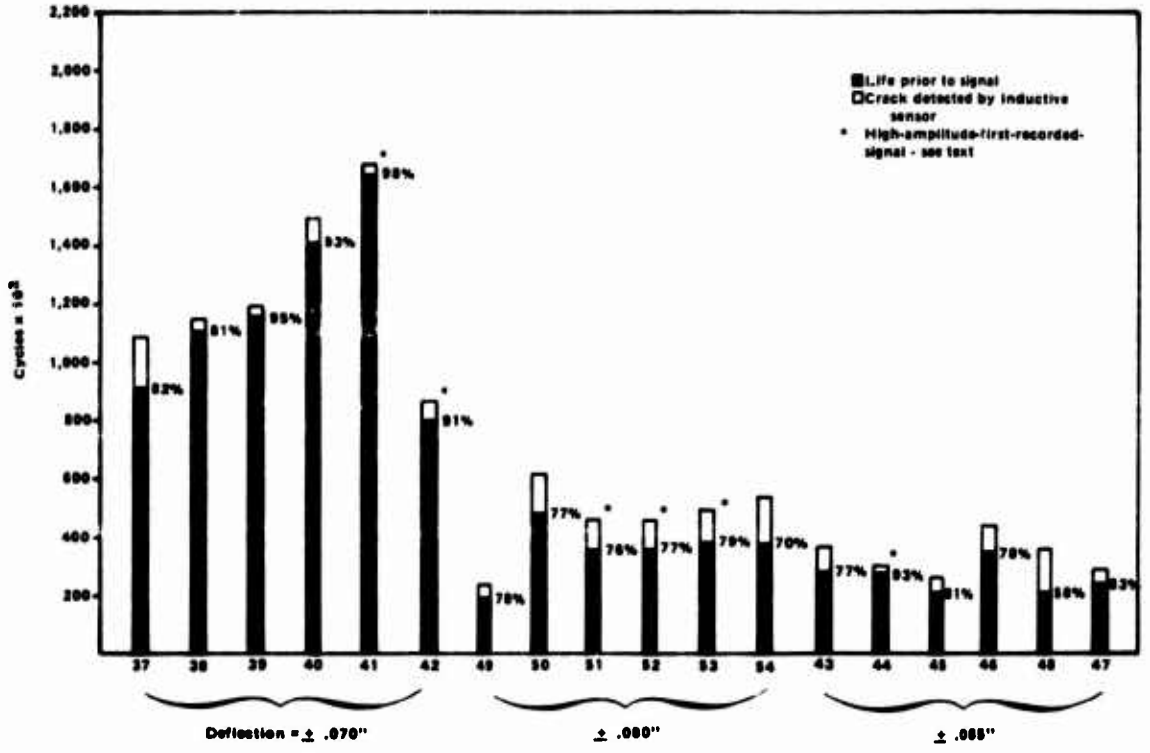

Figure A-10. Graphical Presentation of Results, Steel.

first signal detection were 83.0%, 78.8%, and 77.7%. The overall average percentage of life expended at time of first signal was 79.6%. The earliest signal appeared at 67% of life expended. The latest indication of 93% showed a very large amplitude signal at that point, indicating that the percentage figure could have been lower.

For the 9310 steel, deflections for the three stress levels were set at ±0.070, ±0.080, and ±0.085 inch. The cycles to failure average 1.24×10^6, 0.46×10^6, and 0.32×10^6, respectively. The respective average percentages of life expended at first-signal detection were 90.0%, 76.2%, and 78.3%. The overall average percentage of life expended at the time of first detected signal was 81.5%. All the tests that showed a percentage figure greater than 90% were considered conservative.

The use of modern microanalytical techniques and classical metallography indicates that microcracks as well as larger cracks are responsible for the signals.

For the roll tests, twelve samples were prepared from 8620-H steel. The samples were heat treated to a hardness of RC-63 with a case depth of 0.073 inch. The samples were run in contact with a crowned roller with a maximum Hertz compressive stress of up to 450 psi.

Figure A-11 shows excerpts from a recorder trace of a typical roll test. The baseline remained smooth and regular through 10 readings to 479,000 cycles. At 532,000 cycles, a small, repeated signal appeared. Three thousand cycles later, a large pit developed, which has been defined as evidence of failure.

Instrumentation

An example of an inductive sensing system which can readily be packaged for field use without sacrifice of utility or sensitivity consists of a probe, oscillator, bridge circuit, and detector.

The probe (solenoid) consists of a "U" shaped core constructed of soft iron wire wound on one leg such that the probe is axially symmetric about the wound leg. A second equivalent probe is placed behind the first one to provide temperature compensation. The two coils are then connected in a half-bridge configuration into the A.C. bridge circuit. The signal from the bridge is fed to a synchronous detector and filter, whose output is a D.C. signal corresponding to bridge unbalance. The probe is positioned so that the sample material forms the flux path. The bridge is initially balanced, and the probe is then scanned over the sample. If the standoff distance is held constant, then any bridge unbalance relates to the local characteristics of the material being examined. Test frequencies can range

anywhere from 60 Hz to 6 MHz. Normally selection of a test frequency is a compromise. Penetration is greater at lower frequencies; however, as the frequency is lowered the sensitivity to small flaws decreases. Normally one selects a test frequency as high as possible that still permits the penetration depth required.

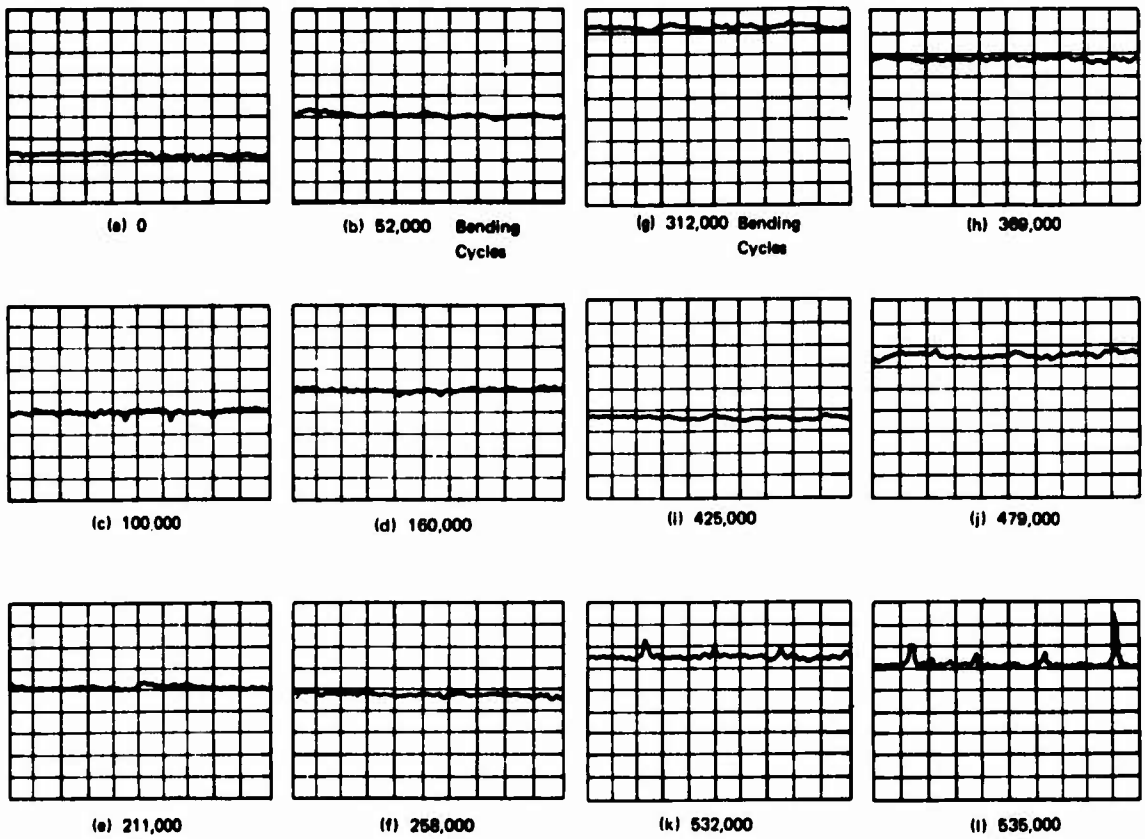

Figure A-11. Roll Test, Steel Sample 9.

Summary

The test results indicate that inductive sensing is capable of detecting microcracks in metals. Where early detection was possible on beam specimens as the cracks propagated normal to the surface, very late detection was evident on the roll specimens as the cracks propagated parallel to the surface. While the tests indicate that an inductive sensing system is of some value in detecting metal fatigue during vibratory beam tests, there has not been developed a model to analytically predict signal amplitudes as a function of either the number of fatigue cycles or the crack propagation rate. Additionally, there is a high degree of uncertainty present whenever the first signal encountered is of high amplitude. It is then difficult to predict remaining fatigue life by comparison with laboratory data that was taken by relatively continuous monitoring.

While inductive sensing is capable of flaw detection, it cannot be considered a satisfactory fatigue life indicator for helicopter components.

FOIL GAGE

Theory

Any strain action will induce strain hardening in a ductile metal which is hardenable by cold working. Dislocation theory in metallurgy proposes that cold working the metal lattice blocks the motion of the crystal boundaries by raising the stress level necessary to allow slip to occur. Since physicists seem to agree that a scattering of electrons as a result of dislocations causes a change in resistivity, cold working should induce a resistance change in a ductile metal. This resistance change is permanent and irreversible under normal conditions. The foil gage utilizes this resistance change due to fatigue-induced strain hardening as a memory capability to store its accumulated strain history. If the foil gage is adequately attached to a structure of interest, then both structure and gage should experience the same strain history at the point of attachment

Discussion

The foil fatigue gage was developed and patents applied for by the Boeing Company. Since then, exclusive manufacturing and distributing rights for the -S/N-Fatigue-life gage^{R} (trademark, Micro-Measurements, Inc., Romulus, Michigan) have been granted to Micro-Measurements, Incorporated.

The -S/N-Fatigue-life gage has the general appearance of a foil strain gage, and is manufactured with the same basic processes. The gage consists of a specially treated constantan foil grid, encased in a glass-fiber/epoxy laminate. It is available in a range of different sizes. The fatigue gage is bonded to the test surface using standard strain gage adhesives and installation techniques.

The fatigue gage manufacturer claims that the cumulative resistance change in the gage is a highly repeatable function of the cyclic strain history to which the gage has been subjected. An earlier study[22] investigated this functional relationship, employing a series of cantilever beam tests. The

---

[22] Harting, Darrell R., THE -S/N-FATIGUE-LIFE GAGE: A DIRECT MEANS OF MEASURING CUMULATIVE FATIGUE DAMAGE, Experimental Mechanics, February 1966.

relationship was found to be of the form

$$\Delta R = K_g(\varepsilon_R - \varepsilon_o)n^h$$

where

ΔR = percentage gage resistance change

ε_R = maximum reversed strain

ε_o = threshold strain, below which the resistance will not change

n = number of applied cycles

h = empirically determined

K_g = gage constant

Another earlier study[23] investigated the repeatability and response of the fatigue gage through a series of coupon tests under constant amplitude and variable amplitude loading. The constant amplitude tests were established for net section stress levels of 35 and 20 ksi at frequencies of 2 and 5 cps, respectively. The variable amplitude test setup was identical to that used for the constant amplitude tests except that the test machine was controlled by a digital programmer instead of a cyclic function generator. The limit load stress was 30 ksi. While the results from both sets of tests agree that the gage does experience a resistance change that can be related to nominal stress history, the test data demonstrate that the results are not consistent for a group of nominally identical structural members experiencing the identical nominal stress history.

The repeatability and response of the gage were again examined with a series of coupon tests[24]. The tests were designed to evaluate the effects on the gage of a range of environmental conditions. The test specimens were fabricated from 7075-T6 bare aluminum and 8Al-1Mo-1V titanium alloy. The majority of the coupons were evaluated under axial loading conditions. A few constant moment bending beams were evaluated to correlate the effect of bending strains versus axial strains upon the gage. It was concluded that the gage makes no distinction regarding direction of strain (tension or compression) or whether strains are bending or axial.

---

[23] EVALUATION OF THE -S/N-FATIGUE-LIFE GAGE UNDER CONSTANT AND VARIABLE AMPLITUDE LOADING, NADC-72071-VT, Naval Air Development Center, 5 September 1972.

[24] Horne, Robert S., A FEASIBILITY STUDY FOR THE DEVELOPMENT OF A FATIGUE DAMAGE INDICATOR, AFFDL-TR-66-113, Air Force Flight Dynamics Laboratory, Wright-Patterson AFB, Ohio, January 1967.

A series of coupons were evaluated at several different stress ratios ($A_S^* = 0.818$, $A_S = 0.333$, and $A_S = \infty$). For a given coupon, the stress ratio and strain amplitude were held constant until failure of the coupon. Constant end resistance at specimen failure was observed for a constant stress ratio. When the stress ratio was changed, specimen failure occurred at a different value of gage end resistance. Additionally, it was observed that the gage end resistance at coupon failure was several orders of magnitude higher under reversed strain than cyclic strain about a mean level.

To evaluate the performance characteristics of the gage under weather exposure, two specimens were subjected to a simulated weather environment for one year. A weatherometer was used to simulate rain for three minutes at seventeen-minute intervals with alternate sunshine supplied by carbon arc electrodes. The results demonstrated that when specimen fatigue life is reduced by weather exposure the end resistance of the gage is also reduced. Two of the gages which had been work hardened at room temperature to a fatigue induced resistance increase of 2.4% were subjected to a 90-hour heat soak at 400°F. It was found that the "irreversible" resistance increase could be reversed approximately 30% by a prolonged heat soak. Specimens were then tested at a 60 ksi stress level at both room temperature and -65°F. The specimen tested at room temperature had a fatigue life of 36,000 cycles, while the specimen tested at -65°F had a life of 179,000 cycles. Yet both gages demonstrated very nearly the same resistance at the end of the test.

The preponderance of evidence from the coupon tests indicated that the fatigue gage resistance at specimen failure is not a constant, and proper utilization of the gage requires calibrating the structure with statistical loading averages. The applicability of the fatigue gage on full-scale aircraft structures was examined in previous studies[24],[25]. A set of guidelines was formulated for application of the gage to aircraft structure:

---

* A_s(Alternating - Mean Ratio) = $\frac{S_a}{S_m}$ (Stress amplitude) / (Mean stress)

---

[24] Horne, Robert S., A FEASIBILITY STUDY FOR THE DEVELOPMENT OF A FATIGUE DAMAGE INDICATOR, AFFDL-TR-66-113, Air Force Flight Dynamics Laboratory, Wright-Patterson AFB, Ohio, January 1967.

[25] Horne, Robert S., and Freyre, Oscar L., ANNEALED FOIL FATIGUE SENSOR DEVELOPMENT, AFFDL-TR-71-127, Air Force Flight Dynamics Laboratory, Wright-Patterson AFB, Ohio, March 1972.

1) The structure's history of accumulated aerodynamic loadings can best be determined by locating each gage in higher strain areas free from stress concentrations.

2) The number and location of the gages on the structure should be sufficient to reliably evaluate the aircraft's degree of exposure to repeated load occurrences. Therefore, all critical fatigue sources should be instrumented.

3) Gages should be applied to the aircraft structure prior to accumulating any flight time.

4) To minimize effect of temperature variation, periodic data should be recorded under controlled ambient conditions or else a temperature correction factor should be applied.

Reference 25 also presents a methodology for relating the fatigue damage of the gage to the fatigue damage of the test item.

Instrumentation

Indications are that no structural modifications would be required on service aircraft prior to gage installation. Gage attachment techniques are well developed, and installation can be accomplished by technicians in field areas. The gage is essentially inexpensive compared to the value of the structure being monitored. Complex data acquisition systems are not required.

Summary

It has been shown that a functional correlation between structural fatigue damage and gage resistance change can be established. However, it has also been shown that the gage resistance at component failure is not a constant, and requires of its user a thorough understanding of the gage response and limitations. Some of the immediate problem areas are:

(1) The change in gage resistance is induced by fatigue damage to the gage sensing element, and not by damage to the structure of interest. The measurement of structure fatigue damage is merely implied. This problem is further compounded when low threshold sensitivity of the gage requires a strain multiplier.

(2) In most structures, fatigue failures occur at the locations of stress concentrations, such as holes

and notches. It is often difficult or impossible to mount gages in these locations.

(3) The effects of corrosion, fungus growth, chance effects, or other variables which influence the metallurgical condition of materials would be considered only to the extent that they affect the mechanical response of the structure.

(4) The gage is generally limited to low-cycle or medium-gage fatigue applications. This is impractical for helicopter applications.

(5) Finally, most of the work done to date on the fatigue gage has been directed toward fixed wing application.

CONCLUSIONS

The development of a passive fatigue damage indicator requiring no in-flight instrumentation has long been the aim of the aircraft industry. The annealed foil fatigue gage has shown promise of accomplishing this aim. However, there is a lack of consistency in the gage response under varying loading and environmental conditions. Consequently, it must be concluded that with the currently available gages, it is not possible to correlate a given percent resistance change with the actual fraction of fatigue life expended for a component outside the controlled laboratory environment.

The monitoring of acoustic emission during periodic proof stressing provides a means of detecting the presence and growth of fatigue cracks. Good results have been obtained in controlled situations where the damaging loads and the proof loads are applied in the same manner. However, to proof load components of a helicopter rotor system in a manner equivalent to the complex loads experienced during flight could require new hardware or disassembly of the system. Additionally, successful warning of impending fatigue failure has been demonstrated only for materials with low-cycle fatigue lives and not for the high-cycle fatigue lives encountered in helicopter components.

Because of the importance of helicopter component fatigue life prediction it is felt that work to develop a fatigue damage indicator should continue. Good agreement between experimental results and analytical predictions suggests further investigation of acoustic emission during high-cycle fatigue and complex loading. And the economy and ease of application of the foil gage offer an incentive for the further development of the gage element response.

APPENDIX B
COMPUTER PROGRAM DISCUSSIONS

FATHIP

FATHIP is a fatigue damage calculation program developed to duplicate the manufacturers' fatigue analysis of the UH-1H and CH-47C. The basis for both analyses is Miner's Rule of Cumulative Damage, which states that the fatigue life of a cyclically loaded structural item can be calculated by

$$T = T_0 \left[\sum_{i=1}^{n} \frac{n_i}{N_i} \right]^{-1} \qquad \text{(B-1)}$$

where n_i = number of cycles of oscillatory load magnitude y_i based on a spectrum of T_0 hours

N_i = number of cycles to failure at load magnitude y_i

n = number of loading conditions (flight conditions) in the loading spectrum

The input to the FATHIP program consists of flight usage spectra, flight loads data, component S-N data, and cycle-count factors. The flight loads data contain each occurrence of a flight condition and its corresponding oscillatory load, y_i. The usage spectra contain each flight condition and the corresponding percentage of spectrum time spent in that flight condition. With this information, n_i can be determined:

$$n_i = C_i \, P_i \qquad \text{(B-2)}$$

where n_i = number of cycles of oscillatory load y_i in T_0 hours

C_i = number of occurrences of ith flight condition in flight loads data

P_i = percentage of spectrum time spent in ith flight condition

FATHIP then uses y_i, S-N data for each component, and an interpolation routine to calculate n_i. The component damage accrued during the ith flight condition can now be computed by

$$D_i = (n_i/N_i)F_i \qquad \text{(B-3)}$$

where D_i = component damage accrued during ith flight condition

F_i = cycle-count factor for the ith flight condition.

The CH-47C fatigue substantiation report is based on damage calculations where the values of n_i are applied to loads, each load being the maximum recorded in the corresponding flight test data record. Generally, the true damage for the record, obtained by a cycle-by-cycle count, is considerably lower. The ratio of cycle-counted damage to life-calculation damage (damage caused by the same number of cycles at the top-of-scatter load) is the cycle-count factor. The values of F_i for each flight condition can be found in the manufacturers' fatigue substantiation report. For the UH-1H fatigue substantiation, the manufacturer does not compute cycle-count factors. The load range of flight records for high load maneuvers was broken down into several smaller ranges. A damage fraction was calculated for each of the small load ranges. These damage fractions were then summed to give the flight record (flight condition) damage fraction. The values of F_i for the UH-1H FATHIP runs were all set equal to one. The flight loads data for the high load maneuvers were modified to yield flight condition damage fractions for the design spectrum equal to those in the fatigue substantiation.

Substitution of Equation (B-3) into Equation (B-1) yields the component fatigue life T:

$$T = T_0 \left[\sum_{i=1}^{n} D_i/F_i \right]^{-1} \qquad \text{(B-4)}$$

The FATHIP logic was tested by using the design spectrum of the UH-1H and CH-47C as the usage spectrum. For the UH-1H, all but one of the FATHIP fatigue lives were within 1 percent of the manufacturer's fatigue substantiation lives.

For the main rotor blade, the FATHIP life was 3 percent high. For the CH-47C, all of the FATHIP lives were within 1 percent of the manufacturer's fatigue substantiation lives. These accuracies were considered satisfactory. Next, the upper bounds on component replacement times for the UH-1H and CH-47C were calculated for the mild, average, and severe usage spectra. A sample calculation performed by FATHIP on the UH-1H main rotor grip is shown in Table B-1.

TABLE B-1. SAMPLE OUTPUT OF FATHIP PROGRAM, DESIGN SPECTRUM FOR THE MAIN ROTOR GRIP OF THE UH-1H HELICOPTER

UH-1H HELICOPTER
FATIGUE LIFE DETERMINATION

MAIN ROTOR GRIP, P/N 204-011-121

FLIGHT CONDITIONS	FREQUENCY OF OCCURRENCE: % OF FLIGHT TIME TOTAL	% OF FLIGHT TIME INCREMENTAL	CYCLES PER 100 HOURS N	BEARING STRESS IN RETENTION BOLT-HOLE PSI	NUMBER OF CYCLES TO FAILURE Ni	DAMAGE FRACTION N/Ni	ACCUMULATED DAMAGE SUM N/Ni
I. GROUND CONDITIONS							
A. NORMAL ROTOR START		.530	0.000	0.000	INFINITE	0.000000	
B. NORMAL SHUTDOWN	1.0000	.500	0.000	0.000	INFINITE	0.000000 0.000000	0.000000
II. POWER-ON FLIGHT							
A. VERTICAL TAKE-OFF	.4000	.400	0.000	0.000	INFINITE	0.000000 0.000000	0.000000
B. HOVERING I.G.E.							
1. STEADY		3.290	0.000	0.000	INFINITE	0.000000	
2. RIGHT TURN		.133	0.000	0.000	INFINITE	0.000000	
3. LEFT TURN		.133	0.000	0.000	INFINITE	0.000000	
	3.4900					0.000000	0.000000
4. CONTROL REVERSAL							
A. LONGITUDINAL		.010	191.000	1920.000	.1342E+08	.000014	
B. LATERAL		.010	191.330	1613.930	INFINITE	0.000000	
C. RUDDER		.010	0.000	0.000	INFINITE	0.000000	
5. NORMAL ACCELERATION		1.000	0.000	0.000	INFINITE	0.000000	
6. NORMAL DECELERATION		1.000	0.000	0.000	INFINITE	0.000000	
7. MAX RATE ACCEL.		.250	0.000	0.000	INFINITE	0.000000	
8. MAX RATE DECEL.		.250	0.000	0.000	INFINITE	0.000000	
	2.5300					.000014	.000014
9. SIDEWARD FLIGHT							
1. TO THE RIGHT		.250	0.000	0.000	INFINITE	0.000000	
2. TO THE LEFT		.250	0.000	0.000	INFINITE	0.000000	
	.5000					0.000000	.000014
H. REARWARD FLIGHT		.250	.000	0.000	INFINITE	0.000000	
I. FULL POWER CLIMB		4.000	0.000	0.000	INFINITE	0.000000	
	4.2900					0.000000	.000014
J. FORWARD LEVEL FLT.							

UH-1H HELICOPTER
FATIGUE LIFE DETERMINATION

MAIN ROTOR GRIP, P/N 204-011-121

FLIGHT CONDITIONS	FREQUENCY OF OCCURRENCE: % OF FLIGHT TIME TOTAL	% OF FLIGHT TIME INCREMENTAL	CYCLES PER 100 HOURS N	BEARING STRESS IN RETENTION BOLT-HOLE PSI	NUMBER OF CYCLES TO FAILURE Ni	DAMAGE FRACTION N/Ni	ACCUMULATED DAMAGE SUM N/Ni
1. 0.2 VNE		1.000	0.000	0.000	INFINITE	0.000000	
2. 0.3		1.000	0.000	0.000	INFINITE	0.000000	
3. 0.4		2.000	0.000	0.000	INFINITE	0.000000	
4. 0.5		3.000	0.000	0.000	INFINITE	0.000000	
5. 0.6		7.000	0.000	0.000	INFINITE	0.000000	
6. 0.7		8.000	0.000	0.000	INFINITE	0.000000	
7. 0.8		15.000	0.000	0.000	INFINITE	0.000000	
8. 0.9 VNE		25.000	0.000	0.000	INFINITE	0.000000	
9. VNE		15.000	2871000.000	1132.000	INFINITE	0.000000	
	77.0000					0.000000	.000014
K. PART-POWER DESCENT		1.000	0.000	0.000	INFINITE	0.000000	
	1.0000					0.000000	.000014
L. RIGHT TURNS							
1. 0.3 VH		.500	0.000	0.000	INFINITE	0.000000	
2. 0.6 VH		1.000	0.000	0.000	INFINITE	0.000000	
3. 0.9 VH		.500	0.000	0.000	INFINITE	0.000000	
	2.0000					0.000000	.000014
M. LEFT TURNS							
1. 0.3 VH		.500	0.000	0.000	INFINITE	0.000000	
2. 0.6 VH		1.000	0.000	0.000	INFINITE	0.000000	
3. 0.9 VH		.500	0.000	0.000	INFINITE	0.000000	
	2.0000					0.000000	.000014
N. CYCLIC PULL-UPS							
1. 0.6 VH		.200	3828.000	1227.300	INFINITE	0.000000	
2. 0.9 VH		.050	957.000	1910.000	.1424E+08	.000067	
	.2500					.000067	.000081
O. COLLECTIVE PULL-UPS							
1. 0.6 VH		.200	3827.000	1999.000	.4747E+07	.000436	
2. 0.9 VH		.050	957.000	2805.000	.6552E+06	.001461	
	.2500					.001896	.001978
P. 0.9 VH CONTROL REV.							

TABLE B-1 - Concluded

UH-1H HELICOPTER FATIGUE LIFE DETERMINATION MAIN ROTOR GRIP, P/N 204-011-121	FREQUENCY OF OCCURRENCE			BEARING STRESS IN RETENTION BOLT-HOLE	NUMBER OF CYCLES TO FAILURE	DAMAGE FRACTION	ACCUMULATED DAMAGE
	% OF FLIGHT TIME		CYCLES PER 100 HOURS				
FLIGHT CONDITIONS	TOTAL	INCREMENTAL	N	PSI	Ni	N/Ni	SUM N/Ni
1. LONGITUDINAL		.050	957.000	2109.300	.552946E+07	.000173	
2. LATERAL		.050	957.000	2041.300	.728668E+07	.000131	
3. RUDDER		.050	957.000	1013.300	INFINITE	0.000000	
	.1500					.000304	.002282
Q. NORMAL LANDING							
1. 6500 LB GROSS WT.		.100	0.000	0.300	INFINITE	0.000000	
2. 7400 LB GROSS WT.		.300	0.000	0.300	INFINITE	0.000000	
3. 8500 LB GROSS WT.		.450	0.000	0.300	INFINITE	0.000000	
4. 9500 LB GROSS WT.		.150	17217.000	1680.300	.649084E+06	.000265	
	1.0000					.000265	.002547
III. TRANSITIONS							
A. PWR. TO AUTO.							
1. 0.3 VH		.130	0.000	0.000	INFINITE	0.000000	
2. 0.6 VH		.230	0.000	0.300	INFINITE	0.000000	
3. 0.8 VH		.050	0.000	0.300	INFINITE	0.000000	
	.3500					0.000000	.002547
B. AUTO. TO PWR.							
1. 0.4 VH		.100	0.000	0.300	INFINITE	0.000000	
2. 0.6 VH		.230	0.000	0.000	INFINITE	0.000000	
3. 0.8 VH		.050	0.000	0.000	INFINITE	0.000000	
	.3500					0.000000	.002547
IV. AUTOROTATION							
A. STEADY FWD. FLIGHT							
1. 0.4 VH		.030	0.000	0.300	INFINITE	0.000000	
2. 0.6 VH		1.000	0.000	0.000	INFINITE	0.000000	
3. 0.8 VH		.280	0.000	0.300	INFINITE	.000000	
	2.0000					0.000000	.002547
B. 60 KT. CONTROL REV.							
1. LONGITUDINAL		.010	0.000	0.000	INFINITE	0.000000	
2. LATERAL		.010	0.000	0.300	INFINITE	0.000000	
3. RUDDER		.010	0.000	0.300	INFINITE	0.000000	
	.0300					0.000000	.002547
C. RIGHT TURNS							

UH-1H HELICOPTER FATIGUE LIFE DETERMINATION MAIN ROTOR GRIP, P/N 204-011-121	FREQUENCY OF OCCURRENCE			BEARING STRESS IN RETENTION BOLT-HOLE	NUMBER OF CYCLES TO FAILURE	DAMAGE FRACTION	ACCUMULATED DAMAGE
	% OF FLIGHT TIME		CYCLES PER 100 HOURS				
FLIGHT CONDITIONS	TOTAL	INCREMENTAL	N	PSI	Ni	N/Ni	SUM N/Ni
1. 0.6 VH		.230	0.000	0.300	INFINITE	0.000000	
2. 0.8 VH		.250	0.000	0.000	INFINITE	0.000000	
3. 1.0 VH		.050	0.000	0.000	INFINITE	0.000000	
	.9000					0.000000	.002547
D. LEFT TURNS							
1. 0.6 VH		.200	0.000	0.300	INFINITE	0.000000	
2. 0.8 VH		.250	0.000	0.300	INFINITE	0.000000	
3. 1.0 VH		.053	0.000	0.300	INFINITE	0.000000	
	.9000					0.000000	.002547
E. AUTO LDG APPR W/PWR REC							
1. 0.6 VH		.000	0.000	0.300	INFINITE	0.000000	
2. 0.8 VH		.100	0.000	0.300	INFINITE	0.000000	
3. 1.0 VH		.020	0.000	0.000	INFINITE	0.000000	
	.2000					0.000000	.002547
F. FULL AUTO LANDING		.250	0.000	0.000	INFINITE	0.000000	
	.2500					0.000000	.002547
					TOTAL DAMAGE IN 100 HRS.(D) =		.002547

FATIGUE LIFE = 100/D = 39258.78HOURS

FCMMOD

The computer program FCMMOD was written to compute the flight condition category damage rates for the 12 FCM recording systems. The program utilizes a design flight spectrum and component damage fractions taken from the manufacturer's fatigue substantiation. These fractions represent the amount of fatigue damage accrued by a component due to a particular flight condition in the design flight spectrum. For each FCM recording system, FCMMOD requires data defining the distribution of the flight conditions among the flight condition categories. With this information, FCMMOD can compute the fatigue damage accrued by a component due to a particular flight condition category:

$$D_k = \sum_{i=1}^{n} (P_{ik})(DC_i) \left(\frac{TC_i}{TS_i}\right) \qquad \text{(B-5)}$$

where D_k = component damage due to kth flight condition category

P_{ik} = percentage of ith flight condition appearing in the kth flight condition category

DC_i = component damage fraction for the ith flight condition

TS_i = flight time spent in the ith flight condition of flight spectrum

TC_i = weighted flight time spent in ith flight condition

n = number of flight conditions in flight spectrum

The value of TC_i is determined in FCMMOD from the percentage of total damage that the ith flight condition produces. If a component damage fraction is greater than 5% of the total damage to the component, then TC_i is defined such that $(TC_i/TS_i) > 1$. If a component damage fraction is between 0.01% and 5% of the total damage to the component, then TC_i is defined such that $(TC_i/TS_i) = 1$. If a component damage fraction is less than 0.01% of the total damage to the component, then TC_i is defined such that $(TC_i/TS_i) < 1$. This slight modification of the damage fractions introduces a conservatism into the systems by increasing the contribution of highly damaging flight conditions and decreasing the contribution of slightly damaging or nondamaging flight conditions. The amount of flight time spent in each flight condition category is computed in a similar manner:

$$T_k = \sum_{i=1}^{n} P_{ik}\, TS_i \qquad \text{(B-6)}$$

where T_k = amount of flight time spent in kth flight condition category

From the results of Equations (1) and (2), a flight condition category damage rate may be calculated for each component:

$$A_k = D_k/T_k \tag{B-7}$$

where A_k = kth flight condition category damage rate for a particular component

SIMULE

The computer program SIMULE was written to simulate the implementation of the FCM recording systems. For this simulation, SIMULE computes the component fatigue lives by using the flight condition category damage rates generated by FCMMOD and the mild, average, and severe flight usage spectra. For each FCM recording system, SIMULE requires data defining the distribution of the flight conditions among the flight condition categories. With this information, SIMULE can compute the amount of flight time spent in each flight condition category:

$$T_k = \sum_{i=1}^{n} P_{ik}\, TS_i \tag{B-8}$$

where T_k = amount of flight time spent in kth flight condition category

P_{ik} = percentage of ith flight condition appearing in the kth flight condition category

TS_i = flight time spent in the ith flight condition of flight spectrum

n = number of flight conditions in flight spectrum

Multiplying each T_k by its corresponding flight condition category damage rate results in the amount of damage accrued by a particular component due to each flight condition category. These can be summed to yield the total damage accrued by a component in the usage spectrum:

$$D = \sum_{k=1}^{m} A_k\, T_k \tag{B-9}$$

where D = total damage to a component during the usage spectrum

A_k = kth flight condition category damage rate for a particular component

m = number of flight condition categories

The total flight time T_t during the usage spectrum can be found by

$$T_t = \sum_{k=1}^{m} T_k \tag{B-10}$$

From the results of Equations (B-9) and (B-10), the component fatigue life can be calculated:

$$FL = T_t/D \tag{B-11}$$

where FL = component fatigue life

SIMULE performs the above calculations for each of three usage spectra.

COMPONENT LOAD MONITORING MODEL (CLMMOD)

The name "linear programming" is given to any numerical method for finding an extreme value of a linear function of several variables; this value is required to satisfy a set of linear constraints. The linear programming problem may then be represented as

$$\text{MAXIMIZE } g(W_1, \ldots, W_q) = \sum_{j=1}^{q} C_j W_j \tag{B-12}$$

subject to the constraints

$$\sum_{j=1}^{q} k_{\alpha j} W_j \leq d_\alpha \qquad \alpha = 1, \ldots, p \tag{B-13}$$

and

$$W_j \geq 0 \qquad j = 1, \ldots, q \tag{B-14}$$

Equation (B-12) defines the linear function to be optimized and is called the objective function. Equation (B-12) can also describe a minimization problem, since maximizing +q is the same as minimizing -g. If the constraints of a posed problem do not conform to Equation (B-13), the sense of the inequalities can be reversed by multiplication by -1. Equation (B-13) also permits equalities, as well as combinations of equalities and inequalities.

According to Miner's Rule of Cumulative Damage, the fatigue life of a cyclically loaded structural item can be calculated by

$$T = T_0 \left[\sum_{i=1}^{n} \frac{n_i}{N_i} \right]^{-1} \qquad \text{(B-15)}$$

where n_i = number of cycles of oscillatory load magnitude y_i based on a spectrum of T_0 hours

N_i = number of cycles to failure at load magnitude y_i

n = number of loading conditions (i.e., flight conditions) in the loading spectrum

It is now possible to write

$$1/N_i = f(y_i) \qquad \text{(B-16)}$$

$$n_i = \omega_i T_0 \qquad \text{(B-17)}$$

where f = functional representation of the S-N curve

ω_i = relative frequency of occurrence of each loading condition

The function f is of the form

$$f(S) = \begin{cases} \left[\frac{1}{\beta} \left(\frac{S}{S_e} - 1 \right) \right]^{1/\gamma} & \text{for } S \geq E \\ 0 & \text{for } S < E \end{cases}$$

where β, γ, and S_e are constants obtained by a least-square fit of the digitized S-N curve and E is the endurance limit of the component under consideration. Equation (B-15) can then be rewritten as

$$T = \left\{ \sum_{i=1}^{n} \omega_i \, f(y_i) \right\}^{-1} \qquad \text{(B-18)}$$

If y_i (rotating component load) is now approximated as a linear combination of another set of parameters (stationary component loads)

$$\hat{y}_i = A_0 + A_1 X_{i1} + \ldots + A_m X_{im}$$
$$= \sum_{k=0}^{m} A_k X_{ik} \qquad X_{i0} \equiv 1 \qquad \text{(B-19)}$$

then from Equation (B-18) the approximation to the fatigue life of the item can now be written as

$$\hat{T} = \left\{ \sum_{i=1}^{n} \omega_i \, f\left(\sum_{k=0}^{m} A_k X_{ik} \right) \right\}^{-1} \qquad \text{(B-20)}$$

If we now require that

$$\hat{y}_i \geq y_i \qquad i = 1, \ldots, n \qquad \text{(B-21)}$$

then $\hat{T} \leq T$ and the optimal approximation of y_i [Equation (B-19)] is the set of A_k's which maximizes the function $\hat{T}$ [Equation (B-20)] while satisfying Equation (B-21). $\hat{T}$ can be maximized by maximizing the new function

$$\hat{D} = -\sum_{i=1}^{n} \omega_i \, f\left\{ \sum_{k=0}^{m} A_k X_{ik} \right\} \qquad \text{(B-22)}$$

This type of optimization can be formulated as a sequence of linear programming problems by first expanding $\hat{D}$ as a Taylor Series about progressively better estimates, $A_k^{(0)}$, of A_k. Expanding $\hat{D}$ about some initial estimate $A_k^{(0)}$ and neglecting the constant term yields

$$\hat{D} \simeq \sum_{j=1}^{m} \Delta Aj \, \frac{\partial \hat{D}}{\partial Aj} \Big|_{A_j = A_j^{(0)}} \qquad \text{(B-23)}$$

where

$$\Delta Aj = Aj - Aj^{(0)} \qquad \text{(B-24)}$$

Recalling that

$$\hat{y}_i = \sum_{k=0}^{m} A_k X_{ik} \tag{B-25}$$

we can then write

$$\frac{\partial \hat{D}}{\partial A_j} = - \sum_{i=1}^{n} \omega_i \frac{\partial f}{\partial \hat{y}_i} \frac{\partial \hat{y}_i}{\partial A_j} \tag{B-26}$$

and

$$\frac{\partial \hat{y}_i}{\partial A_j} = \sum_{k=0}^{m} \frac{\partial A_k}{\partial A_j} X_{ik} = \sum_{k=0}^{m} \delta_{jk} X_{ik} = X_{ij} \tag{B-27}$$

Substitution of Equation (B-27) into Equation (B-26) yields

$$\frac{\partial \hat{D}}{\partial A_j} = - \sum_{i=1}^{n} \omega_i \frac{\partial f}{\partial y_i} X_{ij} \tag{B-28}$$

and

$$\left. \frac{\partial \hat{D}}{\partial A_j} \right|_{A_j = A_j(0)} = - \sum_{i=1}^{n} \omega_i \left. \frac{\partial f}{\partial \hat{y}_i} \right|_{\hat{y}_i = \hat{y}(0)} X_{ij} \tag{B-29}$$

where

$$\hat{y}_i(0) = \sum_{k=0}^{m} A_k(0) X_{ik} \tag{B-30}$$

Substitution of Equation (B-29) into Equation (B-23) yields

$$\hat{D} \simeq - \sum_{j=1}^{m} \left\{ \sum_{i=1}^{n} \omega_i \left. \frac{\partial f}{\partial \hat{y}_i} \right|_{\hat{y}_i = \hat{y}_i(0)} X_{ij} \right\} \Delta A_j \tag{B-31}$$

Combining Equations (B-19), (B-21), and (B-24) yields

$$\sum_{k=0}^{m} \Delta A_k X_{ik} \geq y_i - \sum_{k=0}^{m} A_k(0) X_{ik} \tag{B-32}$$

If we now define two new terms

$$a_j = -\sum_{i=1}^{n} \omega_i \left.\frac{\partial f}{\partial \hat{y}_i}\right|_{\hat{y}_i = \hat{y}_i(0)} X_{ij} \qquad \text{(B-33)}$$

$$b_i = y_i - \sum_{k=0}^{m} A_k^{(0)} X_{ik} \qquad \text{(B-34)}$$

we can formulate the linear programming problem

$$\text{MAXIMIZE } \hat{D} = \sum_{j=1}^{m} a_j \Delta A_j \qquad \text{(B-35)}$$

subject to the constraints

$$-\sum_{k=0}^{m} \Delta A_k X_{ik} \leq b_i \qquad i = 1, \ldots, n \qquad \text{(B-36)}$$

Each time a solution to Equations (B-35) and (B-36) is found, the $A_j^{(0)}$ are redefined as

$$A_j^{(0)} = A_j^{(0)} + \Delta A_j \qquad \text{(B-37)}$$

until either

$$\Delta A_j \leq T_A \qquad k = 0, \ldots, m \qquad \text{(B-38)}$$

where T_A = some small tolerance, or a predetermined number of iterations has been performed. At this point, $A_j^{(0)}$ [Equation (B-37)] yields the optimal approximation to y_i [Equation (B-25)] subject to Equation (B-21).

Every linear programming problem has a counterpart that is called its "dual." An optimal solution to the dual problem reveals information about the optimal solution of the "primal," or original, problem. This is important since the dual is often easier to work than the primal. The dual of the general linear programming problem represented by Equations (B-12), (B-13), and (B-14), is

$$\text{MINIMIZE } h(U_1, \ldots, U_p) = \sum_{\alpha=1}^{m} U_\alpha d_\alpha \qquad \text{(B-39)}$$

subject to

$$\sum_{\alpha=1}^{p} U_\alpha B_{\alpha j} \geq C_j \qquad j = 1, \ldots, q \qquad \text{(B-40)}$$

and

$$U_\alpha \geq 0 \qquad \text{(B-41)}$$

Since m << n for our particular problem, it is computationally more efficient to replace the linear programming problem posed by Equations (B-35) and (B-36) with its dual.

The optimization problem formulated in the CLM methodology is not consistent with Equation (B-14) of the general linear programming problem in that the ΔA_j must be unrestricted in sign. This condition can be handled by stating without proof the "Unsymmetrical Dual Theorem." If the primal is defined by

$$\text{MAXIMIZE } g(W_1, \ldots, W_n) = \sum_{j=1}^{q} C_j W_j \qquad \text{(B-42)}$$

subject to

$$\sum_{j=1}^{q} B_{\alpha j} W_j = d_\alpha \qquad \text{(B-43)}$$

and

$$W_j \geq 0 \qquad \text{(B-44)}$$

its dual is then defined by

$$\text{MINIMIZE } h(U_1, \ldots, U_m) = \sum_{\alpha=1}^{p} U_\alpha b_\alpha \qquad \text{(B-45)}$$

subject to

$$\sum_{\alpha=1}^{p} U_\alpha B_{\alpha j} \geq C_j \qquad \text{(B-46)}$$

with U_α unrestricted in sign.

A slight modification of the theorem allows us to write the dual of Equations (B-35) and (B-36) as

$$\text{MINIMIZE } D^* = \sum_{i=1}^{n} (-b_i)\, Z_i \tag{B-47}$$

subject to

$$-\sum_{i=1}^{n} X_{ik}\, Z_i = A_j \tag{B-48}$$

and

$$Z_i \geq 0 \tag{B-49}$$

The solution ΔA_j to the primal problem, Equations (B-35) and (B-36), can be obtained quite easily from its dual.

The initial estimate of $A_j^{(0)}$ was arrived at by a least-square fit of y_i; that is, by finding the A_j which minimizes the quantity

$$Z = \sum_{i=1}^{n} (y_i - \hat{y}_i)^2 \tag{B-50}$$

where $\hat{y}_i$ is defined in Equation (B-19).

$$Z = \sum_{i=1}^{n} \{y_i - \sum_{j=0}^{m} X_{ij}\, A_j\}^2 \tag{B-51}$$

Z is minimized by requiring that

$$\frac{\partial Z}{\partial A_k} = 0 \qquad k = 0, \ldots, m \tag{B-52}$$

Substitution of Equation (B-51) into (B-52) yields

$$\frac{\partial}{\partial A_k} \sum_{i=1}^{n} \{y_i - \sum_{j=0}^{m} X_{ij}\, A_j\}^2 = 0 \tag{B-53}$$

Carrying out the partial differentiation in Equation (B-53) results in

$$\sum_{j=0}^{m} A_j \sum_{i=1}^{n} X_{ik}\, X_{ij} = \sum_{i=1}^{n} X_{ik}\, y_i \qquad k = 0, \ldots, m \tag{B-54}$$

The A_j's which satisfy Equation (B-54) are used as the initial values for $A_j^{(0)}$.

A computer program entitled CLMMOD was written to implement the solution scheme presented above. The program consists of 29 subroutines, with most of them designed to facilitate the data input and output and the data handling. The computational core of the program is a library subroutine entitled SIMPLX, which utilizes the simplex method to solve a linear programming problem of the form

$$\text{MINIMIZE} \sum_{j=1}^{n} C_j Z_j \tag{B-55}$$

subject to r constraints

$$\sum_{j=1}^{n} A_{ij} Z_j = B_i \qquad \text{for } i = 1, \ldots, r \tag{B-56}$$

and

$$Z_j \geq 0 \text{ for all } j \text{ values} \tag{B-57}$$

A_{ij}, B_i, and C_j are fixed quantities, and Z_j is unknown.

A second library subroutine entitled SLEQ was used in arriving at the initial values for $A_j^{(0)}$. SLEQ is a simultaneous linear equation solver which handles a set of equations of the form

$$Ax = b \tag{B-58}$$

The input to CLMMOD consists of rotating component loads, corresponding stationary component loads, S-N curve parameters for each rotating component, and various aircraft descriptors.

COST EFFECTIVENESS ANALYSIS PROGRAM (CEAP)

Introduction

During the HIP program the cost benefit of monitoring systems for improved life-cycle helicopter usage was analyzed. This analysis compared the costs for developing, installing, and maintaining the monitoring systems and their corresponding data processing systems with the savings resulting from reduced component inspection, maintenance, and replacement.

Costs

Table B-2 lists the cost categories and gives the type of expense (material, labor, nonrecurring, and recurring) associated with each category. The expenses for each category include overhead. Each category is briefly explained as follows:

TABLE B-2. COST CLASSIFICATION BY CATEGORY

CATEGORY	MATERIAL	LABOR	NON-RECURRING	RECURRING
Prototype Development	X	X	X	
Environmental Testing		X	X	
Preproduction		X	X	
Proof Testing		X	X	
Recorder Components and Miscellaneous Hardware	X		X	X
Assembly		X	X	
Unit Inspection and Testing		X	X	
Material Handling		X	X	X
Technical Orders		X	X	
Aircraft Modification		X	X	
System Shipping Containers	X	X	X	
System Delivery		X	X	
Monitoring System Installation		X	X	
Overhaul and Repair Stations	X	X	X	X
Transmitters	X		X	X
Processing System Development		X	X	
Documentation	X	X	X	X
Data Processing		X		X

1. Prototype Development

Includes all expenses for (1) mechanism and concept proof, (2) detailed layouts, (3) complete detail and assembly drawings, (4) prototype fabrication, (5) finalized drawings and preparation for manufacture, and (6) material.

2. Environmental Testing

Includes all expenses to test the monitoring system's compliance with specifications for military environment. Costs are based on expected sub-contract efforts.

3. Preproduction

Includes all expenses to set up the assembly line production.

4. Proof Testing

Includes all installation and removal fees associated with flight testing of a prototype recording system. Costs for the structure modification to permit recorder installation are included under the Aircraft Modification category rather than under this category.

5. Recorder Components and Miscellaneous Hardware

Includes all material expenses for recording system components and hardware such as timers, counters, transducers, cassettes, wiring, and casing.

6. Assembly

Includes the first board and then all unit assembly expenses incurred during production.

7. Unit Inspection and Testing

Includes all expenses to inspect and test each production recorder unit.

8. Material Handling

Includes all expenses for purchase and acceptance of recorder components.

9. Technical Orders

Includes all expenses to prepare and produce the technical and operational manuals for the description, installation, operation, and repair of the monitoring system.

10. Aircraft Modification

Includes all expenses to (1) prepare detailed drawings for the recording system installation in the helicopter, (2) design and prepare complete detail and assembly drawings of all structural modifications, (3) perform proof installation of the recording system, and (4) prepare finalized drawings.

11. System Shipping Containers

Includes all expenses to package each monitoring system in accordance with military Class A packaging specifications.

12. System Delivery

Includes all expenses to deliver each unit to any location in the Continental United States.

13. Monitoring System Installation

Includes all expenses for Government installation of the monitoring system.

14. Overhaul and Repair Stations

Includes all expenses to outfit the depot assigned for the monitoring system repair.

15. Transmitters

Includes all expenses to develop and maintain a playback unit to place the airborne data on a cassette.

16. Processing System Development

Includes all expenses to develop and implement a data processing system used solely to analyze helicopter usage data.

17. Documentation

Includes all expenses to prepare monthly, interim, and final reports; drawings; and correspondence.

18. Data Processing

Includes all expenses to process and analyze the monitoring system data for one year.

Total Costs

Costs were calculated on a per unit aircraft basis. Unit costs for categories such as Prototype Development, Environmental Testing, Preproduction, Proof Testing, and Processing System

Development were determined by dividing the total nonrecurring costs by the number of helicopters in the fleet. Unit costs for the overhaul and repair stations as well as for playback units were handled similarly but were corrected for their quantity. Except for the Data Processing category, the recurring costs for each category were associated with the replacement of the monitoring system hardware. All recurring costs were determined on a per year as well as a per unit aircraft basis. Consequently, the total cost per unit was determined by multiplying the recurring costs for each helicopter by the helicopter life in years and adding the results to the nonrecurring costs.

Savings

Savings are realized when a helicopter's operational usage is continuously monitored and the fatigue life of its components is constantly known. Components would no longer need to be replaced simply because their design life has been expended. Instead, a component would be replaced when its fatigue life approaches damage allowables. As a result, fewer components are replaced during the helicopter's life.

The number of component replacements saved by using the proposed monitoring system is the basis for savings. To illustrate, the following sample analysis calculates the number of component retirements for both the design and the operational usage and then compares the two numbers to yield the saved replacements. The operational usages and weighting factors for each, as previously described, are used to determine the number of spared replacements.

Replacements

Assume that a helicopter has flown 60 hours per month for 10 years and that a specific helicopter component has a design retirement life of 2500 hours. The number of replacements required for that component in the life of the helicopter is

$$\frac{7200 \text{ hours}}{2500 \text{ hours/replacement}} = 2.9 \text{ replacements}$$

For the same monthly flight time and service life, assume that the helicopter's operational usage is classified as mild, normal, or severe, and that the component's retirement life is 9000, 6000, and 3000 hours, respectively, for these usage classifications. Furthermore, assume that the helicopter has flown 30, 50, and 20 percent of its flight time in the respective usage classifications. The number of replacements for the same component would then be

$$\frac{0.30 \times 7200 \text{ hours}}{9000 \text{ hours/replacement}} = 0.2$$

$$+ \frac{0.50 \times 7200 \text{ hours}}{6000 \text{ hours/replacement}} = 0.6$$

$$+ \frac{0.20 \times 7200 \text{ hours}}{3000 \text{ hours/replacement}} = 0.5$$

1.3 replacements

Thus, by using the monitoring system, the replacements for this component would be reduced from 2.9 replacement to 1.3 for a net reduction of 1.6 replacements. Realistically, partial replacements are not possible so that the actual reduction in replacement would be 1 since three replacements would be made with the current practice and only two replacements would be made with the monitoring system. These saved replacements are, of course, contingent on the assumption that the usage specified in the example occurs. The test usage spectra and weighting factors were assumed to represent the average usage of the fleet.

Savings result from reduced component replacements. These savings are expressed in terms of the saved components, maintenance to replace components, and inspection of replaced components. The savings for the saved components may be expressed as follows:

$$S_R = \sum_i (C_i + CC_i + SC_i) \cdot n_i \cdot \sum_{j=1}^{3} f_j \cdot (r_{d_i} - r_{j_1}) \quad \text{(B-59)}$$

where S_R = component replacement savings

i = component index

C_i = replacement cost for the ith component

CC_i = container cost for the ith component

SC_i = shipping cost for the ith component

n_i = quantity of the ith component

j = operational usage spectrum index where $j = 1, 2, 3$ for mild, normal, and severe, respectively

f_j = weighting factor associated with jth operational usage

r_{d_i} = number of replacements for the ith component as determined by the design usage retirement life

r_{j_i} = number of replacements for the ith component as determined by the jth operational usage retirement life

Since shipping and container costs were not readily available for most of the components considered on the UH-1 and CH-47 helicopters, they were estimated from the known container and shipping costs for the main rotor blade on each helicopter. Tables B-3 and B-4 present these estimates for the UH-1 and CH-47 helicopters, respectively.

TABLE B-3. ESTIMATED COSTS FOR UH-1H COMPONENT CONTAINERS AND SHIPPING

COMPONENT DESCRIPTION	CONTAINER COST	SHIPPING COST
Main Rotor Blade	200.00[26]	90.00[26]
Drag Brace	4.10	1.85
Yoke	43.20	19.45
Pitch Horn	2.10	1.00
Scissors	2.50	1.00
Swashplate Support	8.50	3.80
Collective Lever	2.50	1.00
Stabilizer Bar	16.20	7.30
Retention Strap	9.70	4.35

The savings from reduced maintenance because of the decreased number of component replacements required in the helicopter's life and the corresponding decrease in the paperwork to document component replacement may be expressed as follows:

$$S_M = (M_{m_a} + M_D) \cdot C_m \cdot \sum_{j=1}^{3} f_j \cdot \left(\sum r_{d_i} - \sum_i r_{j_i}\right) \quad \text{(B-60)}$$

where S_M = total savings associated with maintenance

M_{m_a} = average number of man-hours to replace one component

[26] Maloney, Paul F., and Akeley, Carrol R., DESIGN STUDY OF REPAIRABLE MAIN ROTOR BLADES, Kaman Aerospace Corporation; USAAMRDL Technical Report 72-12, U.S. Army Air Mobility Research and Development Laboratory, Fort Eustis, Virginia, July 1972, AD-749-283.

M_D = number of man-hours to document the maintenance required to replace one component

C_m = cost per man-hour

The equation used to determine the average number of man-hours to replace one component is

$$M_{m_a} = \frac{\sum_i n_i \cdot M_{m_i}}{\sum_i n_i} \qquad \text{(B-61)}$$

where M_{m_i} = man-hours to replace ith component

TABLE B-4. ESTIMATED COSTS FOR CH-47C COMPONENT CONTAINERS AND SHIPPING

COMPONENT DESCRIPTION	CONTAINER COST	SHIPPING COST
Aft Rotor Shaft	215.20	33.40
Aft Rotor Hub	129.40	20.10
Aft Rotor Hor. Pin	15.30	2.40
Aft Rotor Blade Socket	31.80	4.90
Aft Rotor Tie Bar	15.50	2.40
Aft Rotor Blade	290.00[27]	45.00[27]
Aft Rotor Pitch Shaft	37.60	5.80
Forward Rotor Blade Socket	32.50	5.00
Forward Rotor Tie Bar	15.50	2.40
Forward Rotor Pitch Shaft	37.60	5.80

The savings accrued for reduced component inspections are a result of a reduction in replacement inspections. Each replacement inspection was assumed to last 0.17 hours, regardless of the component. Savings were calculated as follows:

[27] CH-47A, B, AND C SERIES HELICOPTER ROTOR BLADE FAILURE AND SCRAP RATE DATA ANALYSIS, The Boeing Company, Vertol Division; USAAMRDL Technical Report 71-58, U.S. Army Air Mobility Research and Development Laboratory, Fort Eustis, Virginia, November 1971, AD-739-568.

$$S_I = M_I \cdot C_M \cdot (r_{d_i} - \sum_{j=1}^{3} f_j \cdot r_{j_k}) \qquad \text{(B-62)}$$

where S_I = total savings associated with inspections

M_I = number of man-hours required to conduct one complete inspection

C_M = cost per man-hour

r_{d_i} = number of replacements for the ith component as determined by the design usage retirement life

r_{j_k} = number of replacements for the kth component as determined by the jth operational retirement life

Total Savings

The component replacement, inspection, and maintenance savings were added as follows to yield a total savings to be compared with the costs for developing and implementing the proposed monitoring system.

$$S_T = S_R + S_I + S_M \qquad \text{(B-63)}$$

where S_T = total savings for one helicopter over its projected life

LIST OF SYMBOLS

A	proportionality constant
ACTION	Aircraft Component Time Since Installation, Overhaul, or New
A_{ij}	proportion of time in the ith spectrum for helicopters in the jth mission
A_K	kth flight condition category damage rate for a particular component
A_k	given set of constants, not all equal to zero
ASIP	Aircraft Structural Integrity Program
A_S	stress ratio
BIT	built-in test
B_j	proportion of helicopters in the jth mission
C	damage rate for a given flight condition capacitor
CASIR	Chronological Analysis of Selected Items Record
CEAP	Cost Effectiveness Analysis Program
CGI	cruise guide indicator
CHAOS	Chronological, Historical Aircraft Ownership Summary
C_i	theoretical damage rate for the ith mission segment
C_{ij}, C(I,J)	theoretical damage rate for the jth component type for the ith flight condition category
CLM	component load monitoring
CLMMOD	component load monitoring model (linear programming program to determine optimum linear relationship between rotating and stationary component loads)
CMOS	complementary metal oxide silicon
C_N	theoretical damage rate for the Nth functional assignment
CTMS	Component Tracking Management System
D	total computed fatigue damage

LIST OF SYMBOLS - Continued

ΔD	incremental damage to the component
D_i	component damage accrued during ith flight condition
D_K	component damage due to kth flight condition category
DM	direct monitoring
$\Delta D1, \Delta D2, \ldots \Delta D6$	cumulative damage increments for the rth to (r-1)(r-2)...(r-6) records, separately
E	function error
ECP	engineering change proposal
f	functional representation of the S-N curve
FA	functional assignment
FATHIP	Fatigue Analysis Program
FCM	flight condition monitoring
FCMMOD	flight condition category damage rate calculation program
FDAM	Fatigue Damage Assessment Model
FDAS	Fatigue Damage Assessment System
F_i	weighting factor for the ith spectrum
GLIM	Gains and Losses in the Inventories of Major Items
IGE	in ground effect
IMH	inspection man-hours
IPS	Initial Processing System
LCST	longitudinal cyclic speed trim
L_{Fn}	actual load recorded on the nth fixed component
L_R	actual load experienced on the rotating component
LSB	least significant bit
M	number of component types
m	constant for given material of a particular thickness

m	number of flight condition categories
MIT	Major Item Trends
MMH	maintenance man-hours
MS	mission segment
MTM	mission type monitoring
N	number of cycles to failure at a given load level
N	number of flight condition categories
N	total number of acoustic emission signals resulting from dislocation motion
n	applied cycles of a specific load level
n	number of loading conditions (flight conditions) in loading spectrum
N_i	number of cycles to failure at load magnitude y_i
n_i	number of cycles of oscillatory load magnitude y_i based on a spectrum of T_o hours
ΔN_L	incremental number of landings
ΔN_R	incremental number of rotor start/stop cycles
P	pitch rate
P_{ik}	percentage of ith flight condition appearing in kth flight condition category
PT	pitch rate threshold
ΔQ_R	incremental calendar time
R	roll rate
RAM	random access memory
RAMMIT	Reliability and Maintainability Management Improvement Techniques
RT	roll rate threshold
SIMPLX	library subroutine which utilizes simplex method to solve a linear programming problem

LIST OF SYMBOLS - Continued

SIMULE	computer program which simulates the assesssment of fatigue damage as in the FCM recording system
SLEQ	library subroutine which solves a set of simultaneous linear equations
T	component fatigue life in hours
TASIR	The Aircraft Selected Items Record
TD_i	flight time spent in ith flight condition of usage spectra
ΔT_F	incremental flight time
T(I)	flight time for the ith flight condition category
ΔT_L	incremental log time
T_i	flight time in the ith mission segment
T_K	amount of flight time spent in kth flight condition category
T_L	total log time
T_N	time spent in the Nth functional assignment
T_o	number of hours in flight spectrum
T_R	total record time
ΔTR	time to component removal
ΔT_R, $\Delta T_R(r)$	incremental record time for the rth record
TRCAL	the projected date of component removal
TS_i	flight time spent in ith flight condition of design spectrum
TSN	time since new
T_t	total flight time
$\Delta T1, \Delta T2, \ldots, \Delta T6$	cumulative time increments for the rth to (r-1)(r-2) and (r-6)th records, respectively

$\Delta T_1(r-1)$, $\Delta T_2(r-1)$, ..., $\Delta T_5(r-1)$	cumulative time increments from the previous helicopter
V_H	limit forward airspeed
V_{ne}	velocity never exceeded in forward flight
V_T	threshold voltage of comparator circuit
WOL	wedge opened loading
WUC	work unit code
X_{ik}	stationary component loads
y_i	oscillatory load corresponding to the ith flight condition
$\hat{y}_i$	approximation of the rotating component loads
Z_i	error switch of IPS for the ith flight condition category
α_n	coefficients which define the transfer function for component load monitoring
ω_i	relative frequency of occurrence of each loading condition, y_i
1B,2C, 2CA,3A	designation of recording systems for the UH-1H helicopter
I,II, IIA,IIIA, IVA,VA, VI,VII	designation of recording systems for the CH-47C helicopter
2407 file	record of DA Form 2407 data
2408 file	record of DA Form 2408 data

LIST OF SYMBOLS - Concluded

2410/ 2407/8 file	designation of composite file in RAMMIT that tracks component change information

superscripts

^	approximation
(o)	initial estimate